2023

A DUAL-FUNCTION FILAMENTOUS PF BACTERIOPHAGE PROTEIN MODULATES PSEUDOMONAS AERUGINOSA VIRULENCE POTENTIAL

Caleb Michael Schwartzkopf

A DUAL-FUNCTION FILAMENTOUS PF BACTERIOPHAGE PROTEIN MODULATES *PSEUDOMONAS AERUGINOSA* VIRULENCE POTENTIAL

By

CALEB MICHAEL SCHWARTZKOPF

A.A., Mid-Plains Community College, North Platte, NE, 2014
B.S. Wildlife Biology, The University of Montana, Missoula, MT, 2017

Dissertation

presented in partial fulfillment of the requirements
for the degree of

Doctor of Philosophy
in Cellular, Molecular, and Microbial Biology, Microbiology and Immunology

The University of Montana
Missoula, MT

May 2023

Approved by:

Scott Whittenburg,
Graduate School Dean

Patrick R. Secor
Division of Biological Sciences

Stephen Lodmell
Division of Biological Sciences

Michael F. Minnick
Division of Biological Sciences

Scott Samuels
Division of Biological Sciences

Brandon S. Cooper
Division of Biological Sciences

Angela D. Luis
Department of Ecosystem and Conservation Sciences

Table of Contents

List of Figures

List of Tables

Acknowledgments

I cannot fully express my appreciation towards the many people whose help made this challenge possible, but I'd like to acknowledge:

Patrick R. Secor – I was extremely blessed to have you as my P.I. You have been patient, encouraging, generous, and instructive as a Ph.D. mentor. I am forever grateful for your time, humor, and enthusiasm throughout my time in your lab.

My committee members, Mike Minnick, Brandon Cooper, Scott Samuels, Stephen Lodmell, and Angela D. Luis – Thank you for your teaching and accountability, which has contributed to make me the researcher I am today.

My lab mates – I cannot thank you all enough for the help and support you have given. You have made my time enjoyable and have been so supportive throughout my graduate career. Thank you Alison Coluccio, Laura Jennings, Diane Brooks, Jared McGourty, Autumn Robinson, Robert Brzozowski, Conner Copeland, Madilyn Head, Eleni Wohl, Tyrza Lamma, Alex Joyce, DeAnna Bublitz, Elise Wells, Shelby Cole, Aubrey Schwartzkopf, Audrey Dozier, Devin Hunt, and Jake Cohen. Finally, a special thanks to Dr. Margie Kinnersley and Lia Michaels, I have so appreciated and honored your help, mentorship, and camaraderie.

Dr. Camilla de Mattos, Valery Roman-Cruz, Aaron Held, Amelia Schmitt, and Dominick Faith – To my fellow graduate student friends, thank you for sharing in the struggles, for all the laughs, and good times.

Sarah Weldon, Jill Burke, Ruth Johnson, and Janean Clark– Thank you for wading through the logistics, bureaucracy, and paperwork that have culminated in this degree. Your support was invaluable.

My wife Aubrey Schwartzkopf – Your love and support have been so helpful, and I have been so grateful for our adventures during this season.

My family – Eric, Rebecca, Kathryn, Amelia, and Jorie. Thanks for being so supportive and encouraging throughout my life. Thanks for always being in my corner. I could not have done this without you.

My church family – Luke, Tim, Shaun, Chris, Austin, Jake, Logan, Wayne and Nancy, and the many others, thank you for your encouragement and moral support through thick and thin.

Abstract

Schwartzkopf, Caleb, Ph.D., Spring 2023 Cellular, Molecular, and Microbial Biology

A Dual-Function Filamentous PF Bacteriophage Protein Modulates *Pseudomonas aeruginosa* Virulence Potential

Chairperson: Patrick R. Secor

Pseudomonas aeruginosa is an opportunistic pathogen that often plagues hospitals. More than half of *P. aeruginosa* isolates are infected by temperate Pf bacteriophage. Pf virions protect bacteria from antibiotics, promote biofilm formation, and modulate animal immune responses in ways that promote chronic infection. These virions can be produced without lysing *P. aeruginosa,* but lysis may occur during superinfection. Superinfection is the process whereby virions of the same or similar phage infect an already infected host. Temperate phages typically encode superinfection exclusion mechanisms. Here we elucidate one such mechanism in Pf phage. We observed that superinfection-surviving *P. aeruginosa* were transiently resistant to Pf-infection and deficient in twitch motility. Twitch motility requires type IV pili (T4P), a bacterial cell surface receptor used by Pf to gain entry. We tested the hypothesis that T4P are suppressed by a Pf-encoded protein. We observed that the Pf protein PA0721, which we termed Pf superinfection exclusion (PfsE), suppressed twitch motility, and promoted resistance to Pf infection by binding the T4P protein PilC. Beyond this superinfection exclusion mechanism, we elucidated a second function for PfsE. Upon overexpression, PfsE reduced the production of the virulence factor pyocyanin and transcription of *pqs* quorum sensing genes. Quorum sensing is density-dependent bacterial communication, whereby bacteria can coordinate complex processes, including pathogenesis and phage defense. We found that PfsE interacts with PqsA by folding into an alternate kinked conformation. We subsequently sought to understand how these quorum system effects affect *P. aeruginosa* virulence. *P. aeruginosa* cured of their Pf infection (ΔPf) unsurprisingly show greater *pqs* activation and pyocyanin production. However, we report that this resulted in a loss of virulence against *Caenorhabditis elegans*. This seemingly contradictory finding may be explained by our observation that *C. elegans* mutants were unable to sense bacterial pigments, such as pyocyanin, through their aryl hydrocarbon receptor and are more susceptible to ΔPf infection compared to wild-type *C. elegans*. Collectively, we describe a dual-function Pf-encoded protein PfsE, which conveys superinfection exclusion and suppresses quorum sensing. Furthermore, the suppression of quorum sensing and downstream virulence factors by Pf allows *P. aeruginosa* to evade detection by innate host immune responses.

Chapter I: Introduction and Context

1.1 FILAMENTOUS BACTERIOPHAGES

Filamentous bacteriophages (viruses) engage in complex interactions with their hosts. These phages are prevalent in a wide range of hosts, from bacteria to archaea, and are found in every major microbial habitat (1). They belong to the *Inoviridae, Lipothrixviridae,* and *Rudiviridae* families (2). Phages of the *Inoviridae* family (inoviruses) have a circular, positive-sense, single-stranded DNA (ssDNA) genome of ~5-15 kb packaged in a flexible filamentous capsid, typically 600-2500x6-8 nm in size, which can be longer than the bacteria they infect (1-5). Their genomes typically encode 7-15 proteins and undergo rolling circle replication (4). Although simple, these phages show extensive functional diversity (1, 4). Roux et al. (2019) found this diversity to be on par with phages from *Caudovirales*, which is the largest order of dsDNA phages. Many of the genes analyzed were linked to virion structure, virion extrusion, DNA integration and replication, transcriptional regulation, or toxin-antitoxin modules (1). These gene functions highlight the chronic nature of these phages. These phages exist either episomally or as temperate phages, which undergo a process known as lysogeny and integrate into the chromosome of their host (6).

The typical phage lifecycle starts with adsorption (attachment) to the host cell surface. Phages recognize specific receptors on the cell surface, usually highly conserved in their bacterial host. While many of these structures are unknown for the filamentous phages, the known structures for *Inoviruses* typically are some form of pilus, whether conjugative or the various type-IV pili (T4P) (3, 7). Conjugative pili, such as the F-pilus, are used by bacteria to exchange genetic material from one cell to another, in a process known as conjugation. T4P are distinct genetically, structurally, and mechanistically from the F-pilus, and are used by bacteria and archaea for a range of activities including electron transport, motility, and DNA uptake (8-10). The commonality between these pili that phages capitalize on is that both types of pili retract, thus bringing an adsorbed phage into the cell. It is speculated and spatially verified that the pilus pore is large enough to allow entry of the phage into the periplasmic space (3). Once in the periplasm, the second receptor that the phage interacts with to enter into the cytoplasm is TolA (3). TolA is a part of a larger complex in the Tol-Pal system involved with membrane invagination during cell division and is highly conserved across Gram-negative bacterial species (3, 11, 12). As the phage ssDNA enters the cell, the major coat protein of the phage typically gets incorporated into the inner membrane (3, 6, 13).

Once the ssDNA is inside the cytoplasm, the filamentous phage's genome is known as the infective form (IF) (3). Filamentous phages utilize the host's replication machinery to replicate. In Ff phages, the RNA polymerase σ70 holoenzyme binds a mimicked bacterial -35 and -10 promotor sequence with affinity that is higher than a typical bacterial promotor (3, 14). The RNA polymerase starts synthesizing the + strand of the genome, but stops, creating a primer (15). The host DNA polymerase takes over and finishes synthesis of the + strand (16). This new double-stranded DNA (dsDNA) is known as the replicative form (RF). At this point, the filamentous phage may exhibit one of two life cycles. It may integrate into the host chromosome as a prophage through a process known as lysogeny, whereby it is replicates with the bacterial chromosome or it may exist episomally like a plasmid. As a prophage, much of the phage genome, if not all, is dormant. Phages such as the Pf phages typically utilize lysogeny, while the Ff phages in *E. coli* are episomal. Given certain environmental stimuli, such as the bacterial stress response, the phage excises from the chromosome, existing once again as a RF. The RF serves as a template for protein expression as well as host-independent rolling circle replication. Rolling circle replication generates more RFs as well as IFs. These IFs may get packaged into the proteinaceous filament and extrude from the cell membrane.

The temperate nature of these phages provides an opportunity for mutualistic symbioses with their hosts. This mutualistic relationship breaks the mold of what is typically associated with viruses. For example, these phages do not typically lyse (kill) their host, rather they continuously extrude from the cellular membrane (3). Furthermore, they increase the virulence potentials of their host (3, 17). In *Vibrio cholerae*, the disease causing CTX cholera toxin is encoded on the filamentous CTXφ phage (3). In *Neisseria* and *Ralstonia,* these phages indirectly affect virulence by influencing host colonization abilities and biofilm formation (1, 17-21). In addition to virulence enhancement, several phages convey resistance against other viruses through alterations in the cell surface receptors of their bacterial hosts (22-24). Alternatively, phage resistance can be as economic as the repressor of one phage repressing other phages (24). There are a myriad of different ways phages can benefit theirs hosts and we are a long way from understanding these complex interactions.

1.2 Pf phages

1.2.1 Mutualistic relationship with *Pseudomonas aeruginosa*

Hospital acquired infections are estimated to cost the U.S. nearly $10 billion annually (25). *Pseudomonas aeruginosa* is a common pathogen associated with these infections and has been implicated in causing 10-20% of nosocomial infections in most hospitals (26). This gram-negative opportunistic pathogen terrorizes patients suffering from cystic fibrosis (CF) or burn wounds. Furthermore, it often contaminates medical implants and devices. One of the difficulties with treating *P. aeruginosa* is its ability to develop multi-drug resistance. Indeed, increasing resistance against last-resort antibiotics has led the World Health Organization (WHO) to classify *P. aeruginosa* as a "critical priority pathogen."

A key component of the virulence potential of *P. aeruginosa* are the Pf filamentous phages that infect it. Pf phages increase virulence through influencing biofilm formation, host colonization, motility, and by modulating mammalian immune responses (17, 19, 20, 27-30). These phages are prevalent in 60% of clinical isolates (31), and phage particles are present at sites of *P. aeruginosa* infection (20, 32). Furthermore, Pf phages have also been associated with chronic *P. aeruginosa* infections, antibiotic resistance, and worse disease exacerbations for those suffering from CF (30, 33). This in part is due to their enhancement of the *P. aeruginosa* biofilm, a protective extracellular matrix of DNA and polymers.

During growth in the biofilm, these phage are activated, resulting in the increase of 100-1000 times more phage virions (34). This leads to the abundance of up to 10^{10} phage particles per ml (32). These particles self-organize in the biofilm matrix into a viscous-liquid-crystal-like structure that protects *P. aeruginosa* from desiccation and antibiotics, while also increasing surface attachment (20, 27). Pf phages are also involved in cell death that is dependent on the spatial and temporal organization of cells (28, 35). This death helps shape the biofilm and the removal of the Pf prophage reduces biofilm stability and virulence of *P. aeruginosa* in a mouse pneumonia model (28, 29, 35). These examples indicate the huge impact on biofilm formations Pf phages have.

Beyond effects on biofilm formation, Pf phages also subvert the host immune system, pushing it towards an inappropriate immune response, preventing clearance of *P. aeruginosa* (29). In a study conducted at Stanford (29), researchers found that Pf phage inhibit phagocytosis of *P. aeruginosa* by murine-derived dendritic cells and macrophages, as well as by human macrophages. Intriguingly, Pf phages also inhibited engulfment of *Escherichia coli* by murine phagocytes previously exposed to Pf phages. Beyond disrupting phagocytosis, Pf phages modulated cytokine production by host cells; TNF production, a phagocytosis stimulator, was decreased in response to Pf phage presence, while IL-12

and type-1 interferon were increased (29). These changes, among others in the cytokine profile, biased the immune response towards an antiviral response rather than an antibacterial response (29, 30).

As can be seen, the ways Pf modulate *P. aeruginosa* virulence are various and diverse. From biofilm enhancement to immune modulation, Pf phages interact not only with their prokaryotic host, but also with eukaryotic organisms. There remains much to be discovered about these complex and tripartite interactions.

1.2.2 Pf Phage Life Cycle

The life cycle of Pf phages are similar to other filamentous phages discussed above. Pf phages enter the cell via the T4P. The Pf minor coat protein, CoaA, interacts with the T4P, followed by the secondary receptor, TolA to enter the cell (3, 30). CoaB, the major coat protein, is removed from the ssDNA and retained in the inner membrane as the IF enters the cytoplasm. The IF is used to create the RF by host cell enzymes. The phage may remain an RF if environmental conditions are unfavorable for lysogeny or if the Pf phage is incapable of chromosomal lysogeny, such as Pf1 (36). If the phage is capable of chromosomal lysogeny, then IntF, a phage-encoded tyrosine recombinase, integrates the Pf phage into a bacterial tRNA gene. Both the tRNA gene insertion site and presence of a phage-encoded integrase are common among Pf phages (30). For example, Pf4 (the phage studied in this dissertation) encodes IntF4 which integrates Pf4 into the *P. aeruginosa* strain PAO1 in the tRNA-Gly gene *PA0729.1* (30, 37).

Lysogenic phages, such as Pf phages, utilize various means for determining excision from the chromosome and independent replication, known here as a chronic infection cycle. Phages respond to bacterial population density or nutrient limitation and other types of bacterial stress (30, 38-41). Pf4 phage, for example, responds to the transcriptional regulator OxyR (42) and a recent preprint suggests dephosphorylation of the MvaU protein, as well (43). In the case of OxyR, when exposed to oxidative stress, such as H_2O_2, the cysteine residues in OxyR are oxidized. This in turn, allows it to bind Pf4 between the genes *PA0716* and *PA0719* (42). The *pf4r* repressor c gene, a homologue of the P2 phage repressor C gene, resides in this region (44). As a repressor c protein, Pf4r maintains lysogeny and will prevent superinfection via suppression of the excisionase gene, *xisF4* (37). Therefore, the inhibition of *pf4r* by oxidized OxyR releases *xisF4* transcription and results in the initiation of the chronic infection cycle, whereby XisF4 induces transcription of the operon encoding the RF initiator protein PA0727 and the integrase IntF4 (37). PA0727 binds to the RF origin of replication, recruits the host enzymes DNA polymerase III and the implicated DNA repair helicase UvrD, whereupon rolling circle

replication commences (45). In the case of MvaU, the kinase-kinase-phosphatase (KKP) toxin-antitoxin (TA) system, located on the co-residing prophage Pf6, controls phosphorylation of MvaU (43). MvaU, and its cooperative partner MvaT, are H-NS family DNA-silencing proteins (46, 47). When phosphorylated, MvaU binds to Pf4 on the *xisF4* gene (37, 43, 47). As the KKP system dephosphorylates MvaU, it likely releases repression of the *xisF4* and initiates the chronic infection cycle. It is possible that these two systems work together during biofilm development.

Once rolling circle replication starts, more copies of RF are synthesized, as well as IF ssDNA. PA0720, a single stranded binding protein is synthesized from the RF and quickly coats the IF, stabilizing and protecting the ssDNA (30). Other structural proteins such as CoaB also commence synthesis. CoaB is targeted to the inner membrane via a leader peptide that is translated with the mature CoaB protein. Once properly oriented in the inner membrane the host Sec/YidC enzymes process CoaB into its mature form (30, 48). CoaB then gets processed by morphogenesis machinery, perhaps including PA0726, with the C-terminus of the CoaB extending through the outward-facing ssDNA bases to interact with the phosphate backbone of a twisted and inverted IF (30, 49). The mature phage virion then extrudes from the cell.

1.2.3 Superinfection

With the accumulation of virions outside the cell, the chance that the cell gets reinfected with multiple virions of the same, or similar, phage increases. This process is known as superinfection. Lysogenic phages often encode mechanisms that prevent superinfection, which can provide protection from other phages. This dual protection often occurs when the mechanism preventing superinfection works by altering the bacterial surface receptor commonly used by phages to enter the cell, which is typical of many *P. aeruginosa* phages (24, 50). Common receptors include the O-antigen present in lipopolysaccharide and the T4P (24). T4P (used by Pf4, DMS3, JBD8, and D3112 phages for entry) convey the strongest resistance to superinfection when interfered with by phage proteins (24, 51, 52). Examples of this include the T4P ATPase PilB-binding Tip and Aqs1 proteins, encoded by D3112 and DMS3, respectively (51, 52). Phages may also convey protection through the phage-encoded repression protein, which prevents the initiation of the chronic infection cycle. This protein may share enough similarity with other phages that it prevents their infection. This type of protection is less common than the modification of the cell surface (24). Though it is known that Pf4 encodes the *pf4r* repressor, which does convey partial superinfection exclusion, it has not been shown whether Pf4 may also encode a protein capable of interacting with a cell surface receptor (37, 44). This may be likely as

small colony variants (SCV's) resulting from Pf4 infection show transient, but full, resistance to Pf4 superinfection.

Though Pf4 encodes various superinfection exclusion mechanisms, as addressed in this dissertation, superinfection still occurs and is important for *P. aeruginosa* biofilm development. Indeed, superinfection influences biofilm formation by affecting biofilm maturation, cell death, dispersion, and the development of SCVs (20, 27, 28, 30, 35, 44, 53). Biofilms start as cells attach to a surface and form microcolonies (54). In PAO1, as these microcolonies mature, the center of these colonies suffer Pf4 phage-dependent cell lysis and consequent release of DNA into the extracellular environment (eDNA) (28). This eDNA is important for structural integrity of the biofilm and cellular respiration, as sequestered microcolonies are subject to a lower abundance of oxygen and an increased exposure to reactive oxygen and nitrogen species (53, 55-57). The stresses present in these microcolonies make them hotspots for genetic mutations with mutation frequencies 100-fold higher than in planktonically grown cultures (53, 58).

Intriguingly, from these microcolonies, superinfective Pf variants emerge that contain mutations in the repressor *c* gene *pf4r.* These variant Pf can cause cellular lysis. As previously stated, Pf phages do not typically lyse the cell. However, lysis can occur when enough Pf virions infect the same cell or when infected by superinfective Pf variants (37, 44, 59). The formation of these superinfective Pf variants are linked to improper oxidative stress response and a hindered MMR (methyl-directed mismatch repair) DNA repair system (53); mutations in the MMR system are often observed in the clinical setting (60). The mutation in *pf4r* leading to the superinfective variant renders Pf4r unable to dimerize and bind its native promotor, resulting in dysfunctional repression (44). It is suspected that uncontrolled phage production destabilizes the cytoplasmic membrane, perhaps through accumulation of CoaB, thus causing cell lysis (30, 44). It was observed that cellular lysis due to Pf superinfection is limited by the two-component regulator BfmR, which mediates lysis through PhdA (PA0691) (61). A PAO1 Δ*bfmR* mutant showed increase susceptibility to Pf4-mediated superinfection and lysis. BfmR was found to target the *phdA* promotor, PhdA being homolog of the prevent-host-death (Phd) family of proteins. Further investigation showed that the PAO1 Δ*phdA* mutant exhibited increased cell death and other phenotypes comparable to PAO1 Δ*bfmR.* Furthermore, upon overexpression of PhdA, PAO1 became more resistant to Pf4 superinfection (61).

Pf-mediated cell lysis creates a selective pressure that leads to the formation of SCVs. One feature of these SCVs is that they often lack functional T4P. The loss of T4P is attributed to the Pf phage

resistance these cells gain. Some studies have found that this loss of T4P increases the size of microcolonies found in the biofilm (62, 63). Other have found microcolony establishment is incumbent upon having function T4P (64). It seems likely this discrepancy has to do with experimental methods (27). Beyond loosing T4P, SCVs are coated in interwoven Pf filaments that likely aid in greater attachment and adhesion to surfaces (27). SCVs also exhibited enhanced microcolony development. These features, along with their high abundance in biofilm runoff, underscore the dispersion advantages these cells have (27, 53).

1.3 Bacterial Quorum Sensing

1.3.1 Lux-type quorum sensing in *Pseudomonas aeruginosa*

Quorum sensing (QS) is cell-to-cell communication used by many bacteria, which allows them to collectively regulate behaviors in response to their surrounding microbial communities (65). In *P. aeruginosa*, small chemical messengers, known as autoinducers (AIs), are secreted that typically diffuse freely through the cellular membrane and interact with cognate receptors residing in the cytoplasm of the bacterium. Antiactivators keep the bacterial cells from sensing their own AIs (66). Once a threshold concentration of AI is reached, the receptor-AI pair will initiate transcription of a variety of genes.

There are two canonical circuits to the QS system of *P. aeruginosa*, *las* and *rhl*, which regulate nearly 10% of the *Pa* genome (67, 68). These two systems operate by synthesizing the acyl-homoserine lactone (AHL) AIs through autoinducer synthases, LasI and RhlI. LasI produces *N*-(3-oxododecanoyl)-HSL (3OC12-HSL) (69) and RhlI produces *N*-butyryl-HSL (C4-HSL) (70). 3OC12-HSL and C4-HSL bind their cognate receptors: LasR and RhlR, respectively. Each AI-receptor pair increases transcription of itself, acting as a feed-forward loop. Additionally, LasR increases transcription of the other circuits of the QS system and is therefore known as the master regulator. These circuits include two other non-AHL circuits: *pqs* and *iqs.* In the *pqs* (*Pseudomonas* quinolone signal) system, PQS (2-heptyl-3-hydroxy-4-quinolone), and its precursor HHQ (4-hydroxy-2-heptylquinoline), bind their cognate receptor PqsR (also known as MfvR) and the AI-receptor pair regulate a set of genes overlapping the *rhl* circuit (71-73). Finally, the *iqs* (integrated quorum sensing signal) system, which has an unidentified receptor, is thought to be able to take over some of the functions of a nonfunctional *las* system under low-phosphate conditions (68, 74, 75). This complex system of regulation allows *P. aeruginosa* to fine-tune its behavior to suit its environment.

Genes regulated by QS are involved in bacterial behaviors including, but not limited to, cytotoxicity, biofilm formation, motility (including T4P), danger signaling, immune evasion, iron scavenging, and secretion of extracellular DNA (28, 67, 68, 76, 77). As hinted above, each QS system regulates its own set of genes, though there is some overlap. For example, both the *pqs* and *rhl* systems regulate phenazines, potent redox-active virulence factors (78). Phenazines are nitrogen-containing aromatic molecules that are easily observed due to their bright pigmentation (79). The blue-green color typical of *P. aeruginosa* cultures is due to the phenazine, pyocyanin. Pyocyanin is used by *P. aeruginosa* to respire in oxygen-limited environments, such as the interior of the biofilm (56, 80). Indeed, its respiratory properties make it a toxin because it generates reactive oxygen species. Unfortunately, pyocyanin is often abundant in the sputum of cystic fibrosis patients infected with *P. aeruginosa* (81, 82). Due to the harmful nature of this molecule, as well as its ease in detection, pyocyanin is commonly used as an indicator for *P. aeruginosa* virulence.

1.3.2 PQS quorum sensing

As mentioned above the *pqs* system operates like the other AHL systems, using an AI and receptor pair to initiate gene transcription. The *pqs* system uses both HHQ and PQS as AI molecules (83, 84). Unlike the AHL systems, PQS and HHQ belong to a family of molecules that derive from 4-hydroxy-2-alkylquinolines (HAQs) (85). The precursor molecule to these HAQs is anthranilic acid (AA) and is produced from the *phnAB* genes of the anthranilate synthesis operon. Anthranilic acid then becomes the substrate for the *pqsABCDE* operon, resulting in the production of HHQ. The last gene in the *pqsABCDE* operon, *pqsE,* is not necessary for HHQ or PQS production, as its enzymatic activity is believed to be complemented by the thioesterase TesB (86). However it plays a multifunctional role in establishing virulence phenotypes by interacting with rhlR (87). PQS is synthesized from HHQ with the action of *pqsH,* a gene located elsewhere on the bacterial chromosome (83, 88, 89). When PQS or HHQ interact with PqsR the complex increases transcription of the *pqsABCDE* and *phnAB* operon, creating another forward-feed loop (83, 84, 88).

The *pqs* system is tied to the other QS systems in several ways. The other systems have influence over the *pqs* system. For example, the genes *pqsH* and *pqsR* are positively regulated by lasR, (83, 88, 89). Additionally, *pqsR* is negatively regulated by the *rhl* system, specifically rhlR (83, 90-92). Deleting *rhlR* and *rhlI* result in increased expression of *pqsA* (87). RhlR may compete with PqsR for the promotor of the *pqsABCDE* operon (87, 91-93). Furthermore, the aforementioned PqsE complexes with RhlR, enhancing RhlR's affinity for binding DNA, likely including the *pqsABCDE* promotor (87). The *pqs*

system also exerts it's influence on the others. Mutation of *pqsR* results in decreased pyocyanin, exoprotein, and elastase production (primarily under the control of the *las* system), nearly complete abolishment of the transcription of the coregulated *pqsABCDE* and *phnAB* genes, and a reduction in 3OC12-HSL generation (88, 94, 95). Though, mutations in *pqsR* do not seem to affect the production of C4-HSL and RhlR, PQS itself enhances the *rhl* system (increasing both RhlR and C4-HSL) (95). Indeed, the PQS signal is required for the induction of *rhl* phenotypes during the transition to stationary phase (95). This aligns with the timing of PQS production. The *phAB* and *pqsABCDE* operons are maximally transcribed during the end of exponential/early stationary phase (85), with PQS itself being detected during exponential growth, more substantially during the transition into stationary phase, and maximally during late stationary phase (95). It is speculated that the *pqs* system is important for *lasR*-independent activation of the *rhl* system during late stationary phase. This complex and at times seemingly contradictory regulation, may allow for intricate control of these systems.

The *pqs* system is involved in many different aspects of virulence development. PQS influences the production of rhamnolipids, elastase, LecA, pyocyanin, and biofilm development (83). This system is required for full virulence towards plants (96), nematodes (89), and mice (68, 96, 97). Furthermore, PQS has roles outside of QS. PQS chelates ferric iron (98) and although it holds iron in a non-deliverable way, it is hypothesized that PQS is used to store iron (83). Also, as a hydrophobic molecule, PQS promotes outer membrane vesicle (OMV) formation and is delivered to other cells through OMVs (99). To accomplish this, PQS integrates into the outer membrane, interacts with Lipid A of LPS, and induces membrane curvature (100). Lastly, PQS itself acts as a danger signal to other cells, indicating the presence of phage or antibiotic challenge (101). The role of PQS in phage defense and its population density-dependent regulation make this molecule a prime target for phage interaction.

1.3.3 Phages inactivate bacterial quorum sensing.

Interacting with bacterial QS conveys distinct advantages to phages, especially when considering the lysis-lysogeny lifecycle of phages. Lysogeny is a strategy that seems to work best when the density of host cells is too low to support lytic infection, in environments where downturns for the host can be severe, or where phage populations can become isolated (such as those related to bacterial infections) (102-104). The ability of phages to switch between their chronic or lysogenic life cycle gives them flexibility to maximize success in such environments. Even over the course of phage infection, the host environment changes. It has been modelled and experimentally observed that during a phage infection, selection pressures favor a more virulent phage strain early on, when the density of susceptible cells is

high, and a more lysogenic phage strain later, when the density of susceptible cells is low (102). This is likely because virulent phage can run out of hosts to infect.

Tuning into bacterial communication allows for greater flexibility in dynamic environments where host cell density changes can be dramatic and quick. In *Vibrio cholerae*-infecting phage VP882, the phage encodes a receptor that interacts with a host derived quorum molecule to directly detect host population density (40). Many phages also modulate bacterial quorum sensing systems (105, 106). Examples in *P. aeruginosa* include phage DMS3, which encodes a quorum-sensing anti-activator protein called Aqs1 that binds to and inhibits LasR (51). Another *P. aeruginosa* phage called LUZ19 encodes Qst, a protein that binds to and inhibits the PqsD protein in the PQS signaling pathway (107). In both cases, it is thought that inhibition of *P. aeruginosa* QS makes the bacterial host more susceptible to phage infection, as bacterial QS controls phage defense mechanisms (108, 109). Intriguingly, phage JBD44 was recently found to restore *pqsH* production in a *P. aeruginosa* strain PA14 Δ*lasI* mutant, leading to a reduced HHQ-dependent autolysis and re-establishing quorum product production through the PQS pathway (108). This study speculated that phage infection resulted in PA14 responding with an increased production of PQS, which can act to alarm other cells of phage challenge (108).

With studies such as these in mind, we hypothesize that Pf4 also interacts with QS. We have observed a relationship with Pf4 infection and the production of the QS product, pyocyanin, that hints at this. Furthermore, with the incredible ways that Pf4 interacts with *P. aeruginosa* biofilm formation and pathogenesis, and Pf4's temperate nature, interactions with QS seem likely.

1.4 Thesis aims

My dissertation aims to (1) characterize a novel superinfection exclusion mechanism for the Pf4 phage, (2) identify Pf4's interaction with *P. aeruginosa* QS and elucidate how this interaction effects *P. aeruginosa* virulence, and (3) detail the mechanism of how Pf4 interacts with *P. aeruginosa* QS and what benefits this interaction provides Pf4. This research adds to the knowledgebase of how Pf4 interacts with *P. aeruginosa*, and furthers the framework of understanding on how phages interact with their bacterial hosts and what affect that may have on bacterial fitness.

Chapter 2: A Filamentous Bacteriophage Protein Inhibits Type IV Pili to Prevent Superinfection of *Pseudomonas aeruginosa*

Amelia K. Schmidt[1], Alexa D. Fitzpatrick[4], Caleb M. Schwartzkopf[1], Dominick R. Faith[1], Laura K. Jennings[1], Alison Coluccio[1], Devin J. Hunt[1], Lia A. Michaels[1], Dave W. Dorward[2], Jenny Wachter[3], Patricia A. Rosa[3], Karen L. Maxwell[4], and Patrick R. Secor[1#]

[1] Division of Biological Sciences, University of Montana
[2] Research Technologies Branch, & [3] Laboratory of Bacteriology, Rocky Mountain Laboratories, National Institute of Allergy and Infectious Diseases, National Institutes of Health
[4] Department of Biochemistry, University of Toronto
[#] Corresponding author: patrick.secor@mso.umt.edu

Note: My contribution to this work consisted primarily in generating the preliminary data necessary to publish this paper. To this end, I performed a myriad of plaque and twitch assays that developed our understanding that Pf4 conveys resistance to coinfecting phages. Furthermore, I constructed many of the clones used in this assay, including: ΔPf4 and Δ*intF/pfsE* and I prepared the bacterial samples for TEM. I also wrote a draft introduction for this paper.

2.1 Abstract

Pseudomonas aeruginosa is an opportunistic pathogen that causes infections in a variety of settings. Many *P. aeruginosa* isolates are infected by filamentous Pf bacteriophage integrated into the bacterial chromosome as a prophage. Pf virions can be produced without lysing *P. aeruginosa.* However, cell lysis can occur during superinfection, which occurs when Pf virions successfully infect a host lysogenized by a Pf prophage. Temperate phages typically encode superinfection exclusion mechanisms to prevent host lysis by virions of the same or similar species. In this study, we sought to elucidate the superinfection exclusion mechanism of Pf phage. Initially, we observed that *P. aeruginosa* that survive Pf superinfection are transiently resistant to Pf-induced plaquing and are deficient in twitching motility, which is mediated by type IV pili (T4P). Pf utilize T4P as a cell surface receptor, suggesting that T4P are suppressed in bacteria that survive superinfection. We tested the hypothesis that a Pf-encoded protein suppress T4P to mediated superinfection exclusion by expressing Pf proteins in *P. aeruginosa* and measuring plaquing and twitching motility. We found that the Pf protein PA0721, which we termed Pf superinfection exclusion (PfsE), promoted resistance to Pf infection and suppressed twitching motility by binding the T4P protein PilC. Because T4P play key roles in biofilm formation and virulence, the ability of Pf phage to modulate T4P via PfsE has implications in the ability of *P. aeruginosa* to persist at sites of infection.

2.2 Introduction

Pseudomonas aeruginosa is an opportunistic pathogen that causes infection in wounds, on medical hardware, and in the airways of people with cystic fibrosis. *P. aeruginosa* itself can be infected by a variety of bacteriophages (phages). For example, many *P. aeruginosa* isolates are infected by temperate filamentous Pf phage, which can integrate into the bacterial chromosome as a prophage (17, 31). During *P. aeruginosa* growth as a biofilm or at sites of infection, the Pf prophage is induced, and filamentous virions are produced (29, 32, 34, 110). Like other filamentous phages, Pf can be extruded from the host cell without killing the host, allowing Pf virions to accumulate to high titers in biofilms (10^{11}/mL) (111) and infected tissues (10^{7}/gram) (20). However, cell lysis can occur when Pf superinfects *P. aeruginosa*, which occurs when multiple virions infect the same cell or when superinfective Pf variants emerge that contain mutations in the phage *c* repressor gene *Pf4r* (37, 111). Pf4-mediated cell lysis contributes to the maturation and dispersal stages of the *P. aeruginosa* biofilm lifecycle (112-115).

Temperate phages typically encode superinfection exclusion mechanisms to stave off infection by competing phages in the environment. A common theme amongst superinfection exclusion mechanisms are proteins that inhibit or modify phage cell surface receptors such as type IV pili (T4P) (7), a common cell surface receptor for phages, including Pf4 (116). Many *P. aeruginosa* phages encode proteins that inhibit T4P to prevent superinfection (117). Specific examples include the Aqs1 protein encoded by phage DMS3 and the Tip protein encoded by phage D3112, which both inhibit T4P by binding to the T4P ATPase PilB (51, 52). Pf4 use T4P as a cell surface receptor (116); however, a superinfection exclusion mechanism has not been characterized for the Pf phages that reside in *P. aeruginosa* genomes.

In this study, we show that the smallest protein encoded by Pf4, which we call PfsE (Pf superinfection exclusion), transiently inhibits T4P assembly through an interaction with the T4P platform protein PilC, providing resistance to further infection by T4P-dependent phages. By introducing point mutations to PfsE, we identified two aromatic residues (Y16 and W20) that may be required for PilC binding, T4P inhibition, and resistance to T4P-dependent phages. Furthermore, phage Pf4 engineered to lack the *pfsE* gene is able to kill *P. aeruginosa* more efficiently than the wild-type phage, demonstrating that this mechanism of superinfection reduces *P. aeruginosa* cell lysis. Filamentous Inoviruses such as Pf are widespread amongst Bacterial genomes with even a few examples infecting Archaea (118). Thus, the superinfection exclusion mechanism described here may be relevant to many

species of filamentous phage that infect diverse bacterial hosts.

2.3 Results

2.3.1 Type IV Pili are transiently suppressed in response to Pf4 Superinfection

While working with phage Pf4 we noticed an interesting phenomenon where the surviving cells in a culture of PAO1 superinfected with Pf4 showed a decrease in twitching motility (**Fig 2-1A**). As Pf4 uses T4P as a cell surface receptor (116), we tested the ability of these non-twitching cells to mediate resistance to Pf4-induced plaquing. We found that these cells were highly resistant to lysis by Pf4 virions (**Fig 2-1B**) as compared to uninfected PAO1, which retain the ability to twitch (**Fig 2-1C)** and are sensitive to Pf4 superinfection (**Fig 2-1D**). The resistance observed was similar to that seen for a PAO1 Δ*pilA* mutant, which completely lacks pilus on the cell surface (**Fig 2-1E and F**). To determine if Pf4 superinfection selected for T4P-null mutants or transiently suppressed T4P expression, bacteria collected from Pf4-resistant lawns were sub-cultured in phage-free growth medium for 18 hours and then their ability to twitch and sensitivity to Pf4-induced plaquing was tested. Twitching motility and sensitivity to Pf4 superinfection was restored in sub-cultured bacteria (**Fig 2-1G and H**), indicating that heritable mutations in T4P genes were not responsible for the twitch-deficient and Pf4-resistance phenotypes.

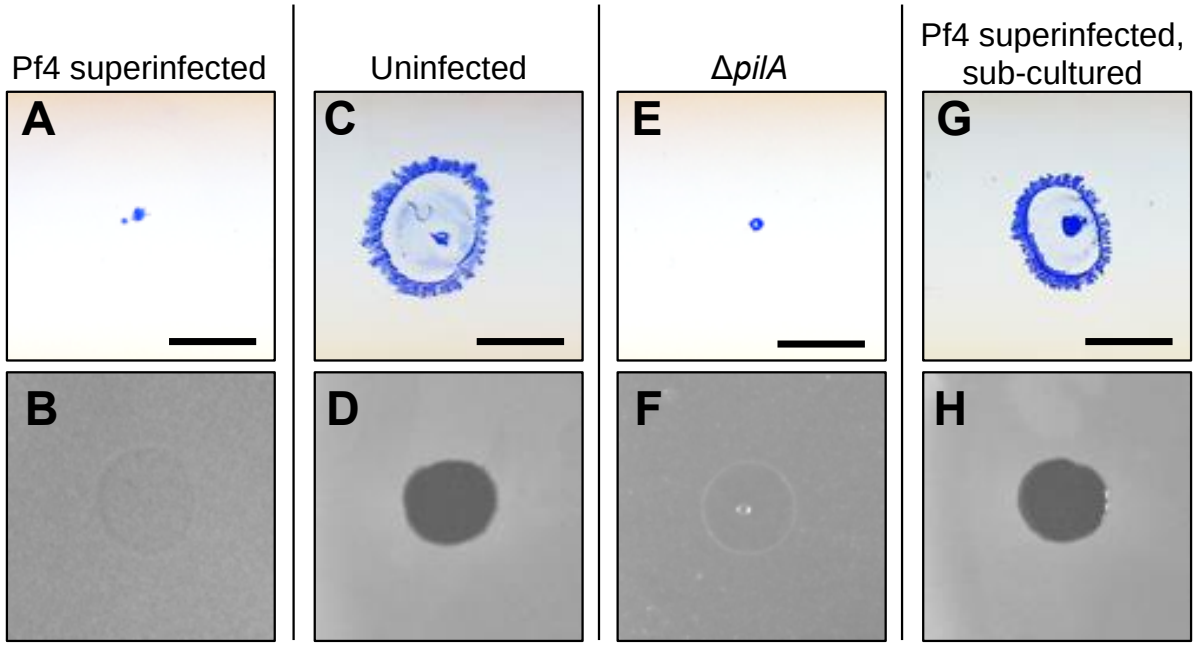

Figure 2-1. Pf4 superinfection transiently suppresses twitching motility and promotes resistance to Pf4-induced plaquing. Twitch assays were performed by stabbing the indicated strain through the agar on a Petri dish to the plastic surface below. After 24h, the agar was removed and bacteria on the plastic dish were stained with Coomassie (upper panels **A, C, E & G**). To measure sensitivity of *P. aeruginosa* to Pf4 superinfection, lawns of the indicated strains were spotted with 10^6 PFUs of Pf4 in 3 µL (lower panels **B, D, F & H**). Strains tested

include (**A and B**) PAO1 superinfected with Pf4, (**C and D**) uninfected PAO1, (**E and F**) the twitch-deficient type IV pili mutant Δ*pilA*, and (**G and H**) Pf4 superinfected PAO1 that was sub-cultured in phage-free broth and re-plated. Scale bar 5 mm.

2.3.2 PfsE suppresses twitching motility and protects *P. aeruginosa* from Pf4 superinfection

Many temperate phages possess superinfection exclusion mechanisms that prevent re-infection of an already infected cell (119). We hypothesized that a Pf4-encoded protein would suppress T4P as a mechanism to prevent Pf4 superinfection and lysis of the host cell. To test this hypothesis, we first deleted the Pf4 prophage from our in-house PAO1 strain (PAO1$^{\Delta Pf4}$). Pf4 proteins encoded by *PA0717-PA0728* in the core Pf4 genome (**Fig 2-2A**) were then expressed individually from a plasmid in PAO1$^{\Delta Pf4}$ and twitching motility and sensitivity to Pf4-mediated lysis were then assessed. We identified two proteins, PA0721 and PA0724, that suppressed twitching motility when overexpressed (**Fig 2-2B**) and promoted resistance to Pf4 plaquing (**Fig 2-2C**). PA0721 is a small 30 residue uncharacterized protein and PA0724 is the Pf4 minor coat protein CoaA, which is involved in receptor binding during the initial steps of infection (17). These results were consistent with a previous study that found these proteins promote resistance to T4P-dependent long-tailed dsDNA phages DMS3m and JBD30 (118).

To determine if the observed twitching inhibition and phage resistance was a direct result of the biological function of these proteins or was due to toxicity of the overexpressed proteins, we examined the growth rates of cells expressing these proteins. We found that PAO1$^{\Delta Pf4}$ expressing PA0724 grew poorly compared to cells expressing PA0721 or PAO1$^{\Delta Pf4}$ carrying an empty expression vector (**Fig 2-2D**). These observations suggest that PA0724 expression is toxic to *P. aeruginosa,* and it is possible that the twitch-deficient and phage resistance phenotypes associated with PA0724 expression are a result of this toxicity rather than a specific superinfection exclusion mechanism. Therefore, we turned our attention towards characterizing PA0721, which we refer to herein as PfsE (Pf superinfection exclusion).

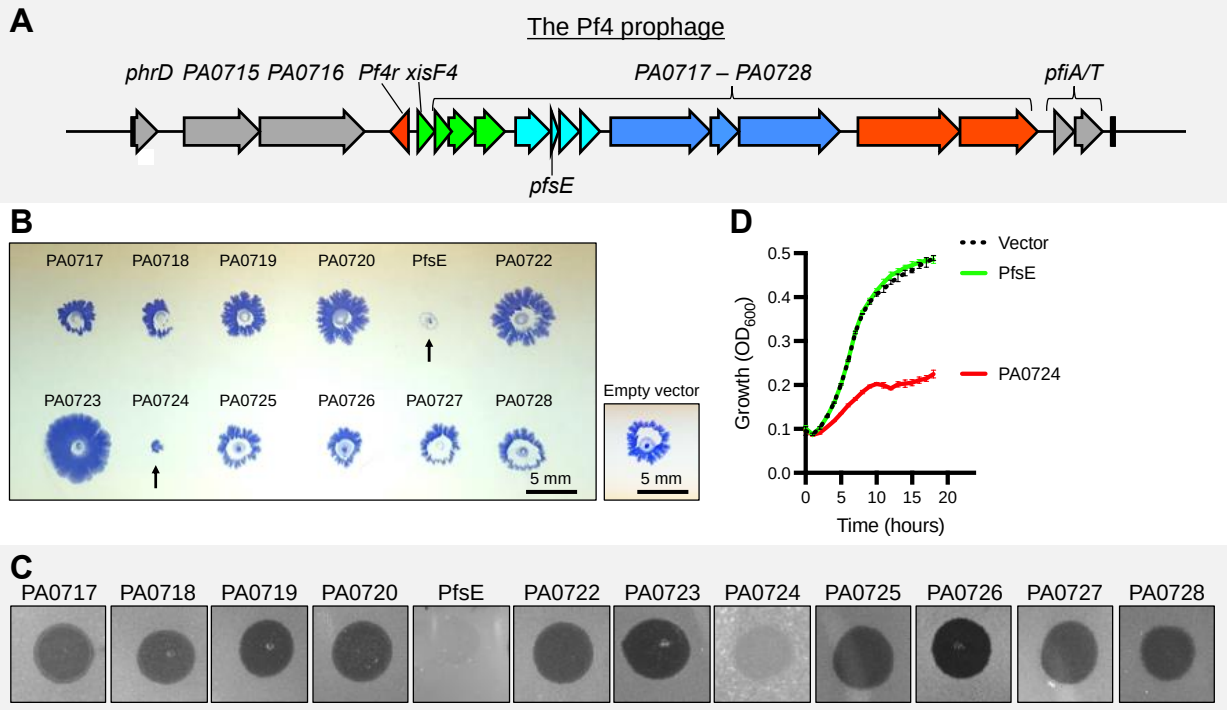

Figure 2-2. PfsE suppresses twitching motility and protects *P. aeruginosa* from Pf4 superinfection. (**A**) The Pf4 prophage is composed of core genes that are essential for the phage to complete its lifecycle (*Pf4r* to *PA0728*) and flanking moron regions (gray) that add "more on" to the core genome (105). (**B**) Genes *PA0717–PA0728* in the core Pf4 genome were placed under the control of an arabinose-inducible promoter and expressed individually in *P. aeruginosa* PAO1$^{\Delta Pf4}$. Twitching was measured in the indicated strains after 24 hours; arrows indicate strains with reduced twitching motility. Bar 5 mm. (**C**) 10^6 PFUs of Pf4 were spotted onto lawns of PAO1$^{\Delta Pf4}$ expressing the indicated phage protein. (**D**) Growth curves in liquid culture for PAO1$^{\Delta Pf4}$ bacteria carrying the indicated expression vector. Cultures were grown in LB supplemented with 0.1% arabinose. Results are the mean ±SEM of three experiments.

2.3.3 T4P are not apparent on cells expressing PfsE

Twitching motility requires bacteria to extend their pili outwards from the cell surface and then retract them to move along solid surface. Thus, PfsE could inhibit twitching motility by either preventing pilus retraction or extension. If PfsE inhibits T4P retraction, cells are anticipated to have a piliated or hyperpiliated morphology. If PfsE inhibits T4P extension, then cells are expected to have few or no pili. To determine if PfsE interferes with extension or retraction we used transmission electron microscopy to look for the presence of pili on the cell surface. We found that cells expressing PfsE showed no visible pili on the surface (**Fig 2-3**) while wild-type PAO1 cells had structures consistent with T4P (**Fig 2-3**). The lack of pili observed on the cells expressing PsfE was similar to a PAO1 Δ*pilA* mutant (**Fig 2-3**), which is known to completely lack surface piliation (120). These data suggest that PfsE inhibits T4P extension rather than retraction.

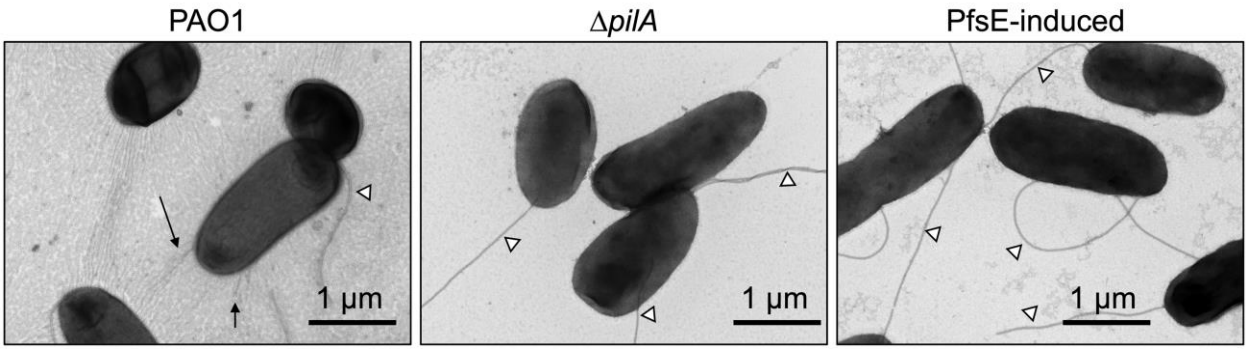

Figure 2-3. Type IV pili are not apparent on cells expressing PfsE. Transmission electron microscopy of the indicated strains of *P. aeruginosa* was performed. Mid-logarithmic cells were washed, fixed, placed on a grid, and negatively stained with uranyl acetate. Arrows indicate potential pili on PAO1 cells. White triangles indicate flagella.

2.3.4 PfsE protects *P. aeruginosa* from other T4P-dependent phage species

Many phages use the T4P as a cell surface receptor to infect bacteria (7). We hypothesized that the transient T4P suppression by PfsE that protected against Pf4 superinfection would also protect *P. aeruginosa* from non-filamentous phages. To test this hypothesis, we examined the ability of phage JBD26, a temperate long-tailed dsDNA phage that uses the pilus as a cell surface receptor, to form plaques on lawns of PAO1, PAO1 Δ*pilA*, PAO1 superinfected with Pf4, PAO1 superinfected with Pf4 and then sub-cultured in phage-free media, or PAO1 expressing PfsE from a plasmid. Like Pf4, JBD26 was not able to infect cells that were superinfected by Pf4 or cells expressing PfsE (**Fig 2-4**). We also tested the ability of phage CMS1, which does not depend on the pilus for infection, to form plaques on these strains. As expected, the plaquing ability of these phages was not affected by the absence of T4P (Δ*pilA*), expression of PsfE, or superinfection by Pf4 (**Fig 2-4**). Furthermore, Pf4 superinfection and expression of PfsE was able to prevent infection by phage OMKO, a lytic pili-dependent phage, but not LPS-5, another pili-independent phage species (**Fig 2-S1**). These results demonstrate that PfsE protects *P. aeruginosa* from T4P-dependent phage species.

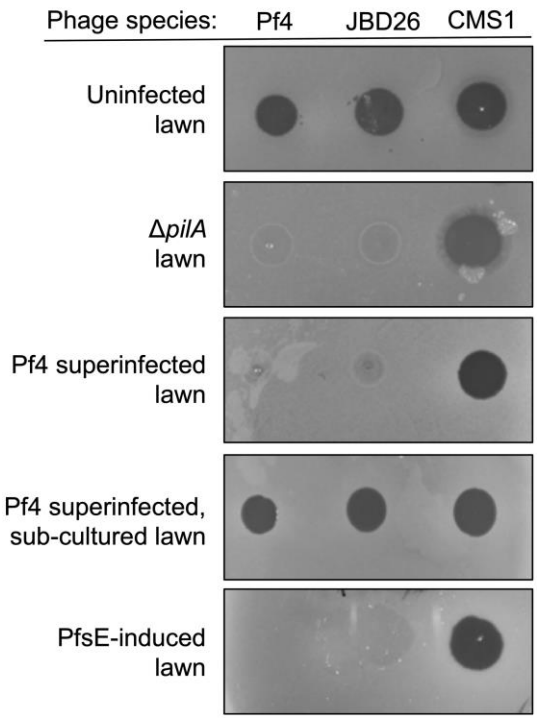

Figure 2-4. Pf4 superinfection and expression of PfsE promotes resistance to type IV pili (T4P)-dependent bacteriophages. Representative images of *P. aeruginosa* PAO1 lawns spotted with 10^6 PFUs of Pf4, JBD26 (both T4P-dependent phages), or CMS1 (a T4P-independent phage). See also Figure S1.

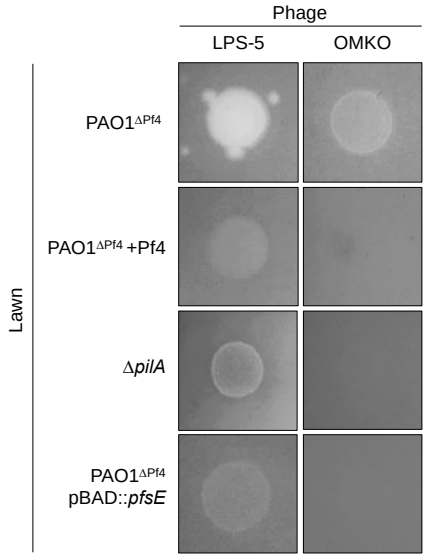

Figure 2-S1. Pf4 superinfection and expression of PfsE promotes resistance to type IV pili (T4P)-dependent lytic bacteriophages. Representative images of *P. aeruginosa* PAO1 lawns spotted with 10^6 PFUs OMKO (T4P-dependent lytic phage), or LPS-5 (a T4P-independent lytic phage). Note plaques are visualized as bright spots in these images.

2.3.5 Deletion of *pfsE* increases Pf4 virulence against *P. aeruginosa*

To definitively show that PsfE expression from Pf phage provides resistance to superinfection, we

attempted to delete the *pfsE* gene from Pf4. All attempts to delete *pfsE* from the Pf4 prophage integrated into the PAO1 chromosome failed. We hypothesized that inactivating *pfsE* resulted in unregulated replication of Pf4, killing *pfsE* mutants, similar to how Pf4 kills *P. aeruginosa* PAO1 when the global repressors *mvaT* and MvaU are both disabled (116). To test this hypothesis, we attempted to delete *pfsE* from the PAO1 Δ*intF4* background. IntF4 (PA0728) is a Pf4-encoded site-specific tyrosine recombinase that catalyzes Pf4 prophage integration and excision (20, 37). In Δ*intF4*, the Pf4 prophage is trapped in the chromosome, preventing infectious virions from being produced (20, 116). We were successful in deleting *pfsE* from Δ*intF4* creating the double mutant Δ*intF4/pfsE*, suggesting that when *pfsE* is inactivated, Pf4 replication kills *P. aeruginosa*.

We hypothesized that Δ*intF4/pfsE* Pf4 virions that lack the *pfsE* gene would not be able to regulate superinfection of the host bacterium, increasing host cell lysis. To test this, we induced and collected Pf4 virions from wild type, Δ*intF4*, and Δ*intF4/pfsE P. aeruginosa*. To induce Pf4 virions from these strains, the Pf4 excisionase XisF4 was expressed *in trans* from a plasmid under the control of an arabinose-inducible promoter (37). To complement the Δ*intF4* mutation, IntF4 was also expressed from a plasmid in all strains tested. After overnight growth (18h) in LB supplemented with 0.1% arabinose, bacterial supernatants were filtered, DNase-treated, and Pf4 titers measured by qPCR, as previously described (121). Phage titers in each supernatant (wild type, Δ*intF4*, and Δ*intF4/pfsE*) were normalized to 6.95×10^7 virions per mL and were plated on a lawn of $PAO1^{\Delta Pf4}$ to determine how infective the mutant phages were. While the Δ*intF4* mutant phage titer was equal to wild-type Pf4, the Δ*intF4/pfsE* mutant phage was approximately 1,000-fold more infective (**Fig 2-5**), indicating that *pfsE* restricts Pf4 infection and thereby protects the bacterial host from lysis.

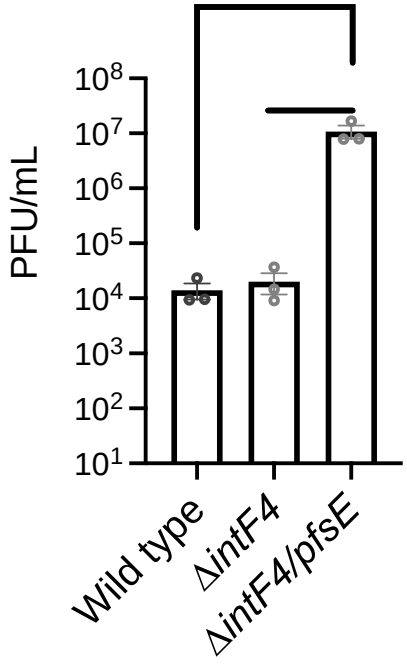

Figure 2-5: Pf4 virions not encoding *pfsE* are more virulent against *P. aeruginosa*. Wild-type and mutant Pf4 virions were induced by expressing both the Pf4 excisionase (*xisF4*) and integrase (*intF4*) *in trans* in wild type, Δ*intF4*, or Δ*intF4/pfsE* backgrounds. Note that deletion of *pfsE* alone from the Pf4 prophage was not possible. Wild-type, Δ*intF4*, and Δ*intF4/pfsE* Pf4 virion titers were measured by qPCR and normalized to $6.95x10^7$ virions per mL. Virions were then spotted as a 10x dilution series on lawns of ΔPf4 to enumerate PFUs. Results are mean ± SEM of three experiments, unpaired Student's *t* test, ****P<0.0001.

2.3.6 Aromatic residues in PfsE are required to inhibit twitching motility and promote Pf4 resistance

PfsE contains a conserved cluster of aromatic residues, **Y**A**W**G**W** (**Fig 2-6A and B**). Clusters of aromatic residues often facilitate protein-protein binding interactions (122, 123). Therefore, we hypothesized that the cluster of aromatic residues in PfsE is required for suppression of twitching motility and resistance to T4P-dependent phages. To test this hypothesis, we introduced into PfsE the following point mutations: $PfsE^{Y16V}$, $PfsE^{W18A}$, $PfsE^{W20A}$, and $PfsE^{Y16V/W18A/W20A}$. The mutant proteins were then expressed in $PAO1^{\Delta Pf4}$ and twitching motility and phage resistance were measured. $PfsE^{Y16V}$, $PfsE^{W20A}$, and $PfsE^{Y16V/W18A/W20A}$ all lost the ability to suppress twitching motility (**Fig 2-6C**) and did not promote resistance to the T4P-dependent phages Pf4 or JBD26 (**Fig 2-6D**). $PfsE^{W18A}$, however, only partially suppressed both twitch motility and infection by T4P-dependent phages, indicating residue W18 is not critical for PfsE to inhibit T4P. The difference in phenotypes between the point mutants may be related to the location of the aromatic residues on the PfsE α-helix; Y16 and W20 are located on the same side of the PfsE α-helix while W18 is oriented in the opposite direction (**Fig 2-6E**). We also tested

the ability of PfsE to inhibit flagellum-dependent swimming motility. PAO1$^{\Delta Pf4}$ expressing wild-type PfsE or PfsE point mutants did not affect swimming motility compared to PAO1$^{\Delta Pf4}$ carrying an empty expression vector (Fig S2 in published manuscript), indicating that PfsE does not affect flagellum-dependent swimming motility, which is consistent with our previous observation that Pf4 superinfection does not affect swimming motility in *P. aeruginosa* PAO1 (110).

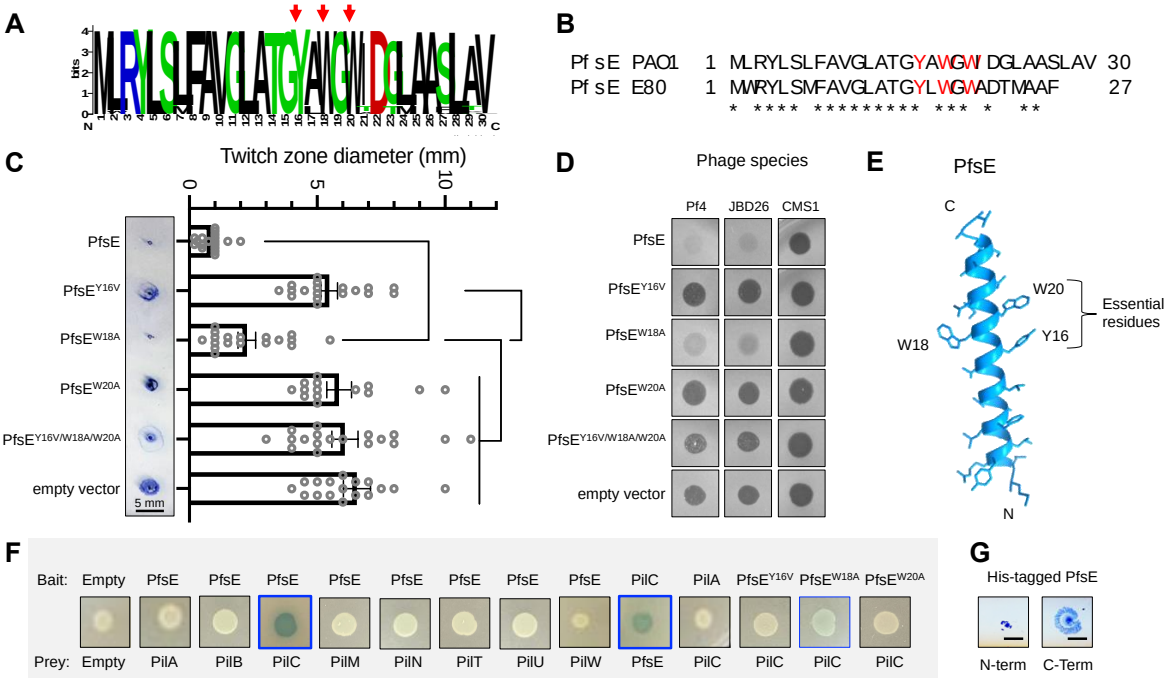

Figure 2-6: Conserved aromatic residues in PfsE are essential for the inhibition of type IV pili and resistance against Pf4 superinfection. (**A**) WebLogo (124) was used to construct a protein sequence logo for 312 PfsE sequences from Pf prophages infecting *P. aeruginosa* strains in the *Pseudomonas* genome database (125). Note that aromatic residues in the YXWGW motif (residues 16-20) are conserved (arrows). (**B**) There is 66% sequence identity (20/30) between two of the most highly diverged PfsE homologues found in Pf prophages residing in the *P. aeruginosa* PAO1 or E80 chromosomes. (**C**) Twitch motility was measured in PAO1$^{\Delta Pf4}$ expressing wild-type or modified PfsE. Results are mean ± SEM of 16 experiments, unpaired Student's *t* test, **p<0.01, ****p<0.0001. (**D**) Lawns of PAO1$^{\Delta Pf4}$ carrying the indicated expression vectors were induced with 0.01% arabinose and spotted with 3 µl of 10^9 PFU/ml stocks of Pf4, JBD26 (pili-dependent phages), or CMS1 (a pili-independent phage). (**E**) AlphaFold (126) was used to predict the structure of PfsE. (**F**) A bacterial adenylate cyclase two-hybrid (BACTH) assay (127) was used to detect interactions between PfsE and the indicated T4P proteins. Interactions between bait and prey proteins are detected by β-galactosidase activity, as indicated by the production of blue pigment. Representative colonies are shown. (**G**) A 6x-His tag was added to the N- or C-terminus of PfsE, expressed in PAO1$^{\Delta Pf4}$, and twitching was measured. Scale bar 5mm.

2.3.7 PfsE binds to the T4P inner-membrane protein PilC

The T4P complex consists of four subcomplexes: the outer membrane complex, an alignment complex that spans the periplasm, and two inner membrane complexes (8). Because PfsE is predicted to localize in the inner membrane (125), we hypothesized that PfsE would interact with inner membrane

proteins of the T4P complex or proteins that interact with the T4P inner membrane complex. To test this hypothesis, we used a bacterial adenylate cyclase two-hybrid (BACTH) assay (127) to detect interactions between PfsE and the T4P proteins PilA, PilB, PilC, PilM, PilN, PilT, PilU, or PilW. In the BACTH assay, interactions between bait (PfsE) and prey (pili proteins) is detected by β-galactosidase activity. High levels of β-galactosidase activity were observed only when PfsE was expressed with PilC (**Fig 2-6F)**, an inner membrane protein essential for T4P pilus biogenesis (128). Similar activity was observed with PilC as bait and PfsE as prey. When the PfsE^{Y16V} or PfsE^{W20A} point mutants were used as bait with PilC as the prey, β-galactosidase activity was not detected. The PfsE^{W18A} mutant produced little to no β-galactosidase activity in the BACTH assay, consistent with its intermediate twitch and phage resistance phenotypes. We attempted to confirm the expression of His-tagged wild-type and mutant PfsE in *E. coli* used in the BACTH assay by western blot. However, we were unable to detect expression of PfsE^{Y16V} or PfsE^{W20A} point mutants using anti-His antibodies, raising the possibility that the loss of interaction between the PfsE point mutants and PilC was due to low expression of mutant PfsE rather than the point mutations. Alternate explanations include poor recovery of PfsE from membrane fractions. Additional experiments will be required to characterize the role of these aromatic amino acids in PfsE-PilC binding interactions.

The binding of PfsE to the inner membrane protein PilC is consistent with the prediction that PfsE is itself an inner membrane protein. To determine the orientation that PfsE inserts itself into the inner membrane, we tagged the N- or C-terminus of PfsE with a poly-histidine (His) tag, which are positively charged and unable to insert into lipid membranes. Tagged PfsE was expressed in PAO1$^{\Delta Pf4}$ and twitching motility measured. The N-terminal His tag had no impact on the ability of PfsE to inhibit twitching while the C-terminal His tag prevented PfsE-mediated twitching inhibition (**Fig 2-7G**). These results suggest that PfsE inserts into the inner membrane with the N-terminus oriented towards the cytoplasm.

As PilC is highly conserved across many different strains of *P. aeruginosa* (128), we tested the ability of PfsE to inhibit twitching motility in *P. aeruginosa* strains PA14, PAK and E90. We found that the PfsE sequence from Pf4 inhibited twitching in each of these strains (**Fig 2-6A**). When the divergent PfsE sequence from P. aeruginosa strain E80 (see **Figure 2-6B**) was expressed in *P. aeruginosa* PAO1$^{\Delta Pf4}$, twitching motility was similarly inhibited (**Fig 2-7B**). These results indicate a conserved mechanism of action.

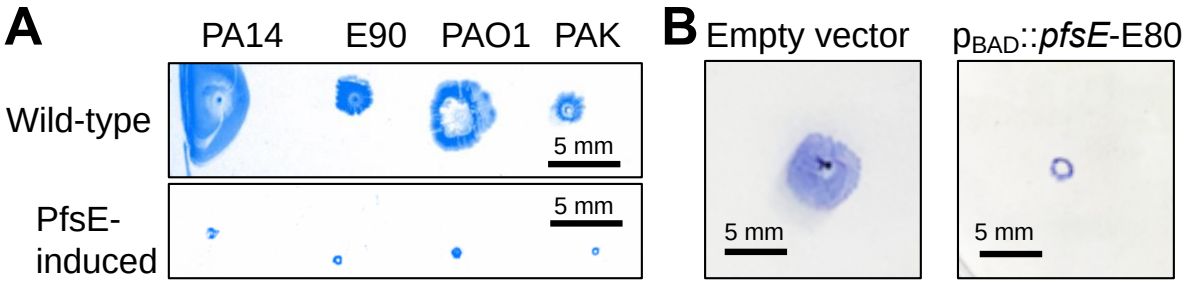

Figure 2-7: Divergent PfsE sequences inhibit twitching motility in various *P. aeruginosa* strains. (A) PfsE was expressed *in trans* in the indicated strains of *P. aeruginosa* and twitching motility measured after 24h. Representative images are shown. **(B)** Twitching motility was assessed in PAO1$^{\Delta Pf4}$ carrying either the empty vector pHERD20T or p_{BAD}-*pfsE*-E80 by standard twitch assay. Representative images are shown.

2.4 Discussion

Many *P. aeruginosa* isolates are Pf lysogens (i.e., they harbor one or more Pf prophage in their chromosome) (17, 31). Lysogenized bacteria defend against infection by the same or similar phage through a mechanism called superinfection exclusion. For example, previously characterized superinfection exclusion mechanisms employed by *P. aeruginosa* phages include proteins Aqs1 from phage DMS3 (51) and Tip from phage D3112 (52), both of which inhibit T4P by binding to the T4P assembly ATPase PilB, which energizes pilus extension (128). This is the first report, to our knowledge, of a phage protein binding PilC to suppress T4P and prevent superinfection. Our data support a model where the Pf-encoded protein PfsE mediates superinfection exclusion by transiently suppressing T4P by binding to PilC to prevent pilus extension, which inhibits twitching motility and prevents infection by T4P-dependent phages. PfsE interactions with PilC may inhibit T4P by either blocking PilC from rotating, PilA loading, or by interfering with interactions between PilC and other pili proteins such as PilB.

To our knowledge, a transient superinfection exclusion phenotype has not previously been described for a phage. However, transient superinfection exclusion has been observed in animal viruses such as the RNA Pestivirus that causes bovine viral diarrhea (129). The transient nature of PfsE-mediated T4P inhibition may be related to highly stable PfsE-PilC binding interactions. If true, then if PfsE is downregulated as Pf re-enters the lysogenic replication lifecycle, tight binding interactions between PfsE and PilC may titrate out PfsE as the cells divide, restoring T4P function. Alternatively, the conserved acidic residue D22 (see **Fig 2-6A**) may pull the C-terminus of PfsE into the periplasmic space where PfsE could interact with periplasmic proteins that could disrupt PfsE-PilC binding (e.g., a periplasmic protease could degrade PfsE).

Our data suggest that PfsE inhibits pili extension. By inhibiting extension of the T4P cell surface receptor, PfsE may reduce the number of Pf virions that are “wasted” on non-productive infections of an already infected host. This would allow Pf virions to accumulate in the environment, allowing Pf phage to spread and infect naïve *P. aeruginosa* hosts. *P. aeruginosa* also benefits from the accumulation of filamentous Pf virions in the environment—as Pf virions accumulate in polymer-rich environments such as the biofilm matrix or host secretions (e.g., mucus), they spontaneously align, creating a large liquid crystalline lattice that protects *P. aeruginosa* from desiccation and some antibiotics (20, 130, 131). When encountered by immune cells, Pf virions induce a type I interferon antiviral response, which reduces the phagocytic uptake of bacteria by macrophages (29). Collectively, these phenotypes help explain why in *P. aeruginosa* PAO1 deleting the Pf4 prophage from the chromosome reduces bacterial virulence in murine lung (112) and wound (29) infection models.

PfsE inhibition of T4P may affect other bacterial behaviors. For example, in *P. aeruginosa*, T4P play important roles in virulence and biofilm formation (64, 132). T4P are critical virulence determinants in *P. aeruginosa* (132) and inhibition of T4P by PfsE could affect *P. aeruginosa* virulence potential. This possibility is consistent with our previous work demonstrating that Pf4 superinfection promotes a non-invasive infection phenotype *in vivo* (110). Under some conditions such as nutrient limitation, suppression of T4P is thought to contribute to biofilm dispersion (133). Pf4 superinfection contributes to the biofilm lifecycle as well by inducing cell death and lysis, which produces the characteristic voids in the center of mature microcolonies of biofilms grown in flow cells (112-114). In dispersed cell populations, Pf4 gene expression is upregulated while T4P genes are downregulated (133, 134). Thus, it is possible that in response to Pf4 superinfection, PfsE expression contributes to biofilm dispersal by suppressing T4P.

Phage therapy holds great potential in combating multidrug-resistant bacterial infections in several settings (135-140). Unfortunately, bacteria can develop resistance to therapeutic phages causing treatment failure ((141) and references therein). In some cases, heritable phage resistance mutations cannot account for phage therapy failure as bacteria remain sensitive to phage infection *ex vivo* (141-144). Because Pf prophages are prevalent amongst *P. aeruginosa* clinical isolates and PfsE is encoded by all Pf lysogens, it is possible that PfsE could cause some phage therapies to fail. Conversely, PfsE could be leveraged as a therapeutic. Recent work demonstrates that the Tip protein from phage D3112 inhibits T4P by blocking the activity of PilB (52). A peptide mimic of the Tip protein inhibits T4P *in vitro,* and when given topically to *P. aeruginosa*, the peptide reduced virulence in a

Drosophila infection model (145). This approach could potentially be adapted to PfsE by synthesizing a peptide that contains the aromatic amino acid motif YAWGW.

2.5 Materials and Methods

2.5.1 Bacterial Strains, plasmids and growth conditions

Strains, plasmids and their sources are listed in **Table 2-1** and primers are listed in **Table 2-2.** Unless indicated otherwise, bacteria were grown in lysogeny broth (LB) at 37 °C with shaking and supplemented with antibiotics (Sigma) or 0.1% IPTG when appropriate. Unless otherwise noted, antibiotics were used at the following concentrations: gentamicin (10 or 30 µg ml^{-1}), ampicillin (100 µg ml^{-1}), kanamycin (50 µg ml^{-1}), carbenicillin (50 µg ml^{-1}).

2.5.2 Construction of strain ΔPf4

The Pf4 prophage was deleted from the PAO1 chromosome by allelic exchange (146), producing a clean and unmarked ΔPf4 deletion with the Pf4 att site intact. All primers used for strain construction are given in **Table 2-2**. The Pf4 prophage contains a toxin-antitoxin (TA) pair (147). The presence of the Pf4-encoded PfiTA system likely explains the low efficiency at which the Pf4 prophage can be deleted from the PAO1 chromosome (112); deletion of the Pf4 prophage results in loss of the antitoxin gene *pfiA* and cells without the antitoxin are killed by the longer-lived toxin PfiT (147). Thus, the *pfiT* toxin gene was first deleted from PAO1 by allelic exchange (146). Briefly, the upstream region of *pfIT (pfiT')* and the downstream region of *pfIT ('pfiT)* were amplified using the primer pairs attB1-pfiT-UpF/pfiT-UpR and PfiT-DownF/attB2-PfiT-DownR, respectively (**Table 2-2**). These were then assembled using SOE-PCR. The resulting fragment was cloned into pENTRpEX18-Gm, transformed into *Escherichia coli* S17λ*pir*, and subsequently mobilized into *P. aeruginosa* PAO1 via biparental mating. Merodiploid *P. aeruginosa* was selected on Vogel-Bonner minimal medium (VBMM) agar containing 60 µg ml^{-1} gentamicin, followed by recovery of deletion mutants on no-salt LB (NSLB) medium containing 10% sucrose. Candidate mutants were confirmed by PCR and sequencing using primer pair PfiT seq F/PfiT seq R. The remaining Pf4 prophage was then deleted from Δ*pfiT* using the same allelic exchange strategy described for Δ*pfiT* using primers Pf4-UpF-GWL, Pf4-UpR-GM, Pf4-DnF-GM, and Pf4-DnR-GWR (Table 2), producing an unmarked clean deletion of Pf4 with an intact att site. Candidate mutants were confirmed by PCR using primer pair pf4-out F/pf4-out R and sequenced confirmed. Supernatants collected from overnight cultures of ΔPf4 did not produce detectable plaques on lawns of PAO1 or ΔPf4 and the ΔPf4 genotype was routinely PCR confirmed prior to experiments using this strain to confirm that re-infection by exogenous Pf4 virions in the laboratory did not occur.

2.5.3 Phage expression constructs

The indicated Pf4 genes or *pfsE* point mutant genes were cloned into the arabinose-inducible expression constructs pHERD20T or pHERD30T (148) were obtained from reference (118) or made by Genewiz (**Table 2-1**). Final constructs were all sequence verified.

2.5.4 Twitch motility assays

Twitching motility was assessed by stab inoculating the indicated strains through a 1.5% LB agar plate to the underlying plastic dish. Agar was supplemented with 0.1% arabinose or antibiotics when appropriate. After incubation for 24 h, the agar was carefully removed, and the zone of motility on the plastic dish was visualized and measured after staining with 0.05% Coomassie brilliant blue, as previously described (149). Twitch zones were measured by placing the plastic dish onto a ruler and imaging with a BioRad GelDoc GO imaging system using preset parameters for Coomassie-stained gels.

2.5.5 Plaque assays

Plaque assays were performed using ΔPf4 or isogenic PAO1 as indicator strains grown on LB plates. Phage in filtered supernatants were serially diluted 10x in PBS and spotted onto lawns of the indicated indicator strain. Plaques were imaged after 18h of growth at 37°C.

2.5.6 Pf4 phage virion quantitation by qPCR

Pf4 virion copy number was measured using qPCR as previously described (121). Briefly, filtered supernatants were treated with DNase I (10 µL of a 10mg/ml stock per mL supernatant) followed by incubation at 70°C for 10 minutes to inactivate the DNase. Ten µL reaction volumes containing 5 µl SYBR Select Master Mix (Life Technologies, Grand Island, NY), 100 nM of primer attR-F and attL-R (**Table 2-2**), and 2 µl supernatant. Primers attR-F and attL-R amplify the re-circularization sequence of the Pf4 replicative form and thus, do not amplify linear Pf4 prophage sequences that may be present in contaminating chromosomal DNA. Cycling conditions were as follows: 50°C 2min, 95°C 2min, (95°C, 15 sec, 60°C 1 minute) x 40 cycles. A standard curve was constructed using plasmids containing the template sequence at a known copy number per milliliter. Pf4 copy numbers were then calculated by fitting Ct values of the unknown samples to the standard curve.

2.5.7 Pf4 virion induction

P. aeruginosa strains PAO1, Δ*intF4*, and Δ*intF4/pfsE* were made competent by 300 mM sucrose washes (150) and electroporated with the arabinose-inducible expression vectors pHERD20T-*xisF4* and pHERD30T-*intF4.* Double transformants were grown in LB supplemented with gentamicin and carbenicillin to an OD_{600} of 0.3 and induced with 0.1% arabinose. Bacteria were grown for 18h, pelleted by centrifugation, and supernatants were filtered through a 0.22μm filter (Millipore Millex GP) followed by DNase treatment. Pf4 virion titers were measured by qPCR, as described above. Pf4 copy numbers in each supernatant were normalized to the same titer by diluting with PBS.

2.5.8 Growth Curves

Overnight cultures were diluted to an OD_{600} of 0.05 in 96-well plates containing LB and if necessary, the appropriate antibiotics. Over the course of 24h, OD_{600} was measured in a CLARIOstar (BMG Labtech) plate reader at 37C with shaking prior to each measurement.

2.5.9 Transmission Electron Microscopy

Cells were grown to mid-log (OD_{600} 0.4), washed with PBS, fixed with 4% formamide, and placed on a grid and negatively stained with uranyl acetate. Cells were imaged on a Hitachi H-7800 120 kV TEM.

2.5.10 Bacterial two-hybrid assays

Bacterial two-hybrid assays were performed as described previously (127). PfsE was cloned into plasmid constructs (pKT25, pUT18C) using relevant primers (**Table 2-2**). *Escherichia coli* BTH101 cells were co-transformed with plasmid constructs containing different sets of genes. Three independent colonies were grown overnight at 30°C in LB media containing the appropriate selection, 2μl of each was plated onto X-gal and MacConkey agar plates containing the appropriate selection and 1mM IPTG and incubated at 30°C for 48 hours. A colour change on both plates indicates an interaction between the genes encoded in the plasmids.

2.5.11 PfsE Modeling

AlphaFold (126) was used to predict the secondary structure of PfsE. The .pdb file was downloaded for PfsE 'model one' and visualized using UCSF ChimeraX (151).

Table 2-1. Bacterial strains, phage, and plasmids used in this study.

Strain	Description	Source
Escherichia coli		
DH5α	New England Biolabs	(116)
S17	λpir-positive strain	(116)

P. aeruginosa		
PAO1	Wild type	(152)
PAO1 Δ*pilA*	Clean deletion of *pilA* from PAO1	(153)
PAO1 Δ*intF4*	Clean deletion of *intF4* from PAO1	(20)
PAO1 Δ*intF4/pfsE*	Clean deletion of *pfsE* from PAO1 Δ*intF4*	This study
PAO1 ΔPf4	Clean deletion of the Pf4 prophage from PAO1	This study
PA14	Wild type	(154)
PAK	Wild type	ATCC 25102
E90	Clinical CF *P. aeruginosa* isolate	(155)
Bacteriophage Strains		
Pf4	Inoviridae	(20)
JBD26	Siphoviridae	(119)
CMS1	Podoviridae	This study
DMS3	Siphoviridae	(156)
OMK01	Myoviridae	(157)
LPS-5	Podoviridae	Felix Biotech
Plasmids		
pHERD20T	AmpR, expression vector with araC-P_{BAD} promoter	(148)
pHERD30T	GmR, expression vector with araC-P_{BAD} promoter	(148)
pHERD30T-*PA0717*	pBAD::*PA0717*	(118)
pHERD30T-*PA0718*	pBAD::*PA0718*	(118)
pHERD30T-*PA0719*	pBAD::*PA0719*	This study
pHERD30T-*PA0720*	pBAD::*PA0720*	(118)
pHERD30T-*pfsE*	pBAD::*pfsE*	(118)
pHERD30T-*PA0722*	pBAD::*PA0722*	This study
pHERD30T-*PA0723*	pBAD::*PA0723*	This study
pHERD30T-*PA0724*	pBAD::*PA0724*	This study
pHERD30T-*PA0725*	pBAD::*PA0725*	(118)
pHERD30T-*PA0726*	pBAD::*PA0726*	This study
pHERD30T-*PA0727*	pBAD::*PA0727*	This study
pHERD30T-*intF4*	pBAD::*intF4*	This study
pHERD20T-*xisF4*	pBAD::*xisF4*	(37)
pKT25	BACTH construct	(127)
pUT18C	BACTH construct	(127)
pHERD20T-*pfsE*	pBAD::*pfsE*	This study
pHERD20T- *pfsE* ^{Y16V}	pBAD:: *pfsE* ^{Y16V}	This study
pHERD20T- *pfsE* ^{W18A}	pBAD:: *pfsE* ^{W18A}	This study
pHERD20T- *pfsE* ^{W20A}	pBAD:: *pfsE* ^{W20A}	This study
pHERD20T- *pfsE* $^{Y16A/W18A/W20A}$	pBAD:: *pfsE* $^{Y16A/W18A/W20A}$	This study

Table 2-2. Primers used in this study

Purpose/Name	***Sequence (5'-3')***
Cloning	
PfsE_p18CFwd	TACGTCTAGAGCTCCGCTATCTCTCGCTGTTCGCGGTAGG
PfsE_p18CRev	TACGGGTACCTCAAACAGTCAGGGAGGCCGCTAGG
PfsE_Y16VFwd	CTGGCCACCGGCGTGGCCTGG
PfsE_Y16VRev	CCAGCCCCAGGCCACGCCGGT
PfsE_W18AFwd	ACCGGCTACGCCGCCGGCTGG

PfsE_W18ARev	TCGATCCAGCCGGCGGCGTAGC
PfsE_W20AFwd	TACGCCTGGGGCGCCATCGACG
PfsE_W20ARev	CTAGGCCGTCGATGGCGCCCCAGG
∆***pfiT primers:***	
attB1-pfiT-UpF	ggggataagtttgtacaaaaaagcaggcttcTTCAACCCGCTCATAGGTT
pfiT-UpR	TCAGGAGTAGAAAGCCATCACATTAAACCTCCTTATTCTGG
PfiT-DownF	TGATGGCTTTCTACTCCTGA
attB2-PfiT-DownR	ggggaccactttgtacaagaaagctgggtaAGCCGCTCAACCCGATCTA
PfiT seq F	CCACACGTTCGCCAGTCACTT
PfiT seq R	AATGCCGGCCACTTCATCGAC
∆***Pf4 primers:***	
Pf4-UpF-GWL	tacaaaaaagcaggctTCTGGGAATACGACGGGGGC
Pf4-UpR-GM	tcagagcgcttttgaagctaattcgGATCCCAATGCAAAAGCCCC
Pf4-DnF-GM	aggaacttcaagatccccaattcgCGTCATGAGCTTGGGAAGCT
Pf4-DnR-GWR	tacaagaaagctgggtTGGCAGCAGACCCAGGACGC
pf4-out F	AGTGGCGGTTATCGGATGAC
pf4-out R	TCATTGGGAGGCGCTTTCAT

2.5.12 Statistical analyses

Differences between data sets were evaluated by an unpaired Student's *t* test, using GraphPad Prism version 5.0 (GraphPad Software, San Diego, CA). P values of < 0.05 were considered statistically significant.

2.6 Acknowledgements

We are grateful to Joe Bondy-Denomy, Adair Borges, and Xiaoxue Wang for sharing the inducible Pf plasmids indicated in Table 1. We thank Paul Turner and Felix Biotechnology, Inc. for sharing phages OMK01 and LPS-5. PRS was supported by NIH grants R01AI138981 and P20GM103546. DWD, JW and PAR were supported by the Intramural Research Program of the National Institute of Allergy and Infectious Diseases, National Institutes of Health.

Chapter 3: Tripartite interactions between filamentous Pf4 bacteriophage, *Pseudomonas aeruginosa*, and bacterivorous nematodes

Caleb M. Schwartzkopf[1], Autumn J. Robinson[1], Mary Ellenbecker[1], Dominick Faith[1], Diane M. Brooks[1], Lincoln Lewerke[2], Ekaterina Voronina[1], Ajai A. Dandekar[2,3], Patrick R. Secor[1#]

[1] Division of Biological Sciences, University of Montana, Missoula, Montana, USA
[2] Department of Microbiology, University of Washington, Seattle, Washington, USA
[3] Department of Medicine, University of Washington, Seattle, Washington, USA
[#] Correspondence: Patrick.secor@mso.umt.edu

Note: My contribution to this work consisted in performing *C. elegans* survival assays with Autumn J. Robinson, measuring pyocyanin abundance, procuring the transcriptional reporter data, and testing *C. elegans* permeability. Proteomics were carried out by Diane M. Brooks and Dominick Faith. The transcriptional reporters were gifts from Lincoln Lewerke and Ajai A. Dandekar upon our request. Mary Ellenbecker and Ekaterina Voronina both assisted with *C. elegans* experiments.

3.1 Abstract

The opportunistic pathogen *Pseudomonas aeruginosa* PAO1 is infected by the filamentous bacteriophage Pf4. Pf4 virions promote biofilm formation, protect bacteria from antibiotics, and modulate animal immune responses in ways that promote infection. Furthermore, strains cured of their Pf4 infection (ΔPf4) are less virulent in animal models of infection. Consistently, we find that strain ΔPf4 is less virulent in a *Caenorhabditis elegans* nematode infection model. However, our data indicate that PQS quorum sensing is activated and production of the pigment pyocyanin, a potent virulence factor, is enhanced in strain ΔPf4. The reduced virulence of ΔPf4 despite high levels of pyocyanin production may be explained by our finding that *C. elegans* mutants unable to sense bacterial pigments through the aryl hydrocarbon receptor are more susceptible to ΔPf4 infection compared to wild-type *C. elegans*. Collectively, our data support a model where suppression of quorum-regulated virulence factors by Pf4 allows *P. aeruginosa* to evade detection by innate host immune responses.

3.2 Introduction

Filamentous bacteriophages (phages) of the Inoviridae family infect diverse bacterial hosts (118, 158). In contrast to other phage families, Inoviruses can establish chronic infections where filamentous virions are produced without killing the bacterial host (6, 17, 159), which may allow a more symbiotic relationship between filamentous phages and the bacterial host to evolve. Indeed, filamentous phages

are often associated with enhanced virulence potential in pathogenic bacteria. For example, the filamentous phage CTXϕ encodes the cholera toxin genes that convert non-pathogenic *Vibrio cholerae* into toxigenic strains (160), the MDAϕ Inovirus that infects *Neisseria gonorrhoeae* acts as a colonization factor and enhances bacterial adhesion to host tissues (21), and the filamentous phage ϕRSS1 increases extracellular polysaccharide production and invasive twitching motility in the plant pathogen *Ralstonia solanacearum* (161).

The filamentous phage Pf4 that infects *Pseudomonas aeruginosa* strain PAO1 enhances bacterial virulence in murine lung (112) and wound (29) infection models. Oxidative stress induces the Pf4 prophage (162) and filamentous virions are produced at high titers, up to 10^{11} virions per mL (111, 113). Pf4 virions serve as structural components of biofilm matrices that protect bacteria from antibiotics and desiccation (20, 112, 130). Pf4 virions also engage immune receptors on macrophages to decrease phagocytic uptake (29, 110) and inhibit CXCL1 signaling in keratinocytes, which interferes with wound re-epithelialization (163). These observations outline the diverse ways that Pf4 virions promote the initiation and maintenance of *P. aeruginosa* infections. However, how Pf4 phages modulate bacterial virulence behaviors is poorly understood.

P. aeruginosa regulates the production of a variety of secreted virulence factors using a cell-to-cell communication system called quorum sensing (QS). As bacterial populations grow, concentrations of QS signaling molecules called autoinducers increase as a function of population density (164). When autoinducer concentrations become sufficiently high, they bind to and activate their cognate receptors, allowing bacterial populations to coordinate gene expression (67, 68). *P. aeruginosa* PAO1 has three QS systems, Las, Rhl, and PQS. Las and Rhl QS systems recognize acyl-homoserine lactone signals while the PQS system recognizes quinolone signals.

In this study, we demonstrate that deleting the Pf4 prophage from *P. aeruginosa* PAO1 (ΔPf4) activates PQS quorum sensing and increases production of the pigment pyocyanin, a potent virulence factor. However, like observations in vertebrate infection models (29, 112), the virulence potential of ΔPf4 is reduced compared to PAO1 in a *Caenorhabditis elegans* nematode infection model. We resolve this apparent controversy and report that *C. elegans* strains lacking the ability to sense bacterial pigments through the aryl hydrocarbon receptor (AhR) are more susceptible to ΔPf4 infection compared to wild-type *C. elegans* capable of detecting bacterial pigments. Collectively, our data support a model where Pf4 suppresses the production of quorum-regulated pigments, allowing *P. aeruginosa* to evade detection by host immune responses.

3.3 Results

3.3.1 Pf4 protect *P. aeruginosa* from *Caenorhabditis elegans* predation

Prior work demonstrates that Pf4 enhances *P. aeruginosa* PAO1 virulence potential in mouse models of infection by modulating innate immune responses (29, 110, 112). Because central components of animal innate immune systems are conserved, we hypothesized that Pf4 would affect *P. aeruginosa* virulence in other animals such as bacterivorous nematodes. To test this hypothesis, we used *Caenorhabditis elegans* nematodes in a slow-killing *P. aeruginosa* infection model were nematodes are maintained on minimal NNGM agar with a bacterial food source for several days (165).

We first confirmed that PAO1 and ΔPf4 grew equally well on NNGM agar without *C. elegans* (**Fig 3-1A**) by homogenizing and resuspending three-day-old bacterial lawns in saline and measuring colony forming units (CFUs) by drop-plate. Resuspended cells were then pelleted by centrifugation and Pf4 virions in supernatants were measured by plaque assay. In the absence of *C. elegans*, neither PAO1 nor ΔPf4 produced any detectable Pf4 virions (**Fig 3-1B**).

Subsequently, we tested the effect of *C. elegans* grazing on PAO1 and ΔPf4. Young adult N2 *C. elegans* were plated onto 24-hour old bacterial lawns and incubated for an additional 48 hours. In the presence of *C. elegans*, PAO1 CFUs were comparable to PAO1 CFUs recovered from lawns grown without *C. elegans* at approximately 10^{10} CFUs/mL (**Fig 3-1C**, black bar, compare to Fig 1A). CFUs recovered from ΔPf4 lawns exposed to *C. elegans* were ~100-fold lower than ΔPf4 lawns grown without *C. elegans* (**Fig 3-1C**), indicating that Pf4 protects *P. aeruginosa* from *C. elegans* predation.

We did not detect Pf4 virions in ΔPf4 lawns exposed to *C. elegans* (**Fig 3-1D**), but we did recover ~1 x 10^6 Pf4 plaque forming units (PFUs) from PAO1 lawns exposed to *C. elegans* (**Fig 3-1D**, black bar). These results indicate that *C. elegans* predation induces Pf4 virion replication.

When filamentous Pf4 virions accumulate in the environment, they enhance *P. aeruginosa* adhesion to mucus and promote biofilm formation (20, 110). Because *P. aeruginosa* colonization of the *C. elegans* digestive track is a primary cause of death in the slow killing model (165), we hypothesized that Pf4 virions may accumulate in the *C. elegans* digestive track. To test this hypothesis, we topically applied 1x10^9 fluorescently labeled Pf4 virions to bacterial lawns and imaged *C. elegans* by fluorescence microscopy after 24 hours of grazing. *Escherichia coli* OP50 were used for these experiments to avoid Pf4 replication and any potential bacterial lysis (Pf4 cannot infect *E. coli* hosts). After 24 hours, Pf4 virions accumulated in the upper intestine of *C. elegans* (**Fig 3-1E**), raising the possibility that Pf4 virions physically block the digestive track, which could increase *C. elegans* killing by *P. aeruginosa*.

When *C. elegans* was challenged with PAO1 in the slow killing model, nematode killing was complete after five days (**Fig 3-1F** black line) whereas complete *C. elegans* killing took eight days when challenged with ΔPf4 (**Fig 3-1F** green line), indicating that Pf4 enhances the virulence potential of *P.*

aeruginosa, consistent with prior work in mice (29, 110, 112). Collectively, these results indicate that *C. elegans* induces Pf4 replication and that Pf4 protects *P. aeruginosa* from *C. elegans* predation.

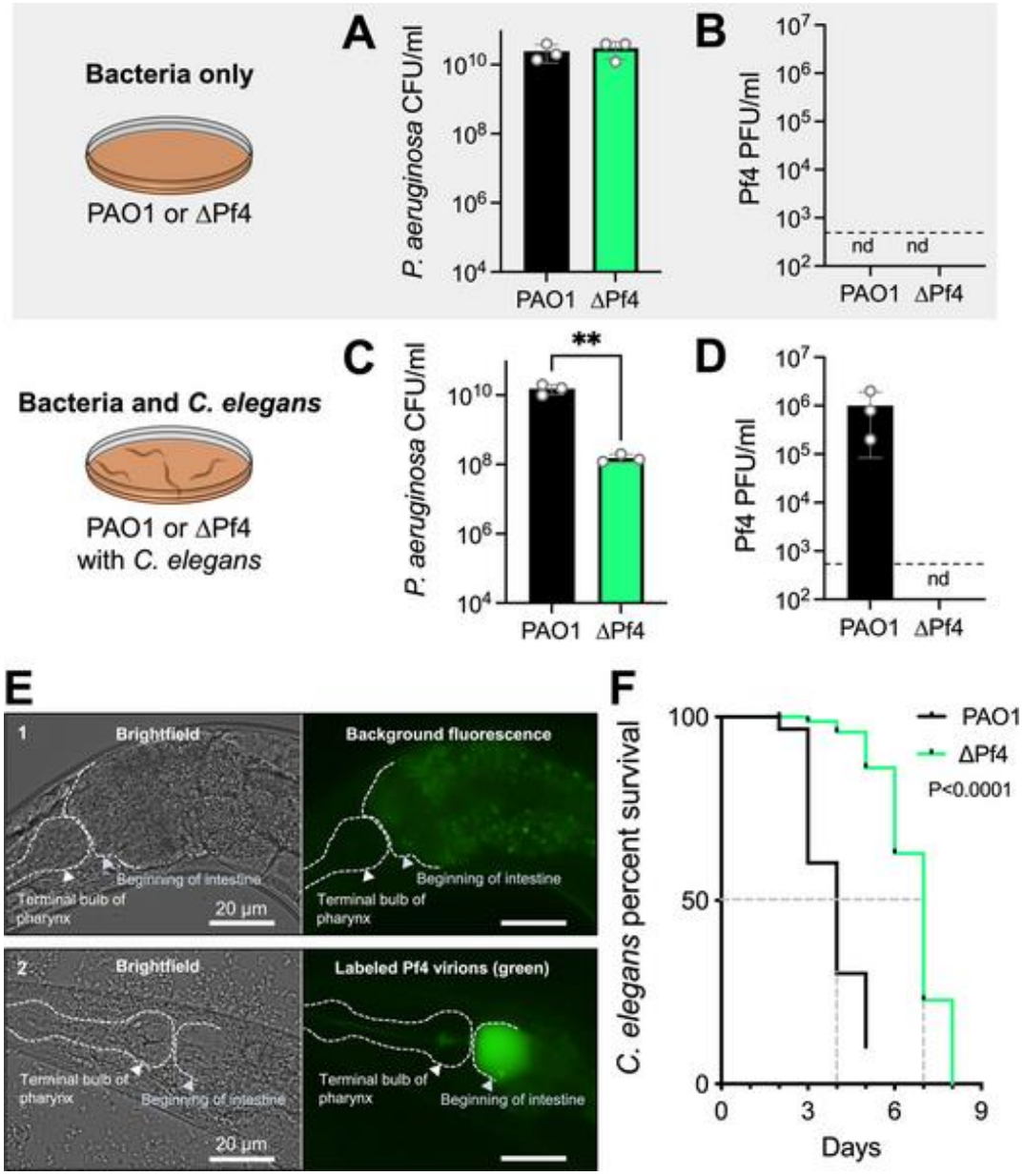

Figure 3-1. *C. elegans* predation induces Pf4 replication and enhances *P. aeruginosa virulence*. **(A-D)** Bacterial CFUs and Pf4 PFUs were enumerated after three days in the absence (A-B) or presence (C-D) of *C. elegans*. nd, not detected (below detection limit of 333 PFU/mL indicated by dashed line). Results are the mean ±SD of three experiments, **P<0.01, Student's *t*-test. **(E)** Wild-type N2 *C. elegans* were maintained on lawns of 1) *E. coli* OP50 (non-pathogenic nematode food) or 2) OP50 supplemented with 10^9 Pf4 virions labeled with Alexa-fluor 488 (green). Representative brightfield and fluorescent images after 24 hours are shown. **(F)** Kaplan-Meier survival curve analysis of *C. elegans* exposed to *P. aeruginosa*. N=90 worms per condition (three replicate experiments of 30 worms each). The mean survival of *C. elegans* maintained on lawns of PAO1 was four days compared to seven days for nematodes maintained on lawns of ΔPf4 (dashed gray lines). Note that worms that may have escaped the dish rather than died were withdrawn from the study, explaining why the black PAO1 line does not

reach zero percent survival.

3.3.2 PQS quorum sensing is activated and pyocyanin production enhanced in ΔPf4

During routine propagation of *P. aeruginosa*, we noted that production of the green pigment pyocyanin (**Fig 3-2A**) was significantly (P<0.003) higher in ΔPf4 compared to PAO1 (**Fig 3-2B and C**). Pyocyanin is a redox-active phenazine that shuttles electrons to distal electron acceptors, which enhances ATP production and generates proton-motive force in *P. aeruginosa* cells living in anoxic environments (166, 167). The redox activity of pyocyanin also makes it a potent virulence factor that passively diffuses into phagocytes and kills them by redox cycling with NAD(H) to generate reactive oxygen species that indiscriminately oxidize cellular structures (168).

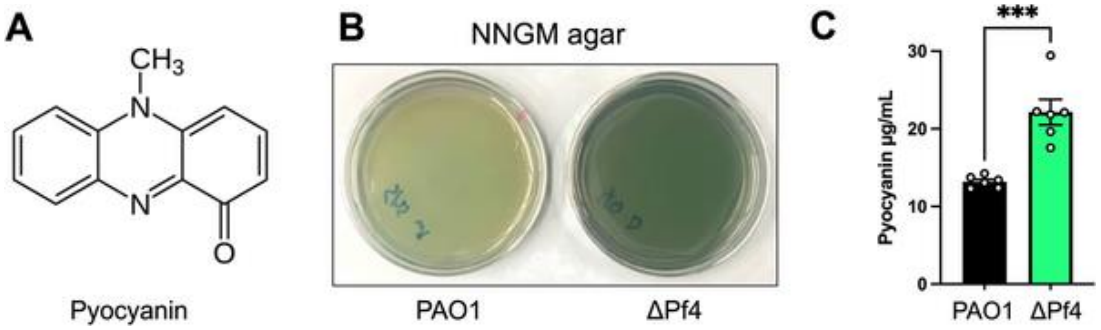

Figure 3-2. Pyocyanin production is enhanced in ΔPf4 compared to PAO1. (A) The structure of pyocyanin, a redox-active green pigment produced by *P. aeruginosa*. **(B)** Representative images of PAO1 and ΔPf4 growing on NNGM agar plates after 24 hours at 37°C. **(C)** Pyocyanin was chloroform-acid extracted from NNGM agar plates, absorbance measured (520 nm), and values converted to µg/mL. Data are the mean ±SEM of six replicate experiments. ***P<0.003, Student's *t*-test.

Expression of many *P. aeruginosa* virulence genes, including the phenazine biosynthesis genes responsible for pyocyanin production, are regulated by quorum sensing (72, 73, 89, 169-173). We used fluorescent transcriptional reporters to measure Las (P_{rsaL}::*gfp*), Rhl (P_{rhlA}::*gfp*), and PQS (P_{pqsA}::*gfp*) quorum sensing (174-176). In ΔPf4, regulation of Las and Rhl gene targets was not significantly different from PAO1 after 18 hours of growth **(Fig 3-3A and B**). However, PQS activity in ΔPf4 was significantly (P<0.001) higher compared to PAO1 after 18 hours (**Fig 3-3C**). Fluorescence was not detected in empty vector controls (**Fig 3-3D**). These results suggest that loss of the Pf4 prophage upregulates PQS quorum sensing, causing pyocyanin to be overproduced.

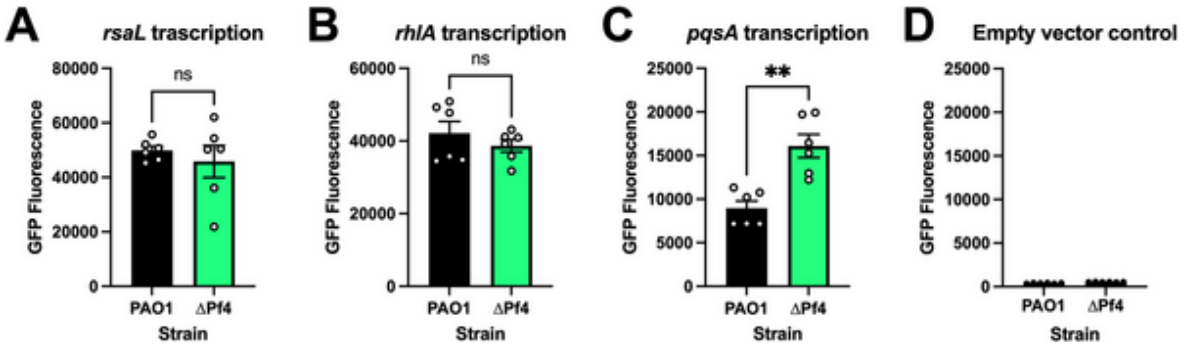

Figure 3-3. PQS quorum sensing is upregulated in *P. aeruginosa* ΔPf4. GFP fluorescence from the transcriptional reporters (**A**) P_{rsaL}-*gfp*, (**B**) P_{rhlA}-*gfp*, (**C**) P_{pqsA}-*gfp* and (**D**) P_{empty}-*gfp* was measured in PAO1 (black) or ΔPf4 (green) at 18 hours in cultures growing in lysogeny broth. For each measurement, GFP fluorescence was corrected for bacterial growth (OD_{600}). Data are the mean ±SEM of six replicates. **P<0.001, Student's *t*-test.

3.3.3 Quantitative proteomics analysis of *C. elegans* exposed to PAO1 or ΔPf4

To gain insight into how Pf4 might affect *C. elegans* responses to *P. aeruginosa*, we performed mass spectrometry-based quantitative proteomics on *C. elegans.* To avoid progeny contamination, we used the *rrf-3(−); fem-1(−)* genetic background that is sterile at temperatures above 25°C (177). Like wild-type N2 nematodes, PAO1 killed the *rrf-3(−); fem-1(−)* strain significantly (P<0.001) faster than ΔPf4 in the slow killing model (**Fig 3-S1**). Nematodes were maintained for two days on lawns of PAO1 or ΔPf4. This timepoint was selected because most *C. elegans* were still alive in both groups (**Fig 3-1F; Fig 3-S1**). Whole nematodes were collected (~320 per replicate, N=4), washed, and proteins purified. Proteins were digested with trypsin and tandem mass tags were used to uniquely label peptides from each biological replicate, allowing all samples to be pooled, fractionated, and analyzed by mass spectrometry in a single run. This approach allows direct and quantitative comparisons between groups.

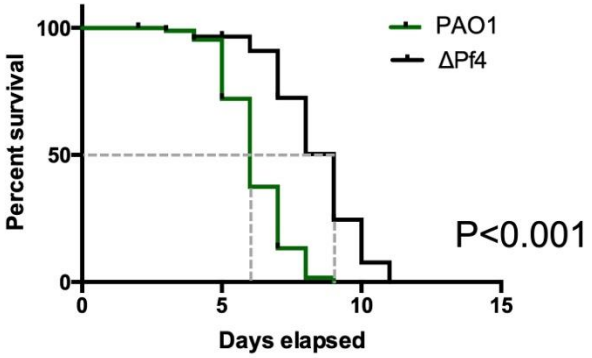

Figure 3-S1. Survival analysis of sterile *rrf-3(-); fem-1(-) C. elegans* challenged with *P. aeruginosa* PAO1 or ΔPf4. Kaplan–Meier survival analysis of N=90 worms per condition (three replicate experiments of 30 worms each) were monitored daily for death. The mean survival of *rrf-3(-); fem-1(-) C. elegans* maintained on lawns of PAO1 was six days compared to nine days for nematodes maintained on lawns of ΔPf4 (dashed gray lines).

We identified 410 proteins that were significantly (P<0.05) up or down regulated at least 1.5-fold (log_2 fold change ≥0.58) in *C. elegans* exposed to ΔPf4 compared to PAO1 (**Fig 3-4A, Supplemental Table S1 found in manuscript**). Enrichment analysis revealed proteins associated with mitochondrial respiration and electron transport were significantly (FDR<0.002) enriched in upregulated proteins (**Fig 3-4B**). As pyocyanin is a redox-active virulence factor known to interfere with mitochondrial respiration (178, 179), these results suggest that respiration is perturbed in *C. elegans* grazing on ΔPf4 lawns that over-produce pyocyanin.

We also noted that proteins associated with muscle cell differentiation and organization were enriched in *C. elegans* challenged with ΔPf4 (**Fig 3-4C**), which could be related to a decline in motility observed in *C. elegans* as they begin to succumb to *P. aeruginosa* infection (165).

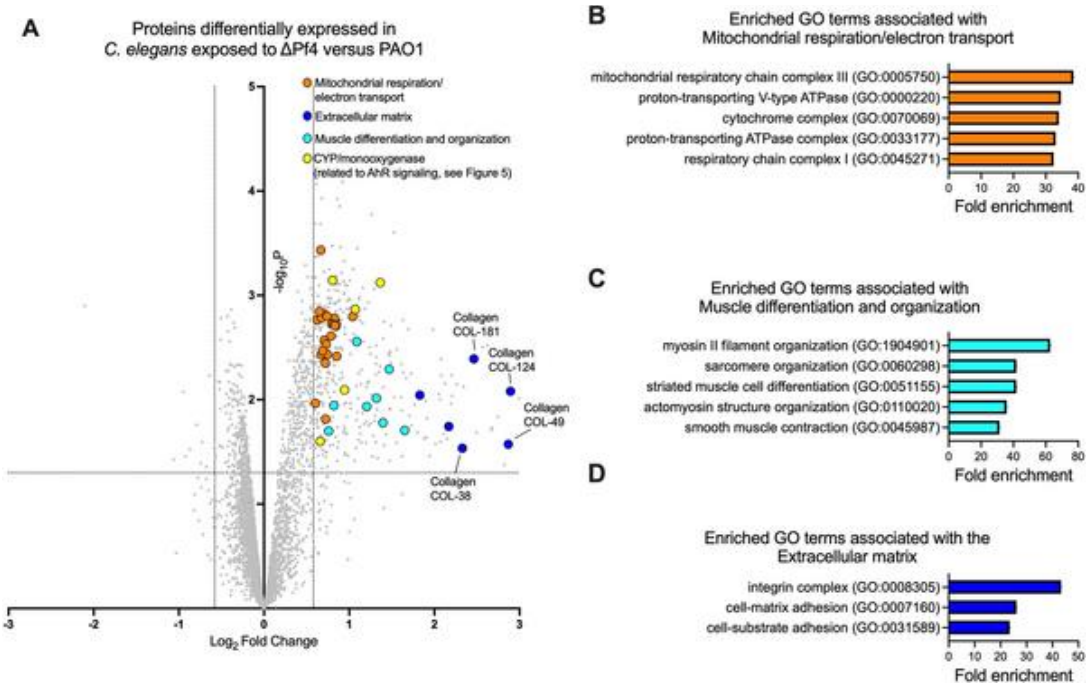

Figure 3-4. Pf4 modulates expression of *C. elegans* proteins associated with respiration, the extracellular matrix, and motility. (A) Volcano plot showing differentially expressed proteins in *C. elegans* maintained on lawns of ΔPf4 compared to *C. elegans* maintained on lawns of PAO1 for three days. The dashed lines indicate proteins with expression levels greater than ±1.5-fold and a false discovery rate (FDR) <0.05. Results are representative of quadruplicate experiments. **(B-D)** Enrichment analysis of significant upregulated proteins shown in (A). Fold enrichment of observed proteins associated with specific Gene Ontology (GO) terms each had an FDR of <0.002.

In *C. elegans* exposed to ΔPf4, proteins associated with the extracellular matrix (e.g., collagen) were also significantly enriched (**Fig 3-4A,** dark blue symbols; **Fig 3-4D**). The tough extracellular cuticle of *C. elegans* is composed predominantly of cross-linked collagen (180). Because PAO1 kills *C. elegans* faster than ΔPf4 (**Fig 3-1F**), lower collagen abundance in PAO1-exposed *C. elegans* may be

an indication of compromised cuticle integrity. To test this, we assessed cuticle integrity in synchronized young adult worms collected from lawns of PAO1 or ΔPf4 after two days and stained with 10 µg/mL Hoechst. Nematodes where stained nuclei were observed were scored as permeable and cuticle integrity compromised (**Fig 3-5A**) whereas worms without stained nuclei were scored as non-permeable with an intact cuticle (**Fig 3-5B**). We find that *C. elegans* cuticle permeability is significantly (P<0.01) higher in *C. elegans* exposed to PAO1 compared to *C. elegans* exposed to ΔPf4 (**Fig 3-5C**). These results correlate with the lower relative collagen protein abundance observed in *C. elegans* exposed to PAO1 compared to ΔPf4 (**Fig 3-4A**) and are consistent with a loss of cuticle integrity and higher morbidity of *C. elegans* exposed *P. aeruginosa* lysogenized by filamentous Pf4 phage.

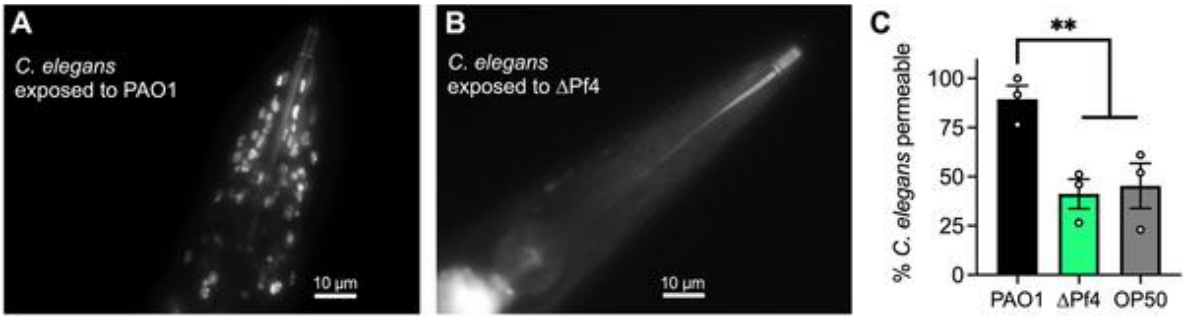

Figure 3-5. PAO1 compromises *C. elegans* cuticle integrity compared to ΔPf4. Synchronized young adult N2 worms were collected from lawns of PAO1, ΔPf4, or *E. coli* OP50 after 48 hours and stained with the nucleic acid stain Hoechst. Cuticle permeability was assessed by visualization of stained nuclei in live nematodes exposed to **(A)** PAO1 or **(B)** ΔPf4. Representative images are shown. **(C)** The percent *C. elegans* with stained nuclei were scored as permeable and plotted. **P<0.01, Student's *t*-test. N=3 replicates of 25-50 animals per replicate, 92-137 total worms per group.

3.3.4 *C. elegans* aryl hydrocarbon receptor signaling regulates antibacterial defense

Compared to PAO1, ΔPf4 produces more of the virulence factor pyocyanin (and likely other quorum-regulated virulence factors). However, ΔPf4 is less virulent in mouse lung (112), wound (29), and *C. elegans* infection models (**Fig 3-1F**). How is it that the ΔPf4 strain that produces more virulence factor is less virulent in animal models of infection?

Prior work demonstrates that vertebrate immune systems can sense *P. aeruginosa* aromatic pigments such as pyocyanin via the aryl hydrocarbon receptor (AhR) pathway (181, 182). AhR is a highly conserved eukaryotic transcription factor that binds a variety of aromatic hydrocarbons and regulates metabolic processes that degrade xenobiotics and coordinate immune responses (181, 182). In vertebrates, AhR's ability to detect pyocyanin and other bacterial pigments provides the host a way to monitor bacterial burden and mount appropriate immune countermeasures (182, 183).

Furthermore, AhR regulates the expression of numerous cytochrome P450 (CYP) enzymes in

both vertebrates (184) and in *C. elegans* (185) that participate in xenobiotic degradation. In our proteomics dataset, we identified five CYP proteins (CYP-29a2, CYP-25a2, CYP-14a5, CYP-37a1, and CYP-35b1) that were significantly upregulated in *C. elegans* exposed to ΔPf4 (**Fig 3-4A**, yellow symbols).

Based on these observations, we hypothesized that AhR signaling would increase *C. elegans* fitness against the pyocyanin over-producing ΔPf4 strain. To test this, we challenged wild-type N2 *C. elegans* or an AhR-null mutant (*ahr-1(ia3)*) with PAO1 or ΔPf4 in the slow killing model. We also included *P. aeruginosa* Δ*pqsA*, a strain where PQS signaling is disabled and pyocyanin production abolished (186). Δ*pqsA* is far less virulent against *C. elegans* compared to wild-type *P. aeruginosa* (**Fig 3-6A-D**, compare black to red), consistent with prior work (187). Disabling AhR signaling in *C. elegans* does not significantly affect nematode survival when challenged with Δ*pqsA* (**Fig 3-6C and D**). This contrasts with the ΔPf4 mutant where disabling AhR signaling significantly (P=0.0002) increases ΔPf4 virulence compared to wild-type nematodes (**Fig 3-6E and F**).

These results indicate that even though pigment production is impaired in Δ*pqsA*, additional virulence determinants are inactivated in the Δ*pqsA* mutant. The results also raise the possibility that the Pf4 prophage is targeted in its inhibition of PQS or other pathways that regulate pigment biosynthesis whose products may be sensed by AhR.

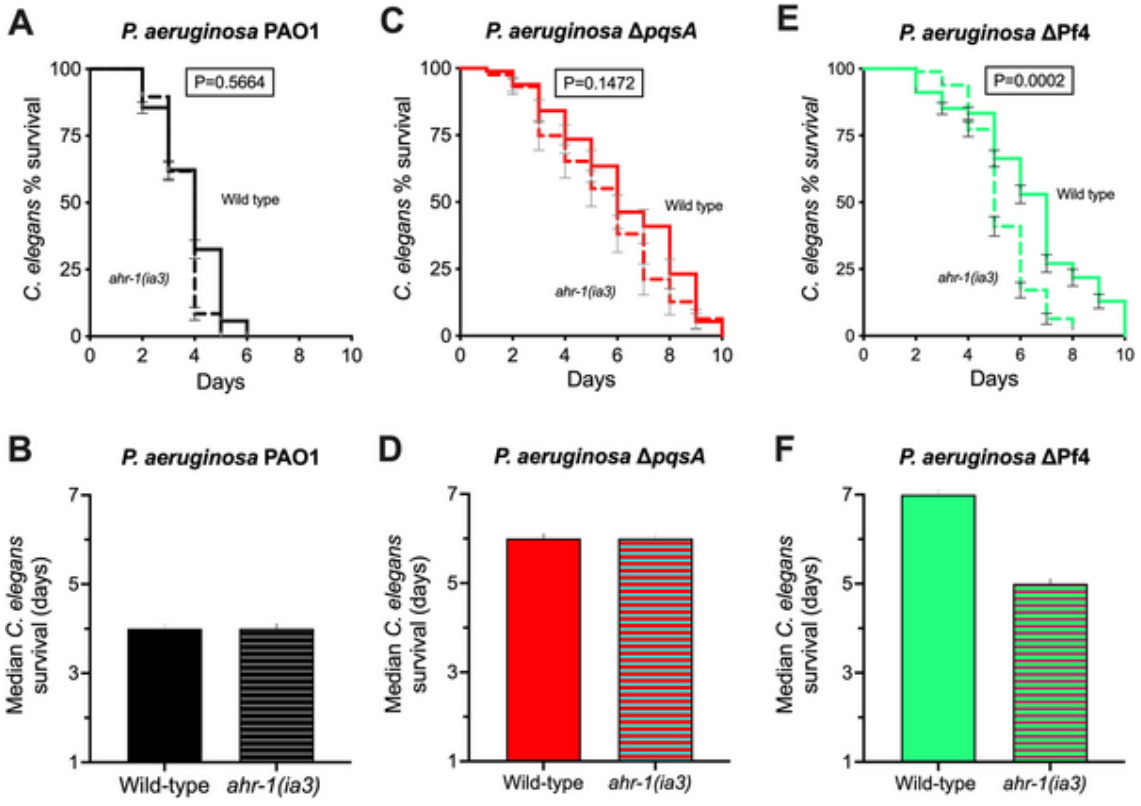

Figure 3-6. Inactivation of AhR signaling in *C. elegans* enhances ΔPf4 virulence. (A, C, and E) Kaplan-Meier survival curve analysis (Log-rank) of wild-type N2 or isogenic *ahr-1(ia3) C. elegans* maintained on lawns of *P. aeruginosa* PAO1, Δ*pqsA*, or ΔPf4 for the indicated times. N=3 groups of 90 animals per condition (270 animals total per condition). Error bars represent standard error of the mean. P-values of pairwise log-rank survival curve analyses are shown. **(B, D, and F)** The median survival of *C. elegans* in days was plotted for each group.

3.4 Discussion

Here, we characterize tripartite interactions between filamentous phage, pathogenic bacteria, and bacterivorous nematodes. Our work supports a model where Pf4 phage suppress *P. aeruginosa* PQS quorum sensing and reduce pyocyanin production, allowing *P. aeruginosa* to evade detection by AhR (**Fig 3-7**).

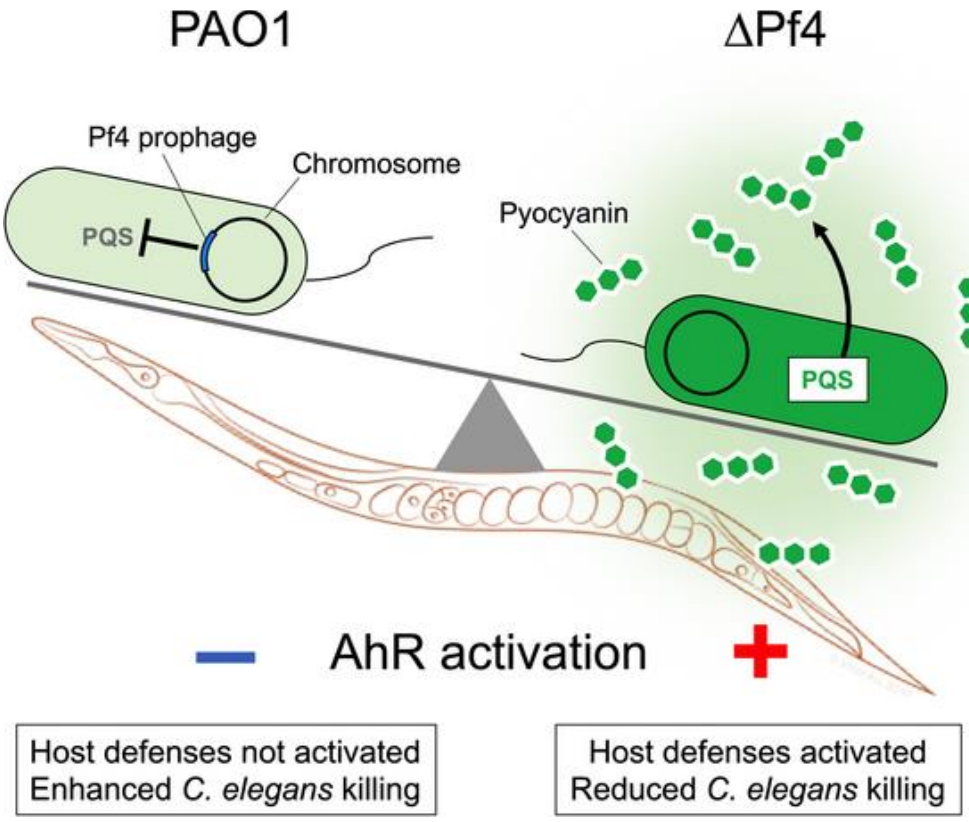

Figure 3-7. Proposed model. Pf4 suppresses the production of quorum-regulated pigments by *P. aeruginosa* allowing bacteria to evade AhR-mediated immune responses in *C. elegans*.

Many phages modulate bacterial quorum sensing systems (105, 106). Examples in *P. aeruginosa* include phage DMS3, which encodes a quorum-sensing anti-activator protein called Aqs1 that binds to and inhibits LasR (51). Another *P. aeruginosa* phage called LUZ19 encodes Qst, a protein that binds to and inhibits the PqsD protein in the PQS signaling pathway (107). In both cases, it is

thought that inhibition of *P. aeruginosa* quorum sensing makes the bacterial host more susceptible to phage infection.

Our finding that PQS signaling is upregulated when the Pf4 prophage is deleted suggests that Pf4 encodes proteins that inhibit PQS signaling. The Pf4 prophage encodes a 5' retron element (188) and a 3' toxin-antitoxin pair (147) and these elements may be acting upon host quorum sensing systems. Another possible mechanism involves genes in the Pf core genome as there are still several with unknown function (e.g., *PA0717-PA0720*).

In the absence of *C. elegans*, PAO1 produces significantly less pyocyanin compared to ΔPf4 and infectious Pf4 virions are not simultaneously produced under these conditions. This indicates that the Pf4 prophage can modulate quorum-regulated pigment production during lysogeny when infectious Pf4 virions are not produced. When *C. elegans* are present, however, Pf4 replication is induced and Pf4 virions appear to accumulate in the *C. elegans* intestine. Pf4 virions are known to promote *P. aeruginosa* biofilm formation and colonization of mucosal surfaces (20, 110, 189). It is possible that Pf4 virions may contribute to *P. aeruginosa* colonization of the *C. elegans* intestine, which is a primary cause of *C. elegans* death in the slow killing model (165).

Our study had some limitations. For example, we only measured pyocyanin production by *P. aeruginosa*. Although pyocyanin is often used as an indicator of *P. aeruginosa* virulence potential (94, 190), there are many other factors that contribute to *P. aeruginosa* virulence, such as hydrogen cyanide (94). We also only used well-defined laboratory strains of *P. aeruginosa* and *C. elegans*. While our study suggests that Pf phages may be broad modulators of bacterial virulence, to accurately predict how different *P. aeruginosa* strains (e.g., clinical vs. environmental) might be affected by Pf, future work is required to characterize the effects various Pf strains have on QS systems in different *P. aeruginosa* hosts. One indication that Pf phages may behave differently in various bacterial hosts are variances in QS hierarchies in different *P. aeruginosa* isolates (191). As quorum sensing can be rewired (e.g., Las dominant verses Rhl dominant hierarchies, (155, 174)), it would not be surprising that Pf phage modulate different behaviors in different *P. aeruginosa* hosts.

Our results support a role for AhR signaling in modulating *C. elegans* sensitivity to *P. aeruginosa* infection. Studies in vertebrates reveal that AhR serves as a pattern recognition receptor that senses aromatic bacterial pigments like pyocyanin to initiate appropriate immune responses (181, 182). However, AhR recognizes a diverse array of ligands and modulation of inflammatory responses by AhR is context specific. For example, exposure of airway epithelial cells to combustion products induces pro-inflammatory AhR-dependent responses (192) while activation of AhR by tryptophan metabolites derived from commensal bacteria in the gut is associated with anti-inflammatory responses and maintenance of intestinal barrier integrity (193). Our proteomics dataset and survival assays

suggest that cuticle integrity is be compromised in *C. elegans* exposed to PAO1 compared to ΔPf4. An interesting research direction would be to link activation of AhR signaling by bacterial pigments to enhanced cuticle integrity as a potential defense mechanism in nematodes.

In addition to AhR, *C. elegans* has other mechanisms to detect bacterial pigments. In environments illuminated with white light, *C. elegans* can discriminate the distinctive blue-green color of pyocyanin to avoid *P. aeruginosa* (194). Our studies were performed predominantly in dark environments; future investigations on how Pf4 may affect *C. elegans* spectral sensing of pathogenic bacteria would be interesting. The existence of multiple bacterial pigment detection mechanisms in *C. elegans* highlights the importance of bacterial pigment detection in nematode survival.

Overall, our study provides evidence that Pf4 phage enhance bacterial fitness against *C. elegans* predation. Prior work demonstrates that Pf4 phage also enhance bacterial fitness against phagocytes by inhibiting phagocytic uptake (29, 110). In the environment, nematodes and other bacterivores such as amoeba can impose high selective pressures on bacteria (195-197). The ability of Pf phage to enhance *P. aeruginosa* fitness against environmental bacterivores may help explain why Pf prophages are so widespread amongst diverse *P. aeruginosa* strains (17, 31, 198). The ability of Pf phage to enhance bacterial fitness against bacterivores in the environment may also translate to increased virulence potential in vertebrate hosts, including humans.

3.5 Materials and Methods:

3.5.1 Strains, plasmids, and growth conditions

Strains, plasmids, and their sources are listed in **Table 3-1.** Unless otherwise indicated, bacteria were grown in lysogeny broth (LB) at 37 °C with 230 rpm shaking and supplemented with antibiotics (Sigma) where appropriate. Unless otherwise noted, gentamicin was used at the at either 10 or 30 µg ml^{-1}.

3.5.2 Plaque assays

Plaque assays were performed using ΔPf4 as the indicator strain grown on LB plates. Phage in filtered supernatants were serially diluted 10x in PBS and spotted onto lawns of ΔPf4 strain. Plaques were imaged after 18h of growth at 37°C. PFUs/mL were then calculated.

3.5.3 Pyocyanin extraction and measurement

Pyocyanin was measured as described elsewhere (199, 200). Briefly, 18-hour cultures were treated by adding chloroform to a total of 50% culture volume. Samples were vortexed vigorously and the different phases separated by centrifuging samples at 6,000xg for 5 minutes. The chloroform layer (dark blue if pyocyanin present) was removed to a fresh tube and 20% the volume of 0.1 N HCl was added and the mixture vortexed vigorously (if pyocyanin is present, the aqueous acid solution turns pink). Once the two layers were separated, the aqueous layer was removed to a fresh tube and absorbance measured at 520 nm. The concentration of pyocyanin in the culture supernatant, expressed as µg/ml, was obtained by multiplying the optical density at 520 nm by 17.072, as described (200).

3.5.4 Quorum sensing reporters

Competent *P. aeruginosa* PAO1 and ΔPf4 were prepared by washing overnight cultures in 300 mM sucrose followed by transformation by electroporation (201) with the plasmids CP1 Blank-PBBR-MCS5, CP53 PBBR1-MCS5 *pqsA*-gfp, CP57 PBBR1-MCS5 *rhlA*-gfp, CP59 PBBR1-MCS5 *rsaL*-gfp listed in **Table 3-1**. Transformants were selected by plating on the appropriate antibiotic selection media. The indicated strains were grown in buffered LB containing 50 mM MOPS and 100 µg ml^{-1} gentamicin for 18 hours. Cultures were then sub-cultured 1:100 into fresh LB MOPS buffer and grown to an OD_{600} of 0.3. To measure reporter fluorescence, each strain was added to a 96-well plate containing 200 µL LB MOPS with a final bacterial density of OD_{600} 0.1 and incubated at 37˚C in a CLARIOstar BMG LABTECH plate-reader. Prior to each measurement, plates were shaken at 230 rpm for a duration of two minutes. A measurement was taken every 15 minutes for both growth (OD_{600}) or

fluorescence (excitation at 485-15 nm and emission at 535-15 nm).

Table 3-1. Bacterial strains, phage, and plasmids used in this study.

Strain	Description	Source
Escherichia coli		
DH5α	Cloning strain	New England Biolabs
P. aeruginosa		
PAO1	Wild type	(112)
PAO1 ΔPf4	Deletion of the Pf4 prophage from PAO1	(112)
Bacteriophage Strains		
Pf4	Inovirus	(20)
C. elegans		
N2	Wild type	*Caenorhabditis* Genetic Center
ZG24	AhR null mutant *ahr-1(ia3)*	(202)
CF512	Temperature-sensitive sterile background *rrf-3(b26) II; fem-1(hc17) IV*	(177)
Plasmids		
CP59 pBBR1-MCS5 *rsaL-gfp*	GFP *lasI* transcriptional reporter	(176)
CP57 pBBR1-MCS5 *rhlA-gfp*	GFP *rhlA* transcriptional reporter	(176)
CP53 pBBR1-MCS5 *pqsA-gfp*	GFP *pqsA* transcriptional reporter	(175)
CP1 pBBR-MCS5-Blank	GFP empty vector control	(176)

3.5.5 *C. elegans* slow killing assay

Synchronized adult N2, *ahr-1(ia3),* or *rrf-3(-); fem-1(-) C. elegans* were plated on normal nematode growth media (NNGM) plates with 30 nematodes for each indicated lawn of *P. aeruginosa* and incubated at 30˚C. Over the course of the assay, nematodes were passaged onto new plates of 24-hour-old *P. aeruginosa* lawns daily and counted. Nematodes were counted as either alive or dead with missing nematodes being withdrawn from the study. The study was ended when all nematodes were either dead or missing.

3.5.6 Preparation of fluorescently tagged Pf4 virions

P. aeruginosa ΔPf4 was grown in LB broth to an OD_{600} of 0.5 at 37°C in a shaking incubator (225 rpm). Five µL of a Pf4 stock containing $5x10^9$ PFU/mL were used to infect the culture. After growing overnight (18h) in the 37°C shaking incubator, bacteria were removed by centrifugation (12,000 xg, 5 minutes, room temperature) and supernatants filtered through a 0.2 µm syringe filter. Pf4 virions were PEG precipitated by adding NaCl to the filtered supernatants to a final concentration of 0.5

M followed by the addition of PEG 8k to a final concentration of 20% w/vol. After incubating at 4°C for four hours, the supernatants became noticeably turbid. At this time, phage were pelleted by centrifugation (15,000 xg, 15 minutes, 4°C), the pellet gently washed in PBS, centrifuged again, and the phage pellet resuspended in 1 mL 0.1 M sodium bicarbonate buffer, pH 8.3. Virions were then labeled with 100 µg of Alexa Fluor 488 TFP ester following the manufacturer's instructions (ThermoFisher). Unincorporated dyes were separated from labeled virions using PD-10 gel filtration columns. PBS was used to elute labeled phages from the column. Titers of labeled phages were measured by qPCR using our published protocol (203). Labeled phages were aliquoted and stored at -20°C.

3.5.7 Fluorescent imaging of nematodes

Approximately 10^9 Alexa Fluor 488-labeled Pf4 virions in 200 µL PBS were added evenly to 24-hour old *E. coli* OP50 lawns growing on NNGM agar. Plates were incubated at 30°C for 30 minutes and synchronized adult N2 *C. elegans* were plated. Routine analysis of *C. elegans* by fluorescence/light microscopy was performed after 24 hours by transferring nematodes to a 5% agarose pad containing levamisole (250 mM), a nematode paralytic agent that enables imaging. Nematodes were examined and imaged using a Leica DFC300G camera attached to a Leica DM5500B microscope.

3.5.8 Protein extraction from *C. elegans*

Proteins were extracted from *rrf-3(-); fem-1(-) C. elegans* as described (204). Briefly, after *P. aeruginosa* exposure for two days, ~320 *C. elegans* were harvested from NMMG plates into 1.5 mL tubes containing 1 mL PBS. Nematodes were gently mixed by hand, pelleted by centrifugation, and resuspended in 1 mL fresh PBS. *C. elegans* were again pelleted and supernatants were discarded, pellets were weighed and frozen at -80°C until proteins were ready to be harvested. Pellets were suspended in reassembly buffer (RAB, 0.1M MES, 1mM EGTA, 0.1mM EDTA, 0.5mM $MgSO_4$, 0.75M NaCl, 0.2M NaF, pH7.4) containing Pierce Protease Inhibitor (ThermoScientific, A32965). Samples were sonicated on ice for 10 cycles of a 2 second pulse with 10 seconds rest between pulses. After 2 minutes rest, sonication was repeated for a total of 8 cycles of 10 x 2 second pulses. Lysates were centrifuged at 20,000xg for 30 minutes at 4°C. Supernatants were transferred to fresh tubes and concentrated to approximately 2µg/µL using 10kDa molecular weight cut off spin columns (VivaSpin 500, Sartorius, VS0102). Protein concentration was determined using a Bradford assay. After visualizing protein integrity by SDS-PAGE (**Fig S2A Not in this manuscript**), 200 µg total protein for each of the four biological replicates for each treatment were sent to the IDeA National Resource for Quantitative Proteomics Center for proteomic analysis.

3.5.9 Mass spectrometry-based quantitative proteomics

Total protein (200 µg) from each sample was reduced, alkylated, and purified by chloroform/methanol extraction prior to digestion with sequencing grade modified porcine trypsin (Promega). Tandem mass tag isobaric labeling reagents (Thermo) were used to label tryptic peptides following the manufacturer's instructions. Labeled peptides were combined into one 16-plex TMTpro sample group that was separated into 46 fractions on a Acquity BEH C18 column (100 x 1.0 mm, Waters) using an UltiMate 3000 UHPLC system (Thermo). Peptides were eluted by a 50 min gradient from 99:1 to 60:40 buffer A:B ratio (Buffer A = 0.1% formic acid, 0.5% acetonitrile. Buffer B = 0.1% formic acid, 99.9% acetonitrile). Fractions were consolidated into 18 super-fractions which was further separated by reverse phase XSelect CSH C18 2.5 um resin (Waters) on an in-line 150 x 0.075 mm column. Peptides were eluted using a 75 min gradient from 98:2 to 60:40 buffer A:B ratio. Eluted peptides were ionized by electrospray (2.4 kV) followed by mass spectrometric analysis on an Orbitrap Eclipse Tribrid mass spectrometer (Thermo) using multi-notch MS3 parameters. MS data were acquired using the FTMS analyzer over a range of 375 to 1500 m/z. Up to 10 MS/MS precursors were selected for HCD activation with normalized collision energy of 65 kV, followed by acquisition of MS3 reporter ion data using the FTMS analyzer over a range of 100-500 m/z. Proteins were identified and quantified using MaxQuant (Max Planck Institute) TMT MS3 reporter ion quantification with a parent ion tolerance of 2.5 ppm and a fragment ion tolerance of 0.5 Da.

3.5.10 Proteomics data analysis

Prior to data analysis, datasets (**Supplementary Table S1 found in manuscript**) were subjected to and passed quality control procedures. To assess if there are more missing values than expected by random chance in one group compared to another, peptide intensity values were Log_2-transformed (**Fig S2B found in manuscript**). Peptide intensities were comparable across all groups. Principal component analysis (PCA) shows that biological replicates cluster within groups (**Fig S2C found in manuscript**). The normalized Log_2 cyclic loess MS3 reporter ion intensities for TMT for the reference *P. aeruginosa* PAO1 proteome (UniprotKB: UP000002438) were compared between wild-type *P. aeruginosa* PAO1 and *P. aeruginosa* PAO1 ΔPf4 conditions. Proteins with ≥ 1.5-fold change (≥ 0.58 log_2FC) and P values < 0.05 were considered significantly differential. Functional classification and Gene Ontology (GO) enrichment analysis were performed using PANTHER classification system (http://www.pantherdb.org/) (205). Analysis results were plotted with GraphPad Prism version 9.4.1 (GraphPad Software, San Diego, CA).

3.5.11 *C. elegans* cuticle permeability assay

Cuticle integrity was assessed by Hoechst 33342 staining of nuclei in whole nematodes, as previously described (206). Briefly, synchronized young adult N2 worms were collected from lawns of PAO1 or ΔPf4 after two days and stained with 10 µg/mL Hoechst 33342 for 30 minutes at room temperature. Unbound stain was removed by washing nematodes with M9 buffer before visualization by fluorescence microscopy using a DAPI filter. Fluorescent images were acquired with a Leica DFC300G camera attached to a Leica DM5500B microscope. All nematodes where stained nuclei were observed were scored as permeable and cuticle integrity compromised.

3.5.12 Statistical analyses

Differences between data sets were evaluated with a Student's *t*-test (unpaired, two-tailed) where appropriate. P values of < 0.05 were considered statistically significant. Survival curves were analyzed using the Kaplan–Meier survival analysis tool. Individual nematodes that were not confirmed dead were removed from the study. The Bonferroni correction for multiple comparisons was used when comparing individual survival curves. GraphPad Prism version 9.4.1 (GraphPad Software, San Diego, CA) was used for all analyses.

3.6 Acknowledgements

We thank Dr. Paul Bollyky and Dr. Laura Jennings for valuable discussions and critical reading of the manuscript. PRS is supported by NIH grants R01AI138981 and P30GM140963. AAD is supported by NIH grant R01GM125714. *C. elegans* strains were provided by the *Caenorhabditis* Genetics Center, which is funded by NIH Office of Research Infrastructure Programs (P40OD010440). The IDeA National Resource for Quantitative Proteomics Center is supported by NIH grant R24GM137786.

Chapter 4: A dual-function filamentous Pf bacteriophage protein inhibits PQS quorum sensing in *Pseudomonas aeruginosa*

Caleb M. Schwartzkopf[1], Véronique L. Taylor[2], Marie-Christine Groleau[3], Amelia K. Schmidt[1], Dominick R. Faith[1], Eric Déziel[3], Karen Maxwell[2], and Patrick R. Secor[1#]

[1] Division of Biological Sciences, University of Montana, Missoula, Montana, USA
[2] Department of Biochemistry, University of Toronto, Toronto, Ontario, Canada
[3] Institut National de la Recherche Scientifique, Montreal, Québec, Canada
[#] Correspondence: Patrick.secor@mso.umt.edu

Note: My contribution to this work consisted in overexpressing Pf4 genes and measuring pyocyanin abundance, extracting QS molecules using ethyl acetate, analyzing RNA-sequencing, procuring the transcriptional reporter data, creating the bacterial strains, quantifying Pf4 and running the plaque assays. Eric Déziel and Marie-Christine Groleau quantified ethyl acetate extractions using mass spectrometry. The BATCH assay was performed by Véronique L. Taylor at our behest. The transcriptional reporters were gifts from Lincoln Lewerke and Ajai A. Dandekar upon our request. Dominick Faith processed the raw RNA-sequencing data. Please see published work for up-to-date results and methods.

4.1 Abstract

Quorum sensing is a bacterial signaling system that coordinates group behaviors as a function of cell density. This system plays an important role in regulating bacterial phage defense mechanisms. In the opportunistic pathogen *Pseudomonas aeruginosa*, PQS signaling is involved in defending against phage infection. Many strains of P. aeruginosa are infected by filamentous Pf phage. We recently discovered that deleting the Pf4 prophage from *P. aeruginosa* PAO1 upregulates PQS signaling, enhancing the production of the phenazine pyocyanin; however, how this occurs is not known. Here, we identify the Pf4 protein PfsE as an inhibitor of PQS signaling that binds to PqsA. PfsE adopts a kinked conformation that orients conserved aromatic residues on PfsE into the hydrophobic catalytic pocket of PqsA. Inhibition of PqsA by PfsE results in more efficient Pf4 replication, suggesting that PQS signaling controls bacterial behaviors that defend against phage infection. Furthermore, PfsE also inhibits type IV pili by binding to PilC, which protects *P. aeruginosa* from infection by type IV pilus-dependent phages. Thus, the simultaneous inhibition of type IV pili and PQS signaling by PfsE may be a strategy to increase the susceptibility of the host while at the same time protecting it from competing phages.

4.2 Introduction

Quorum sensing is a cell-to-cell signaling system that allows bacteria to coordinate group behaviors (207). As bacteria replicate, they constantly produce signaling molecules called autoinducers (164). At sufficiently high concentrations, autoinducers bind to and activate their cognate receptors, allowing bacterial populations to coordinate group behaviors as a function of cell density (67, 68).

Quorum sensing has been studied extensively in the opportunistic pathogen *Pseudomonas aeruginosa*. In *P. aeruginosa*, quorum sensing regulates group behaviors such as motility and the production of secreted virulence factors including elastase, hydrogen cyanide, and pyocyanin (208). *P. aeruginosa* PAO1 has three main quorum sensing systems: *las*, *rhl*, and *pqs*. The *las* and *rhl* QS systems utilize the acyl-homoserine lactone autoinducer signals 3-oxo-C12-HSL and C4-HSL, respectively, while the PQS system utilize the quinolone signals 4-hydroxy-2-heptylquinoline (HHQ) and 2-heptyl-3,4-dihydroxyquinoline, the *Pseudomonas* quinolone signal (PQS).

High density bacterial populations can be prone to viral (phage) infection. Consequently, quorum sensing is implicated in the regulation of bacterial phage defense behaviors such as reduced expression of cell surface receptors used by phage to infect cells (209, 210) and control of phage defense systems such as CRISPR-Cas (211, 212).

PQS signaling plays an important role in defending *P. aeruginosa* against phage infection. For example, in phage infected cells, the *pqsABCDE* and *phnAB* operons that encode quinolone and phenazine biosynthesis enzymes are upregulated (213). This is associated with an increase in abundance of quinolones and related metabolites in phage-infected cells (214). In cells where PQS signaling is active, phage resistant isolates emerge at higher frequencies compared to cells where PQS signaling is disrupted (215), suggesting that PQS signaling regulates host processes that interfere with phage replication. PQS molecules released by phage-infected cells can induce phage avoidance behavior in nearby cells (216). Finally, some phages can manipulate PQS signaling. Phage JBD44 can restore PQS signaling in quorum sensing mutants (217) while *P. aeruginosa* phage LUZ19 encodes a protein that binds to and inhibits the PQS biosynthesis enzyme PqsD (107). These observations indicate that PQS signaling is a target in the evolutionary arms race between phages and bacteria.

P. aeruginosa strains are often infected by filamentous Pf phage which integrates into the bacterial chromosome as a prophage (17, 31, 198). Deleting the Pf4 prophage from the chromosome reduces

the virulence potential of *P. aeruginosa* PAO1 in mouse lung (112), mouse wound (29), and *Caenorhabditis elegans* (218) infection models. Our prior work indicates that the Pf4 prophage suppresses PQS signaling at the transcriptional level and reduces the production of the phenazine pyocyanin (218). However, how Pf4 suppresses PQS signaling was not known.

Here, we identify the Pf4 protein PfsE (PA0721) as a small 3.2 kDa protein that binds to PqsA and inhibits PQS signaling. Structure prediction models suggest that PfsE adopts a kinked conformation that orients conserved aromatic residues on PfsE into the hydrophobic catalytic pocket of PqsA. Inhibition of PqsA by PfsE results in more efficient Pf4 replication, consistent with the idea that PQS signaling controls bacterial behaviors that defend against phage infection. Notably, PfsE has been previously characterized as an inner membrane protein that binds to the type IV pilus protein PilC, which inhibits pilus extension (218). As many phage species use type IV pili as a cell surface receptor, inhibition of type IV pilus assembly by PfsE protects the *P. aeruginosa* host from infection by additional Pf4 virions and from other type IV pilus-dependent phages. As PfsE inhibition of PQS signaling makes *P. aeruginosa* more susceptible to infection, the simultaneous inhibition of type IV pili by PfsE may be a strategy to protect the susceptible host from competing phages.

4.3 Results

4.3.1 Pf4 replication and PQS quorum sensing are inversely regulated in *P. aeruginosa.*

While propagating Pf4 *in vitro*, we noted that successful Pf4 infections were associated with reduced pyocyanin production by *P. aeruginosa* PAO1 (**Fig 4-1A**). Conversely, deleting the Pf4 prophage from the PAO1 chromosome enhances pyocyanin production (**Fig 4-1B and C**) (218). Because pyocyanin is a quorum-regulated phenazine (173), these results suggest that Pf4 replication suppresses quorum sensing in *P. aeruginosa*.

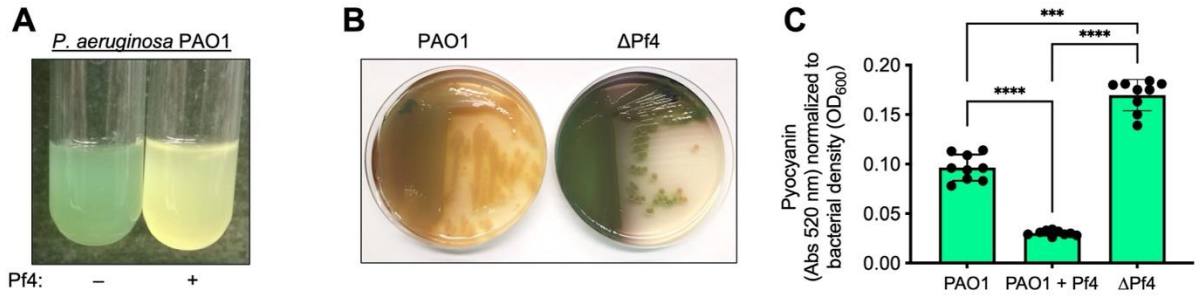

Fig 4-1. Pf4 replication and pyocyanin production are inversely regulated in *P. aeruginosa*. (A) Representative images of PAO1 or PAO1 superinfected with Pf4 virions (PAO1+Pf4) after 18 hours of growth in LB broth. **(B)** Representative images of PAO1 or ΔPf4 grown on LB agar for 18 hours. **(C)** The green pigment pyocyanin was measured in chloroform-acid extracts of bacterial supernatants by

absorbance and normalized to bacterial density (OD_{600}). Data are the mean ±SD of nine replicate experiments, ****P<0.0001, Student's unpaired t-test.

To gain insight onto how the Pf4 phage was affecting quorum sensing pathways, we analyzed RNA sequencing from a superinfecting Pf4 phage (219). We found that numerous quorum sensing genes were significantly (false discovery rate, FDR<0.05) downregulated in Pf4-infected cells as compared to uninfected cells, including *pqs* system genes (**Fig 4-2A and B**) (220). Phenazine biosynthesis genes are also significantly (FDR<0.05) downregulated in Pf4-infected cells (**Fig 4-2C**).

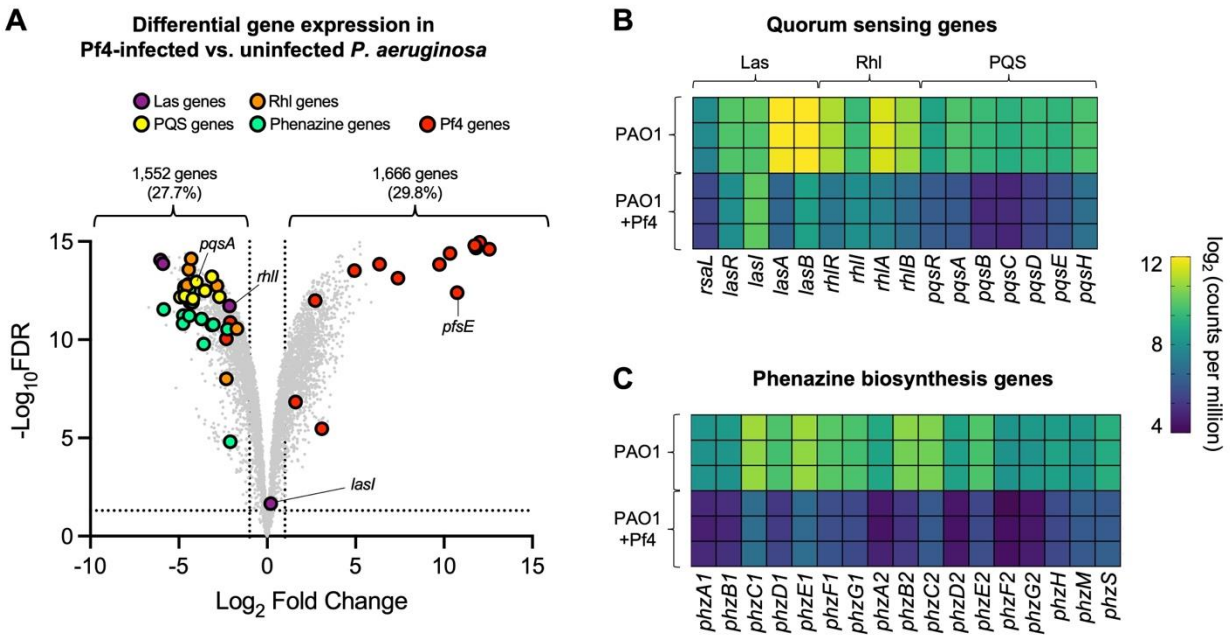

Fig 4-2. Pf4 replication downregulates *P. aeruginosa* quorum sensing genes. (A) Volcano plot showing differentially expressed genes in Pf4 infected verses uninfected *P. aeruginosa*. Dashed lines indicate differentially expressed genes that are $\log_2$[foldchange] > 1 and FDR<0.05 or $\log_2$[fold change] < -1 and FDR<0.05. Data are representative of triplicate experiments. **(B and C)** Heatmaps showing $\log_2$ (counts per million) values for the indicated quorum sensing and phenazine biosynthesis genes are shown for each replicate.

We used HPLC-MS to directly measure quorum sensing autoinducer levels in PAO1, PAO1+Pf4, and ΔPf4 culture supernatants over time. All autoinducer measurements were normalized to viable cell counts (CFUs, **Fig 4-3A**). Levels of the *las* autoinducer 3-oxo-C12-HSL were not significantly different over time in all three cultures (**Fig 4-3B**), which is consistent with the unchanged expression of the autoinducer synthesis gene *lasI* (**Fig 4-2A and B**). Levels of the *rhl* autoinducer C4-HSL were significantly (P<0.02) lower in Pf4-infected cells at the 12-hour time point (**Fig 4-3C**, red square). This result is consistent with the significant (P<0.05) downregulation of *rhlI* in Pf4-infected cells (**Fig 4-2A**

and B). Collectively, these observations suggest that Pf4 replication does not drastically affect *las* signaling but has a negative impact on *rhl* signaling.

Levels of the quinolone signaling molecules HHQ and PQS were comparable in uninfected and Pf4-infected PAO1 over time (**Fig 4-3D** and **Fig 4-3E**, compare squares and circles). In the ΔPf4 strain, however, HHQ levels spike at around 12 hours of growth, followed by a steep decline from 12 to 24 hours (**Fig 4-3D**, blue triangles). The decline of HHQ is accompanied by an increase in PQS levels in ΔPf4 from 12 to 24 hours (**Fig 4-3E**, blue triangles). As HHQ is the direct precursor to the PQS signaling molecule (85), these observations are consistent with HHQ being produced by ΔPf4 during late exponential/early stationary phase followed by HHQ consumption and subsequent PQS production during stationary phase growth. These results indicate that the Pf4 prophage somehow inhibits quinolone biosynthesis to suppress *P. aeruginosa pqs* signaling.

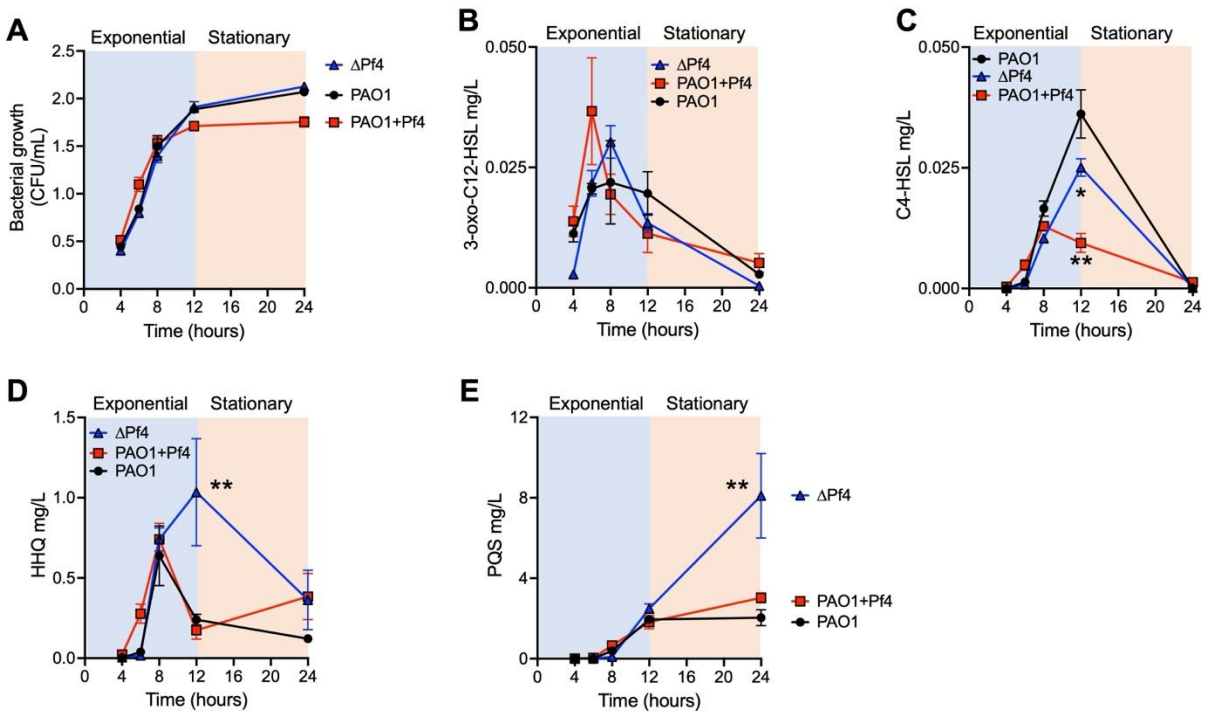

Fig 4-3. Pf4 suppresses C4-HSL, HHQ, and PQS biosynthesis. (A) Growth of the indicated strains was measured by enumerating viable colony forming units (CFUs) at the indicated times, N=4. **(B-E)** The indicated quorum sensing molecules in bacterial supernatants were measured by HPLC-MS at the indicated times and normalized to bacterial CFUs. Data are the mean of triplicate experiments, *P<0.05, **P<0.02 compared to PAO1.

4.3.2 The Pf4 phage protein PfsE binds to PqsA.

Pf4 replication suppresses pyocyanin production (**Fig 4-1A**). To identify Pf4 proteins that may

suppress pyocyanin production, we expressed each protein in the core Pf4 genome (PA0717-PA0728) individually from an expression plasmid in *P. aeruginosa* ΔPf4 and assessed the effects on pyocyanin production. We identified a single protein, PfsE (PA0721), that significantly (P<0.05) reduced pyocyanin production by ΔPf4 compared to the empty vector control (**Fig 4-4A**). Time course experiments confirmed that the expression of PfsE in ΔPf4 significantly (P<0.001) decreased pyocyanin production compared to ΔPf4 carrying an empty expression vector (**Fig 4-4B**). Note the *pfsE* gene is the fifth most highly upregulated gene in Pf4-infected cultures (**Fig 4-2A**).

To determine if PfsE interacts directly with bacterial proteins involved in *pqs* or other quorum sensing pathways, we used a bacterial two-hybrid (BACTH) assay (127) to measure protein-protein interactions between bait (PfsE) and prey (bacterial proteins). Positive interactions are detected as red pigmentation in *E. coli* reporter colonies after 48 hours growth on MacConkey agar. PfsE is known to strongly bind the type IV pilus protein PilC (159), providing a positive control. Colony pigmentation was observed when PfsE was expressed with PilC and PqsA (**Fig 4C and D**), suggesting that in addition to PilC, PfsE also binds to PqsA.

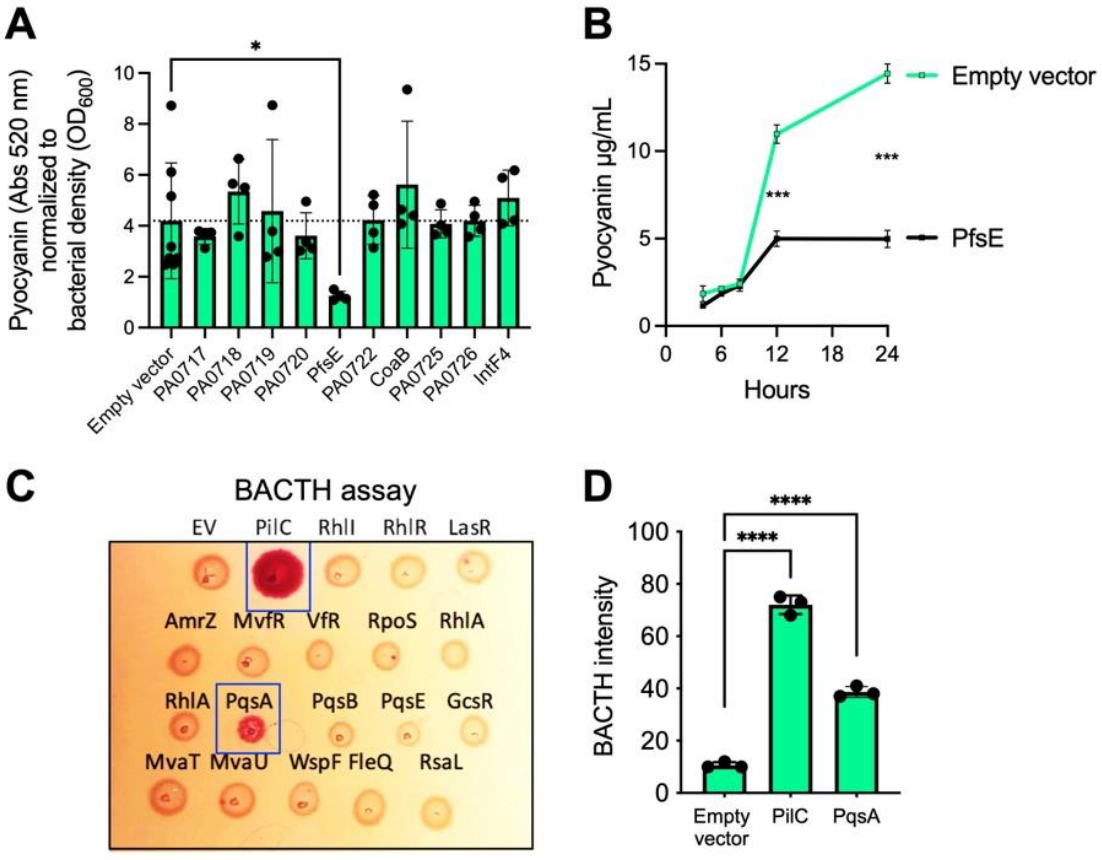

Fig 4-4. The Pf4 phage protein PfsE binds to PqsA and inhibits pyocyanin production. (A) The indicated Pf4 proteins were expressed from an inducible plasmid in ΔPf4. After 18 h, pyocyanin was

extracted, quantified by absorbance, and normalized to bacterial density (OD_{600}). Data are the mean +/- SD, N=4 experiments, *P<0.05. **(B)** Pyocyanin was extracted from ΔPf4 carrying an empty vector or a PfsE expression construct at the indicated times. Data are the mean +/- SD, N=3 experiments, ***P<0.001 comparing each condition at the indicated timepoints. **(C)** A bacterial two-hybrid assay was used to detect interactions between PfsE and the indicated *P. aeruginosa* proteins. Representative colonies are shown. EV = empty vector. **(D)** Pigmentation intensity of colonies expressing PfsE as bait and the indicated prey proteins was measured in image J. Data are the mean +/- SD, N=3 experiments, ***P<0.001.

4.3.3 PfsE binds the catalytic domain of PqsA in a kinked conformation

PfsE is a small 3.2 kDa hydrophobic inner membrane protein that binds to PilC and inhibits type IV pili extension (159). Pf4 (and other phages) use type IV pili as a cell surface receptor to infect cells (116) and expression of PfsE by Pf4 protects the *P. aeruginosa* host from competing phages (159). In the type IV pilus apparatus, PilC forms a homodimer in the inner membrane (221). Protein structure modeling predicts four PfsE molecules bind to the transmembrane domain of the PilC dimer in an extended conformation that is typical of alpha-helical membrane-spanning proteins (**Fig 4-5A and B**). PfsE contains a glycine zipper Gly-XXX-Gly-XXX-Gly motif (**Fig 4-5C and D**). Glycine zippers promote the packing of helical membrane proteins against a neighboring helix (222), which is observed between PfsE proteins in the model (**Fig 4-5A-C**).

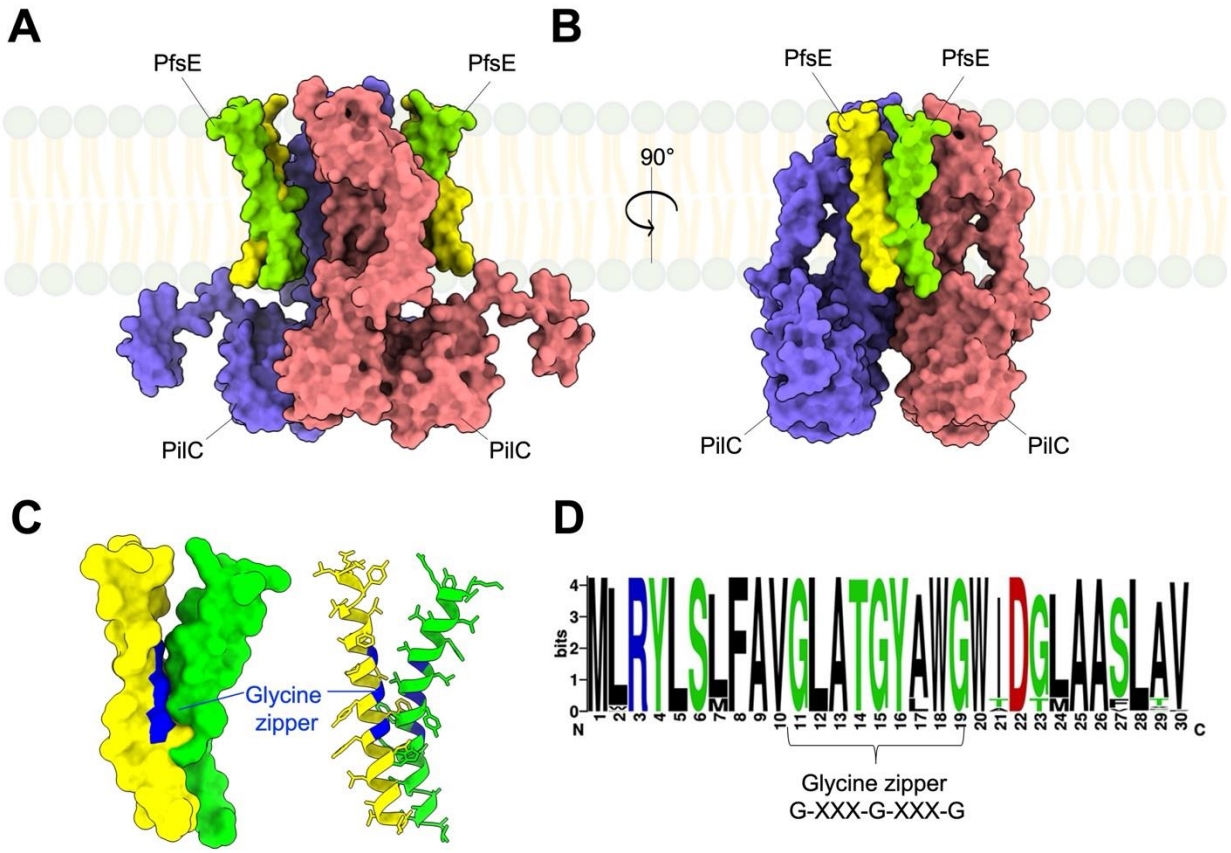

Figure 4-5. PfsE is predicted to bind to the transmembrane domain of the type IV pili protein PilC as a dimer in an extended conformation. (**A and B**) AlphFold 2 was used to predict the structure of the PilC-PfsE complex from *P. aeruginosa* (UniProt A0A367MDJ4). PilC polymers are shown in blue and light red and PfsE polymers are shown in yellow and lime green **(C)** Space filling and ribbon models of PfsE dimers from the PilC-PfsE complex are shown with the glycine zipper highlighted in blue. (**D**) A protein sequence logo was constructed for 312 PfsE sequences from Pf prophages infecting diverse *P. aeruginosa* strains in the *Pseudomonas* genome database. Note the glycine zipper (Gly-XXX-Gly-XXX-Gly) motif is conserved.

The structure of the full *P. aeruginosa* type IV pili complex is not solved. However, PilC is a conserved component of type IV pili in Proteobacteria (223)—the predicted position of PfsE in the solved structure of the type IVa pili complex from *Myxococcus xanthus* (221) is shown in **Fig S1**. Presumably, PfsE binding to PilC restricts pilus assembly and/or extension.

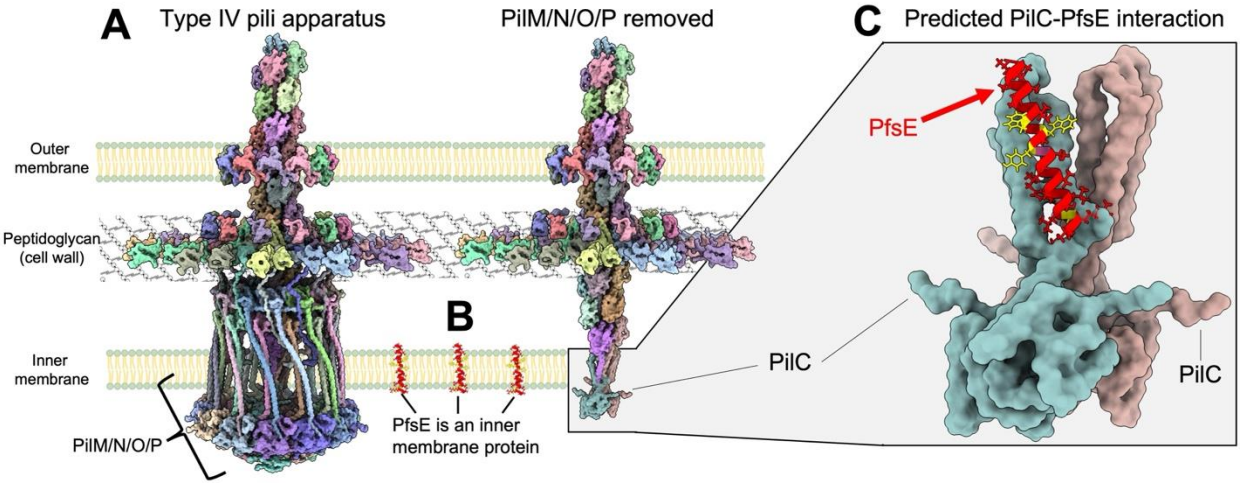

Fig 4-S1. PfsE is predicted to adopt an extended conformation when bound to the type IV pili inner membrane protein PilC. (A) The solved structure of the type IVa pili apparatus (PDB 3jc8) is shown. **(B)** The Pf phage protein PfsE localizes to the inner membrane. **(C)** PfsE is predicted to bind PilC and inhibit pilus extension, preventing re-infection by additional Pf virions or other pili-dependent phages.

PqsA is a cytoplasmic anthranilate-coenzyme A ligase that is required for HHQ and PQS quinolone biosynthesis (224). How might a hydrophobic inner membrane protein such as PfsE bind to a cytoplasmic target like PqsA? The structure of a truncated version *P. aeruginosa* PqsA has been solved (225). Structural modeling predicts that PfsE binds to PqsA in a kinked conformation (**Fig 4-6A-C**). The model predicts that aromatic PfsE residues Tyr-16, Trp-18, and Trp-20 reach into the hydrophobic ligand-binding domain of PqsA (**Fig 4-6D and E**). The kink in PfsE occurs at the conserved central Gly-15 residue and electrostatic interactions between the basic Arg-3 and acidic Asp-22 residues near the N- and C-terminus of PfsE, respectively, may serve to stabilize the kinked conformation (**Fig 4-6F**). Out of 312 PfsE sequences from Pf phage strains infecting diverse *P. aeruginosa* hosts, 22/30 PfsE residues are 100% conserved, including the charged residues Arg-3 and Asp-22, the central Gly-15

that facilitates kinking, and the aromatic residues Tyr-16, Trp-18, and Trp-20 that occupy the ligand-binding domain of PqsA (**Fig 4-6G**).

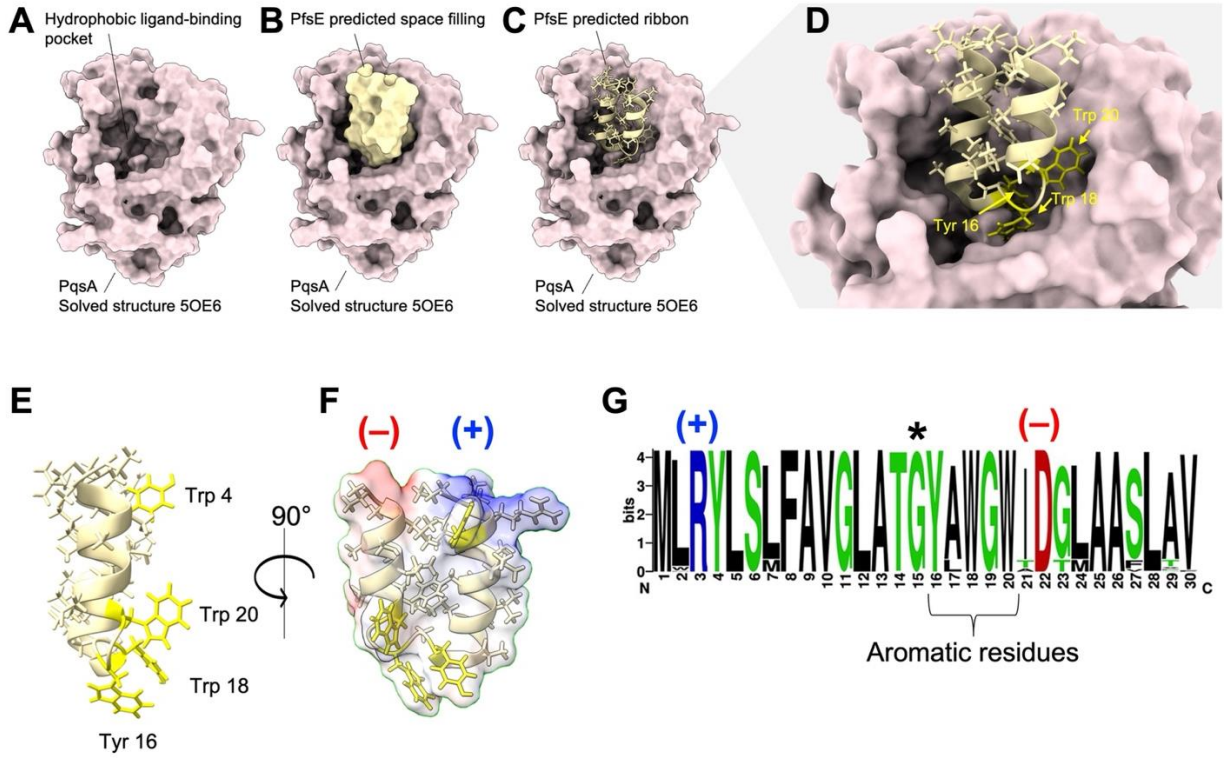

Figure 4-5. PfsE is predicted to adopt a kinked conformation that binds the catalytic domain of PqsA. (A) The solved structure of PqsA (PBD 5OE6) is shown. **(B and C)** AlphaFold2 was used to predict the structure of PfsE (yellow) bound to PqsA (gray). **(D)** Aromatic PfsE residues Tyr 16, Trp 18, and Trp 20 are predicted to reach into the hydrophobic catalytic domain. **(E)** Side view of PfsE in its kinked conformation with aromatic residues highlighted in bright yellow. **(F)** An electrostatic surface representation of PfsE is shown. **(G)** A protein sequence logo was constructed for 312 PfsE sequences from Pf prophages infecting diverse *P. aeruginosa* strains in the *Pseudomonas* genome database.

4.3.4 Disabling PQS signaling by PfsE enhances Pf4 virion infection.

PqsA catalyzes the first step in PQS biosynthesis (224) and PQS signaling is implicated in phage defense behaviors in *P. aeruginosa* (51, 213-216). Thus, we hypothesized that inhibition of PQS signaling would make *P. aeruginosa* more susceptible to infection by Pf4. To test this, we deleted *pqsA* from the ΔPf4 background (ΔPf4/*pqsA*) and infected with Pf4 virions at a multiplicity of infection (MOI) of 0.001. Under these conditions, we did not detect any infectious virions produced by ΔPf4 cultures whereas Pf4 virions could infect ΔPf4/Δ*pqsA* cells (**Fig 4-6A**), suggesting that ΔPf4 cells where PQS signaling is intact are able to suppress infection by Pf4 virions (**Fig 4-6A**). However, ΔPf4 and ΔPf4/*pqsA* lawns were equally susceptible to Pf4 infection when infected at an MOI of one (**Fig 4-S2**). These results indicate that disabling PQS signaling only benefits Pf4 at low MOIs.

When the Pf4 prophage is induced, it is excised from the host chromosome and is initially present as a single circular copy (i.e., the replicative form) in the host cytoplasm. We hypothesized that inhibition of PQS signaling by PfsE at this critical time would be important for Pf4 virion replication. To test this hypothesis, we expressed PfsE from an inducible plasmid in wild-type PAO1 or in ΔPf4. Compared to PAO1 carrying an empty expression vector, expression of PfsE significantly ($P<0.01$) increased Pf4 titers in PAO1 culture supernatants after 18 hours (**Fig 4-6B**). Plaques were not observed under any condition where the ΔPf4 strain was used (**Fig 4-6B**), indicating that plaquing is caused by Pf4 virions. These results suggest that inhibition of PQS signaling by PfsE enhaces Pf4 virion replication efficiency as the phage transitions from lysogenic to active replication.

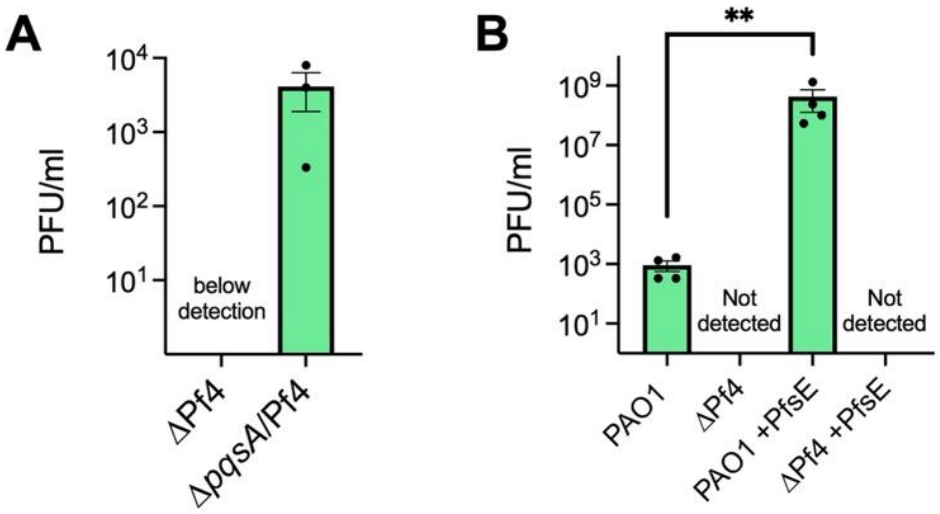

Figure 4-6. Disabling PQS signaling promotes Pf4 virion replication. (A) Liquid cultures of the indicated strains were infected with Pf4 virions (MOI 0.001). After 18 hours of growth at 37°C, Pf4 plaque forming units (PFUs) in cell culture supernatants were enumerated on lawns of *P. aeruginosa* ΔPf4. Data are the mean +/- SD, N=3 experiments. Detection limit = 333 PFU/mL. **(B)** PAO1 or ΔPf4 carrying an empty expression vector or an expression vector carrying an inducible copy of PfsE were grown for 18 hours at 37°C to an OD600 of 2.0. Pf4 PFUs in culture supernatants were then enumerated on lawns of *P. aeruginosa* ΔPf4. Data are the mean +/- SD, N=4 experiments, **P<0.01. Detection limit = 333 PFU/mL.

4.4 Discussion

To maximize replication and genome packaging efficiency, viruses employ several strategies to maintain small genome sizes (226), including the utilization of small genes that encode proteins less than 50 amino acids in length (227). To further maximize efficiency, phage proteins are also often multifunctional. For example, the Cox protein of phage P2 is involved in both prophage excision and a transcriptional repressor that promotes lytic replication (228). Phage P4 encodes an alpha protein that

binds the phage origin of replication that has both helicase and primase activities (229). Phage T7 encodes Gp2.5 that in addition to binding ssDNA, also binds to host DNA polymerase and DNA helicase, regulating their activities (230). Lastly, Aqs1 of phage DMS3 both inhibits twitch motility and represses the *las* system (51).

In this study, we characterized the multifunctional role of the small, highly conserved 30 amino acid Pf phage protein PfsE. Overall, our data support a model where PfsE adopts an extended conformation when it binds to PilC in the inner membrane and a kinked conformation when it binds to the catalytic domain of PqsA in the cytosol (**Figure 4-7**). The inhibition of PQS signaling increases the efficiency of Pf replication while inhibition of type IV pili protects the susceptible host from infection by competing phages.

Quorum sensing plays important roles in shaping the outcomes of phage-bacteria encounters. Other species of *Pseudomonas* phages also target PQS signaling (107), suggesting that PQS signaling regulates phage defense systems. Our results are analogous to the Aqs1 protein encoded by phage DMS3—Aqs1 binds to and inhibits PilB and LasR to simultaneously inhibit type IV pili and disrupt *P. aeruginosa* quorum sensing (51). This prior work along with our results here indicate that the simultaneous inhibition of host quorum sensing and type IV pili provides a fitness advantage to phages.

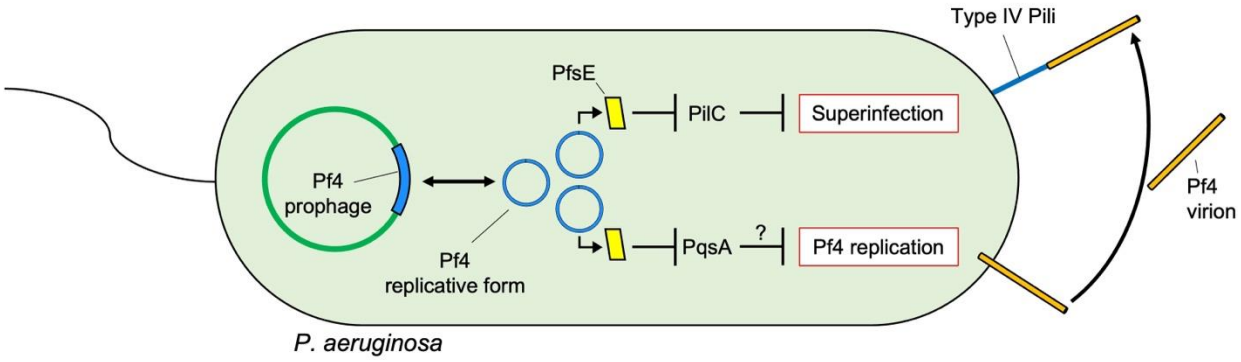

Fig 4-7. Proposed model: PfsE simultaneously binds to and inhibits PqsA (PQS signaling) and PilC (type IV pili). We propose that disabling PQS signaling enhances Pf4 replication and at the same time, protects the susceptible *P. aeruginosa* host from infection by competing phages.

As of yet, our structural data are Alpha Fold predictions, of which there are several. PfsE is also predicted to exist as a dimer and it may bind PilC as a monomer or trimer. Furthermore, our predictions of PfsE's interaction with PqsA were made with the solved, truncated version of PqsA. This may affect the results of the prediction. However, we have crystals of this complex and are in the process of

garnering x-ray crystallography data.

Both expression of PfsE and deletion of *pqsA* affected *P. aeruginosa* susceptibility to phage infection. PfsE may play an important role for lysogens—after prophage induction, a single phage genome (RF) must overcome host defenses to replicate. PfsE inhibition of PQS may be important for this process as opposed to infection from exogenous virions.

PfsE inhibits PQS, but our results suggest that *rhl* signaling also negatively affected. Due to the interactions between QS systems, this might be due to pleiotropic effects of the inhibited *pqs* system, as PQS increases *rhl* signaling (95, 231). Another possibility is that additional Pf proteins modulate host quorum sensing.

Understanding how Pf phages manipulate their bacterial hosts may drive therapeutic innovations for treating *P. aeruginosa* infections. For example, peptide mimics of phage proteins that bind to proteins involved in virulence (such as PilC and PqsA) could be designed to dampen bacterial virulence potential. Inoviruses similar to Pf are pervasive amongst bacteria, especially Gram-negative pathogens such as *Salmonella, Vibrio, E. coli, Yersinia*, and others (118). Thus, understanding how Pf manipulates *P. aeruginosa* may shed light on other filamentous phage-bacteria relationships that have implications for human health and disease.

4.5 Materials and methods

4.5.1 Strains, plasmids, and growth conditions

Strains, plasmids, and their sources are listed in **Table 1.** Unless otherwise indicated, bacteria were grown in lysogeny broth (LB) at 37 °C with 230 rpm shaking and supplemented with antibiotics (Sigma). Unless otherwise noted, gentamicin was used at the at either 10 or 30 μg ml^{-1}.

4.5.2 Construction of strain Δ*pqsA*

The Δ*pqsA* strain was produced in MPAO1 by allelic exchange (146), producing a clean and unmarked Δ*pqsA* deletion. All primers used for strain construction are given in **Table 2**. Using *Escherichia coli* S17λ*pir*, we mobilized the pENTRpEX18-Gm-Δ*pqsA* plasmid, received from the Dandekar lab, into *P. aeruginosa* PAO1 via biparental mating. Merodiploid *P. aeruginosa* was selected on Vogel-Bonner minimal medium (VBMM) agar containing 60 μg ml^{-1} gentamicin, followed by recovery of deletion mutants on no-salt LB (NSLB) medium containing 10% sucrose. Candidate mutants were

confirmed by PCR and sequencing using primer pair attB1-pqsA-UpF/attB2-pqsA-DownR. Supernatants collected from overnight cultures this Δ*pqsA* strain did not produce detectable levels of pyocyanin.

4.5.3 Construction of strain Δ*pqsA*/Pf4

The Pf4 prophage was deleted from the mPAO1 Δ*pqsA* as described in (159) chromosome by allelic exchange (146), producing a clean and unmarked ΔPf4 deletion with the Pf4 att site intact. All primers used for strain construction are given in **Table 2**. The Pf4 prophage contains a toxin-antitoxin (TA) pair (147). The presence of the Pf4-encoded PfiTA system likely explains the low efficiency at which the Pf4 prophage can be deleted from the PAO1 chromosome (112); deletion of the Pf4 prophage results in loss of the antitoxin gene *pfiA* and cells without the antitoxin are killed by the longer-lived toxin PfiT (147). Thus, the *pfiT* toxin gene was first deleted from PAO1 by allelic exchange (146). Briefly, the upstream region of *pflT (pfiT')* and the downstream region of *pflT ('pfiT)* were amplified using the primer pairs attB1-pfiT-UpF/pfiT-UpR and PfiT-DownF/attB2-PfiT-DownR, respectively (**Table 2**). These were then assembled using SOE-PCR. The resulting fragment was cloned into pENTRpEX18-Gm, transformed into *Escherichia coli* S17λ*pir*, and subsequently mobilized into *P. aeruginosa* PAO1 via biparental mating. Merodiploid *P. aeruginosa* was selected on Vogel-Bonner minimal medium (VBMM) agar containing 60 µg ml^{-1} gentamicin, followed by recovery of deletion mutants on no-salt LB (NSLB) medium containing 10% sucrose. Candidate mutants were confirmed by PCR and sequencing using primer pair PfiT seq F/PfiT seq R. The remaining Pf4 prophage was then deleted from Δ*pfiT* using the same allelic exchange strategy described for Δ*pfiT* using primers Pf4-UpF-GWL, Pf4-UpR-GM, Pf4-DnF-GM, and Pf4-DnR-GWR (**Table 2**), producing an unmarked clean deletion of Pf4 with an intact att site. Candidate mutants were confirmed by PCR using primer pair pf4-out F/pf4-out R and sequenced confirmed. Supernatants collected from overnight cultures this ΔPf4 strain did not produce detectable plaques on lawns of PAO1 or ΔPf4 and the ΔPf4 genotype was routinely PCR confirmed prior to experiments using this strain to avoid re-infection by exogenous Pf4 virions in the laboratory environment.

4.5.4 Plaque assays

Plaque assays were performed using the ΔPf4 as the indicator strain grown on LB plates. Phage in filtered supernatants were serially diluted 10x in PBS and spotted onto lawns of ΔPf4 strain. Plaques were quantified after 18h of growth at 37°C.

4.5.5 Pf4 phage virion quantitation by qPCR

Pf4 virion copy number was measured using qPCR as previously described (121). Briefly, filtered supernatants were treated with DNase I (10 µL of a 10mg/ml stock per mL supernatant) followed by incubation at 95°C for 10 minutes to inactivate the DNase. Ten µL reaction volumes containing 5 µl SYBR Select Master Mix (Life Technologies, Grand Island, NY), 400 nM of primer attR-F and attL-R (**Table 2**), and 1 µl supernatant. Primers attR-F and attL-R amplify the re-circularization sequence of the Pf4 replicative form (Pf4-RF) and thus, do not amplify linear Pf4 prophage sequences that may be present in contaminating chromosomal DNA. Cycling conditions were as follows: 98°C 3 min, (95°C 10 sec, 61.5°C 30 sec) x 40 cycles. A standard curve was constructed using a Pf4-RF gBlock (**Table 2**) containing the template sequence at a known copy #/mL. Pf4 copy numbers were then calculated by fitting Ct values of the unknown samples to the standard curve.

4.5.6 Growth Curves

Overnight cultures were diluted to an OD_{600} of 0.01 in 96-well plates containing LB and if necessary, the appropriate antibiotics. Over the course of 24h, OD_{600} was measured in a CLARIOstar (BMG Labtech) plate reader at 37C with orbital shaking at 300 rpm for 2 minutes prior to each measurement.

4.5.7 Pyocyanin extraction and measurement

Pyocyanin was measured as described elsewhere (199, 200). Briefly, ~18-hour cultures were treated by adding chloroform to a total of 50% culture volume. This was vortexed vigorously and the different phases given time to separate. After the aqueous top-layer was discarded, we added 20% the volume of chloroform of 0.1 N HCl and the mixture vortexed vigorously. Once separated, we removed the aqueous fraction and measured its absorbance at 520 nm. The concentration of pyocyanin in the culture supernatant, expressed as µg/ml, was obtained by multiplying the optical density at 520 nm by 17.072 (200).

4.5.8 LC/MS Analysis

Analyses were performed using a Micromass Quattro II triple quadrupole mass spectrometer (Micromass Canada, Pointe-Claire, Canada) in positive electrospray ionization mode, interfaced to an HP1100 HPLC equipped with a 4.5X150-mm reverse-phase C_8 column. Internal standard was added to culture supernatants and the mixture was twice extracted with ethyl acetate, the solvent was evaporated in a speed vacuum concentrator, and the residue was dissolved in a water/acetonitrile.

4.5.9 Quorum sensing reporters

Competent *P. aeruginosa* PAO1 and ΔPf4 were prepared by washing overnight cultures in 300 mM sucrose followed by transformation by electroporation (201) with the plasmids CP1 Blank-PBBR-MCS5, CP53 PBBR1-MCS5 *pqsA*-gfp, CP57 PBBR1-MCS5 *rhlA*-gfp, CP59 PBBR1-MCS5 *rsaL*-gfp listed in **Table 1**. Transformants were selected for by plating on the appropriate antibiotic selection media. The indicated strains were grown in buffered LB containing 50 mM MOPS and 100 µg ml^{-1} gentamicin for 18 hours. Cultures were then sub-cultured 1:100 into fresh LB MOPS buffer and grown to an OD_{600} of 0.3. To measure reporter fluorescence, each strain was added to a 96-well plate containing 200 µL LB MOPS with a final bacterial density of OD_{600} 0.01 and incubated at 37˚C in a CLARIOstar BMG LABTECH plate-reader. Prior to each measurement, plates were shaken at 230 rpm for a duration of two minutes. A measurement was taken every 15 minutes for both growth (OD_{600}) or fluorescence (excitation at 485-15 nm and emission at 535-15 nm).

Table 4-1. Bacterial strains, phage, and plasmids used in this study.

Strain	**Description**	**Source**
Escherichia coli		
DH5α	New England Biolabs	(116)
BL21(DE3)	New England Biolabs	
P. aeruginosa		
PAO1	Wild type	(112)
PAO1 ΔPf4	Deletion of the Pf4 prophage from PAO1	(112)
MPAO1		
MPAO1 ΔPf4	Deletion of the Pf4 prophage from MPAO1	
MPAO1 Δ*pqsA*	Clean deletion of *pqsA* from MPAO1	
MPAO1 Δ*pqsA*/Pf4	Clean deletion of *pqsA* and Pf4 from MPAO1	
Bacteriophage Strains		
Pf4	Inovirus	(20)
Plasmids		
CP59 pBBR1-MCS5 rsaL-gfp	GFP *rsaL* transcriptional reporter	(176)
CP57 pBBR1-MCS5 rhlA-gfp	GFP *rhlA* transcriptional reporter	(176)
CP53 pBBR1-MCS5 pqsA-gfp	GFP *pqsA* transcriptional reporter	(175)
CP1 pBBR-MCS5-Blank	GFP empty vector control	(176)

pHERD20T	AmpR, expression vector with araC-P_{BAD} promoter	(118)
pHERD30T	GmR, expression vector with araC-P_{BAD} promoter	(118)
pHERD30T-*PA0717*	pBAD::*PA0717*	(159)
pHERD30T-*PA0718*	pBAD::*PA0718*	(159)
pHERD30T-*PA0719*	pBAD::*PA0719*	(159)
pHERD30T-*PA0720*	pBAD::*PA0720*	(159)
pHERD30T-*pfsE*	pBAD::*pfsE*	(159)
pHERD30T-*PA0722*	pBAD::*PA0722*	(159)
pHERD30T-*PA0723*	pBAD::*PA0723*	(159)
pHERD30T-*PA0724*	pBAD::*PA0724*	(159)
pHERD30T-*PA0725*	pBAD::*PA0725*	(159)
pHERD30T-*PA0726*	pBAD::*PA0726*	(159)
pHERD30T-*PA0727*	pBAD::*PA0727*	(159)
pHERD30T-*intF4*	pBAD::*intF4*	(159)
pHERD20T-*xisF4*	pBAD::*xisF4*	(37)

Table 4-2. Primers used in this study

Purpose/Name	***Sequence (5'-3')***
Cloning	
PfsE_p18CFwd	TACGTCTAGAGCTCCGCTATCTCTCGCTGTTCGCGGTAGG
PfsE_p18CRev	TACGGGTACCTCAAACAGTCAGGGAGGCCGCTAGG
PfsE_Y16VFwd	CTGGCCACCGGCGTGGCCTGG
PfsE_Y16VRev	CCAGCCCCAGGCCACGCCGGT
PfsE_W18AFwd	ACCGGCTACGCCGCCGGCTGG
PfsE_W18ARev	TCGATCCAGCCGGCGGCGTAGC
PfsE_W20AFwd	TACGCCTGGGGCGCCATCGACG
PfsE_W20ARev	CTAGGCCGTCGATGGCGCCCCAGG
ΔpqsA primers:	
attB1-pqsA-UpF	ggggacaagtttgtacaaaaaagcaggcttcCTACGAAGCCCGTGG
attB2-pqsA-DownR	ggggaccactttgtacaagaaagctgggtaCCGAGGACCTTCTGCAAC
PfiT-DownF	TGATGGCTTTCTACTCCTGA
attB2-PfiT-DownR	ggggaccactttgtacaagaaagctgggtaAGCCGCTCAACCCGATCTA
PfiT seq F	CCACACGTTCGCCAGTCACTT
PfiT seq R	AATGCCGGCCACTTCATCGAC
ΔPf4 primers:	
Pf4-UpF-GWL	tacaaaaaagcaggctTCTGGGAATACGACGGGGGC
Pf4-UpR-GM	tcagagcgcttttgaagctaattcgGATCCCAATGCAAAAGCCCC
Pf4-DnF-GM	aggaacttcaagatccccaattcgCGTCATGAGCTTGGGAAGCT
Pf4-DnR-GWR	tacaagaaagctgggtTGGCAGCAGACCCAGGACGC

pf4-out F	AGTGGCGGTTATCGGATGAC
pf4-out R	TCATTGGGAGGCGCTTTCAT
qPCR primers:	
AttR-F	taggcatttcaggggcttgg
AttL-R	gagctacggagtaagacgcc
Pf4-RF gBlock	GGGGACAAGTTTGTACAAAAAAGCAGGCTTCTAGGCATTTCAGGGGCTTGG CAGGGTGATTTGGAGCGGGCGAAGGGAATCGAACCCTCGTCATGAGCTTGG GAAGCTCAGGTAATGCTAAAATAGGGTTTTGAAGCGTTCCTATACATTCTAAT GCCACTGCCTTCGATTTTTAGGCGTCTTACTCCGTAGCTCTACCCAGCTTTC TTGTACAAAGTGGTCCCC

4.5.10 RNA sequencing

RNA-seq reads were downloaded from GEO accession no. GSE201738 (232). RNA-seq reads were then aligned to the reference *P. aeruginosa* PAO1 genome (GenBank: GCA_000006765.1), mapped to genomic features, and counted using Rsubread package v2.12.3 (233).Count tables produced with Rsubread were normalized and tested for differential expression using edgeR v3.40.2 (234).Genes with ≥ two-fold expression change and a false discovery rate (FDR) below 0.05 were considered significantly differential. RNA-seq analysis results were plotted with ggplot2 v3.4.1 and pheatmap v1.0.12 packages using R v4.2.3 in RStudio v2023.3.0.386, and GraphPad Prism v9.5.1 (www.graphpad.com) (235, 236).

4.5.11 Statistical analyses

Differences between data sets were evaluated with a Student's *t*-test (unpaired, two-tailed) where appropriate. P values of < 0.05 were considered statistically significant. GraphPad Prism version 5.0 (GraphPad Software, San Diego, CA) was used for all analyses.

Chapter 5: Conclusions
5.1 Current Model

Though phages are often genetically smaller and simpler than their hosts, phage-host interaction are varied and complex. The dual functionality of *pfsE* highlights the efficiency present in these simplified genomes. PfsE also exemplifies the mutualistic balance between the bacteria and their temperate phage, both organisms benefiting from each other: Pf4 by propagating with their host, and *P. aeruginosa* by phage resistance and virulence changes. Influencing the realm of bacterial communication is a means for phages to keep their finger on the pulse of a bacterial community and influence virulence potential. The changes to bacterial virulence that ensue have a much broader impact on how the bacteria interact with their hosts.

In this study, we elucidated two distinct functions of the Pf-encoded gene, pfsE. We first noticed the transient loss of twitch motility in Pf4-infected SCVs. Seeking to make sense of this, we observed that PfsE is capable of inhibiting T4P-dependent twitch motility by preventing the extension of T4P. We discovered that PfsE prevents pilus extension by interacting with the T4P subunit, PilC. An interaction mediated through the three highly conserved aromatic residues of PfsE. This resulted in Pf4's inability to infect the cell, a finding consistent with the literature describing PfsE-mediated phage resistance to other T4P-dependent phages. Furthermore, Pf4 lacking *pfsE* had greater virulence against *P. aeruginosa*. However, overexpression of PfsE increased virion production. This seems due to PfsE's second function; PfsE dampens PQS QS. In addition to PilC, PfsE binds to PqsA in an alternate kinked conformation, and inhibits PqsA's enzymatic function. This is apparently beneficial for Pf4 as PqsA plays a role in inhibiting Pf4 replication. This interaction also leads to a decrease in pyocyanin levels, which we learned can potentially benefit *P. aeruginosa* during *C. elegans* predation.

We discovered that the Pf4 protects *P. aeruginosa* from *C. elegans* predation. We found that Pf4 enters the chronic infection cycle upon *P. aeruginosa* predation by *C. elegans*, whereby Pf4 accumulates in the worm's digestive tract, possibly inhibiting digestion. Furthermore, Pf4-infected *P. aeruginosa* exhibited greater virulence towards *C. elegans* than *P. aeruginosa* cured of Pf4. We noted that Pf4-infected *P. aeruginosa* also displayed an enhanced ability to compromise the *C. elegans* cuticle. Consistent with our observation of PfsE, Pf4-infected *P. aeruginosa* also produced less of the virulence factor pyocyanin, seemingly through the inhibition of the PQS pathway. Our running model is that Pf4's reduction in pyocyanin allows *P. aeruginosa* to better evade detection by the worm's AhR. Our confidence in this model was bolstered by AhR-null worms' increased mortality, compared with AhR replete worms, when propagated on *P. aeruginosa* cured of Pf4.

5.2 Loose ends and Summary

We present findings, consistent with current literature (30), in which Pf4's interactions with *P. aeruginosa* results in changes to *P. aeruginosa's* virulence potential. Yet we have only scratched the surface of the multifaceted ways in which these interactions affect bacterial virulence. Future research is needed to identify and elucidate these mechanisms to answer questions such as: Does Pf4 interact directly with the other QS systems, and if so, how?, How does PqsA function to inhibit Pf infection?, What pleiotropic effects does the dampening of the *pqs* system have on *P. aeruginosa*?, What are the functions of other Pf4 proteins?, and What other Pf4 proteins have dual functionality? Furthermore, bacterial QS is still a burgeoning field with much to be discovered. For example, we still lack a full understanding of the regulation of the *pqsABCDE* operon. With phage-host interactions and bacterial quorum sensing open to inquiry, current methods molecular biology seem promising to uncovering new and exciting developments that may aid our understanding of microbiology and provide new avenues for treating human pathogens.

Works Cited

1. Roux S, Krupovic M, Daly RA, Borges AL, Nayfach S, Schulz F, Sharrar A, Matheus Carnevali PB, Cheng JF, Ivanova NN, Bondy-Denomy J, Wrighton KC, Woyke T, Visel A, Kyrpides NC, Eloe-Fadrosh EA. Cryptic inoviruses revealed as pervasive in bacteria and archaea across Earth's biomes. Nat Microbiol. 2019;4(11):1895-906. Epub 2019/07/25. doi: 10.1038/s41564-019-0510-x. PubMed PMID: 31332386; PMCID: PMC6813254.
2. Jia K, Peng Y, Chen X, Jian H, Jin M, Yi Z, Su M, Dong X, Yi M. A Novel Inovirus Reprograms Metabolism and Motility of Marine Alteromonas. Microbiology Spectrum.0(0):e03388-22. doi: doi:10.1128/spectrum.03388-22.
3. Hay ID, Lithgow T. Filamentous phages: masters of a microbial sharing economy. Embo Rep. 2019;20(6). doi: ARTN e47427
10.15252/embr.201847427. PubMed PMID: WOS:000472972600016.
4. Knezevic P, Adriaenssens EM, Consortium IR. ICTV Virus Taxonomy Profile: Inoviridae. The Journal of General Virology. 2021;102(7).
5. Roux S, Krupovic M, Daly RA, Borges AL, Nayfach S, Schulz F, Sharrar A, Matheus Carnevali PB, Cheng J-F, Ivanova NN, Bondy-Denomy J, Wrighton KC, Woyke T, Visel A, Kyrpides NC, Eloe-Fadrosh EA. Cryptic inoviruses revealed as pervasive in bacteria and archaea across Earth's biomes. Nature Microbiology. 2019. doi: 10.1038/s41564-019-0510-x.
6. Rakonjac J, Bennett NJ, Spagnuolo J, Gagic D, Russel M. Filamentous bacteriophage: biology, phage display and nanotechnology applications. Current issues in molecular biology. 2011;13(2):51-76.
7. Bertozzi Silva J, Storms Z, Sauvageau D. Host receptors for bacteriophage adsorption. FEMS Microbiol Lett. 2016;363(4). Epub 2016/01/13. doi: 10.1093/femsle/fnw002. PubMed PMID: 26755501.
8. Burrows LL. Pseudomonas aeruginosa twitching motility: type IV pili in action. Annu Rev Microbiol. 2012;66:493-520. Epub 2012/07/04. doi: 10.1146/annurev-micro-092611-150055. PubMed PMID: 22746331.
9. Averhoff B, Friedrich A. Type IV pili-related natural transformation systems: DNA transport in mesophilic and thermophilic bacteria. Archives of microbiology. 2003;180(6):385-93.
10. Reguera G, McCarthy KD, Mehta T, Nicoll JS, Tuominen MT, Lovley DR. Extracellular electron transfer via microbial nanowires. Nature. 2005;435(7045):1098-101.
11. Click EM, Webster RE. Filamentous phage infection: required interactions with the TolA protein. Journal of bacteriology. 1997;179(20):6464-71.
12. Holliger P, Riechmann L. A conserved infection pathway for filamentous bacteriophages is suggested by the structure of the membrane penetration domain of the minor coat protein g3p from phage fd. Structure. 1997;5(2):265-75.
13. Smilowitz H. Bacteriophage f1 Infection: Fate of the Parental Major Coat Protein. Journal of Virology. 1974;13(1):94-9. doi: doi:10.1128/jvi.13.1.94-99.1974.
14. Higashitani A, Higashitani N, Horiuchi K. Minus-strand origin of filamentous phage versus transcriptional promoters in recognition of RNA polymerase. Proceedings of the National Academy of Sciences. 1997;94(7):2909-14.
15. Zenkin N, Naryshkina T, Kuznedelov K, Severinov K. The mechanism of DNA replication primer synthesis by RNA polymerase. Nature. 2006;439(7076):617-20.
16. Horiuchi K. Initiation mechanisms in replication of filamentous phage DNA. Genes to Cells. 1997;2(7):425-32.
17. Secor PR, Burgener EB, Kinnersley M, Jennings LK, Roman-Cruz V, Popescu M, Van Belleghem JD, Haddock N, Copeland C, Michaels LA, de Vries CR, Chen Q, Pourtois J, Wheeler TJ,

Milla CE, Bollyky PL. Pf Bacteriophage and Their Impact on Pseudomonas Virulence, Mammalian Immunity, and Chronic Infections. Front Immunol. 2020;11:244. Epub 2020/03/11. doi: 10.3389/fimmu.2020.00244. PubMed PMID: 32153575; PMCID: PMC7047154.
18. Varani AM, Monteiro-Vitorello CB, Nakaya HI, Van Sluys MA. The role of prophage in plant-pathogenic bacteria. Annu Rev Phytopathol. 2013;51:429-51. Epub 2013/06/04. doi: 10.1146/annurev-phyto-081211-173010. PubMed PMID: 23725471.
19. Ilyina TS. Filamentous Bacteriophages and Their Role in the Virulence and Evolution of Pathogenic Bacteria. Mol Genet Microbiol+. 2015;30(1):1-9. doi: 10.3103/S0891416815010036. PubMed PMID: WOS:000351489500001.
20. Secor PR, Sweere JM, Michaels LA, Malkovskiy AV, Lazzareschi D, Katznelson E, Rajadas J, Birnbaum ME, Arrigoni A, Braun KR, Evanko SP, Stevens DA, Kaminsky W, Singh PK, Parks WC, Bollyky PL. Filamentous Bacteriophage Promote Biofilm Assembly and Function. Cell Host Microbe. 2015;18(5):549-59. Epub 2015/11/17. doi: 10.1016/j.chom.2015.10.013. PubMed PMID: 26567508; PMCID: PMC4653043.
21. Bille E, Meyer J, Jamet A, Euphrasie D, Barnier JP, Brissac T, Larsen A, Pelissier P, Nassif X. A virulence-associated filamentous bacteriophage of Neisseria meningitidis increases host-cell colonisation. PLoS Pathog. 2017;13(7):e1006495. Epub 2017/07/14. doi: 10.1371/journal.ppat.1006495. PubMed PMID: 28704569; PMCID: PMC5526601.
22. Bondy-Denomy J, Davidson AR. When a Virus is not a Parasite: The Beneficial Effects of Prophages on Bacterial Fitness. J Microbiol. 2014;52(3):235-42. doi: 10.1007/s12275-014-4083-3. PubMed PMID: WOS:000332049700006.
23. Chung IY, Jang HJ, Bae HW, Cho YH. A phage protein that inhibits the bacterial ATPase required for type IV pilus assembly. P Natl Acad Sci USA. 2014;111(31):11503-8. doi: 10.1073/pnas.1403537111. PubMed PMID: WOS:000339807200058.
24. Bondy-Denomy J, Qian J, Westra ER, Buckling A, Guttman DS, Davidson AR, Maxwell KL. Prophages mediate defense against phage infection through diverse mechanisms. Isme Journal. 2016;10(12):2854-66. doi: 10.1038/ismej.2016.79. PubMed PMID: WOS:000394508000008.
25. Zimlichman E, Henderson D, Tamir O, Franz C, Song P, Yamin CK, Keohane C, Denham CR, Bates DW. Health care-associated infections: a meta-analysis of costs and financial impact on the US health care system. JAMA Intern Med. 2013;173(22):2039-46. Epub 2013/09/04. doi: 10.1001/jamainternmed.2013.9763. PubMed PMID: 23999949.
26. Ramos GP, Rocha JL, Tuon FF. Seasonal humidity may influence Pseudomonas aeruginosa hospital-acquired infection rates. Int J Infect Dis. 2013;17(9):E757-E61. doi: 10.1016/j.ijid.2013.03.002. PubMed PMID: WOS:000324172200019.
27. Webb JS, Lau M, Kjelleberg S. Bacteriophage and phenotypic variation in Pseudomonas aeruginosa biofilm development. J Bacteriol. 2004;186(23):8066-73. Epub 2004/11/18. doi: 10.1128/JB.186.23.8066-8073.2004. PubMed PMID: 15547279; PMCID: PMC529096.
28. Rice SA, Tan CH, Mikkelsen PJ, Kung V, Woo J, Tay M, Hauser A, McDougald D, Webb JS, Kjelleberg S. The biofilm life cycle and virulence of Pseudomonas aeruginosa are dependent on a filamentous prophage. ISME J. 2009;3(3):271-82. Epub 2008/11/14. doi: 10.1038/ismej.2008.109. PubMed PMID: 19005496; PMCID: PMC2648530.
29. Sweere JM, Van Belleghem JD, Ishak H, Bach MS, Popescu M, Sunkari V, Kaber G, Manasherob R, Suh GA, Cao X, de Vries CR, Lam DN, Marshall PL, Birukova M, Katznelson E, Lazzareschi DV, Balaji S, Keswani SG, Hawn TR, Secor PR, Bollyky PL. Bacteriophage trigger antiviral immunity and prevent clearance of bacterial infection. Science. 2019;363(6434). Epub 2019/03/30. doi: 10.1126/science.aat9691. PubMed PMID: 30923196; PMCID: PMC6656896.

30. Secor PR, Burgener EB, Kinnersley M, Jennings LK, Roman-Cruz V, Popescu M, Van Belleghem JD, Haddock N, Copeland C, Michaels LA. Pf bacteriophage and their impact on Pseudomonas virulence, mammalian immunity, and chronic infections. Frontiers in Immunology. 2020;11:244.
31. Knezevic P, Voet M, Lavigne R. Prevalence of Pf1-like (pro)phage genetic elements among Pseudomonas aeruginosa isolates. Virology. 2015;483:64-71. Epub 2015/05/13. doi: 10.1016/j.virol.2015.04.008. PubMed PMID: 25965796.
32. Burgener EB, Sweere JM, Bach MS, Secor PR, Haddock N, Jennings LK, Marvig RL, Johansen HK, Rossi E, Cao X, Tian L, Nedelec L, Molin S, Bollyky PL, Milla CE. Filamentous bacteriophages are associated with chronic Pseudomonas lung infections and antibiotic resistance in cystic fibrosis. Sci Transl Med. 2019;11(488). Epub 2019/04/19. doi: 10.1126/scitranslmed.aau9748. PubMed PMID: 30996083; PMCID: PMC7021451.
33. Burgener EB, Sweere JM, Bach MS, Secor PR, Haddock N, Jennings LK, Marvig RL, Johansen HK, Rossi E, Cao X. Filamentous bacteriophages are associated with chronic Pseudomonas lung infections and antibiotic resistance in cystic fibrosis. Science translational medicine. 2019;11(488):eaau9748.
34. Whiteley M, Bangera MG, Bumgarner RE, Parsek MR, Teitzel GM, Lory S, Greenberg EP. Gene expression in Pseudomonas aeruginosa biofilms. Nature. 2001;413(6858):860-4. Epub 2001/10/26. doi: 10.1038/35101627. PubMed PMID: 11677611.
35. Webb JS, Thompson LS, James S, Charlton T, Tolker-Nielsen T, Koch B, Givskov M, Kjelleberg S. Cell death in Pseudomonas aeruginosa biofilm development. J Bacteriol. 2003;185(15):4585-92. Epub 2003/07/18. doi: 10.1128/jb.185.15.4585-4592.2003. PubMed PMID: 12867469; PMCID: PMC165772.
36. Takeya K, Amako K. A rod-shaped Pseudomonas phage. Virology. 1966;28(1):163-5.
37. Li Y, Liu X, Tang K, Wang P, Zeng Z, Guo Y, Wang X. Excisionase in Pf filamentous prophage controls lysis-lysogeny decision-making in Pseudomonas aeruginosa. Mol Microbiol. 2019;111(2):495-513. Epub 2018/11/27. doi: 10.1111/mmi.14170. PubMed PMID: 30475408.
38. Harms A, Diard M. Crowd Controlled-Host Quorum Sensing Drives Phage Decision. Cell Host Microbe. 2019;25(2):179-81. Epub 2019/02/15. doi: 10.1016/j.chom.2019.01.016. PubMed PMID: 30763531.
39. Maxwell KL. Phages Tune in to Host Cell Quorum Sensing. Cell. 2019;176(1-2):7-8. Epub 2019/01/12. doi: 10.1016/j.cell.2018.12.007. PubMed PMID: 30633910.
40. Silpe JE, Bassler BL. A Host-Produced Quorum-Sensing Autoinducer Controls a Phage Lysis-Lysogeny Decision. Cell. 2019;176(1-2):268-80 e13. Epub 2018/12/18. doi: 10.1016/j.cell.2018.10.059. PubMed PMID: 30554875; PMCID: PMC6329655.
41. Lee Y, Song S, Sheng L, Zhu L, Kim J-S, Wood TK. Substrate binding protein DppA1 of ABC transporter DppBCDF increases biofilm formation in Pseudomonas aeruginosa by inhibiting Pf5 prophage lysis. Frontiers in microbiology. 2018;9:30.
42. Wei Q, Le Minh PN, Dötsch A, Hildebrand F, Panmanee W, Elfarash A, Schulz S, Plaisance S, Charlier D, Hassett D. Global regulation of gene expression by OxyR in an important human opportunistic pathogen. Nucleic acids research. 2012;40(10):4320-33.
43. Guo Y, Tang K, Sit B, Gu J, Chen R, Lin J, Lin S, Liu X, Wang W, Gao X. Dual control of lysogeny and phage defense by a phosphorylation-based toxin/antitoxin system. bioRxiv. 2022:2022.09.05.506569.

44. Ismail MH, Michie KA, Goh YF, Noorian P, Kjelleberg S, Duggin IG, McDougald D, Rice SA. The repressor C protein, Pf4r, controls superinfection of Pseudomonas aeruginosa PAO1 by the Pf4 filamentous phage and regulates host gene expression. Viruses. 2021;13(8):1614.
45. Martínez E, Campos-Gómez J. Pf filamentous phage requires UvrD for replication in Pseudomonas aeruginosa. MSphere. 2016;1(1):e00104-15.
46. Castang S, McManus HR, Turner KH, Dove SL. H-NS family members function coordinately in an opportunistic pathogen. Proc Natl Acad Sci U S A. 2008;105(48):18947-52. Epub 2008/11/26. doi: 10.1073/pnas.0808215105. PubMed PMID: 19028873; PMCID: PMC2596223.
47. Castang S, Dove SL. Basis for the essentiality of H-NS family members in Pseudomonas aeruginosa. Journal of bacteriology. 2012;194(18):5101-9.
48. Chen M, Samuelson JC, Jiang F, Muller M, Kuhn A, Dalbey RE. Direct interaction of YidC with the Sec-independent Pf3 coat protein during its membrane protein insertion. Journal of Biological Chemistry. 2002;277(10):7670-5.
49. Liu DJ, Day LA. Pf1 virus structure: helical coat protein and DNA with paraxial phosphates. Science. 1994;265(5172):671-4.
50. Tsao Y-F, Taylor VL, Kala S, Bondy-Denomy J, Khan AN, Bona D, Cattoir V, Lory S, Davidson AR, Maxwell KL. Phage morons play an important role in Pseudomonas aeruginosa phenotypes. Journal of bacteriology. 2018;200(22).
51. Shah M, Taylor VL, Bona D, Tsao Y, Stanley SY, Pimentel-Elardo SM, McCallum M, Bondy-Denomy J, Howell PL, Nodwell JR, Davidson AR, Moraes TF, Maxwell KL. A phage-encoded anti-activator inhibits quorum sensing in Pseudomonas aeruginosa. Mol Cell. 2021. Epub 2021/01/08. doi: 10.1016/j.molcel.2020.12.011. PubMed PMID: 33412111.
52. Chung IY, Jang HJ, Bae HW, Cho YH. A phage protein that inhibits the bacterial ATPase required for type IV pilus assembly. Proc Natl Acad Sci U S A. 2014;111(31):11503-8. Epub 2014/07/23. doi: 10.1073/pnas.1403537111. PubMed PMID: 25049409; PMCID: PMC4128137.
53. Hui JGK, Mai-Prochnow A, Kjelleberg S, McDougald D, Rice SA. Environmental cues and genes involved in establishment of the superinfective Pf4 phage of Pseudomonas aeruginosa. Frontiers in Microbiology. 2014;5. doi: 10.3389/fmicb.2014.00654.
54. Stoodley P, Sauer K, Davies DG, Costerton JW. Biofilms as complex differentiated communities. Annual Reviews in Microbiology. 2002;56(1):187-209.
55. Whitchurch CB, Tolker-Nielsen T, Ragas PC, Mattick JS. Extracellular DNA required for bacterial biofilm formation. Science. 2002;295(5559):1487-.
56. Saunders SH, Edmund C, Yates MD, Otero FJ, Trammell SA, Stemp ED, Barton JK, Tender LM, Newman DK. Extracellular DNA promotes efficient extracellular electron transfer by pyocyanin in Pseudomonas aeruginosa biofilms. Cell. 2020;182(4):919-32. e19.
57. Barraud N, Hassett DJ, Hwang S-H, Rice SA, Kjelleberg S, Webb JS. Involvement of nitric oxide in biofilm dispersal of Pseudomonas aeruginosa. Journal of bacteriology. 2006;188(21):7344-53.
58. Conibear TC, Collins SL, Webb JS. Role of mutation in Pseudomonas aeruginosa biofilm development. PloS one. 2009;4(7):e6289.
59. McElroy KE, Hui JG, Woo JK, Luk AW, Webb JS, Kjelleberg S, Rice SA, Thomas T. Strain-specific parallel evolution drives short-term diversification during Pseudomonas aeruginosa biofilm formation. Proceedings of the National Academy of Sciences. 2014;111(14):E1419-E27.
60. Oliver A, Cantón R, Campo P, Baquero F, Blázquez J. High frequency of hypermutable Pseudomonas aeruginosa in cystic fibrosis lung infection. Science. 2000;288(5469):1251-3.
61. Petrova OE, Schurr JR, Schurr MJ, Sauer K. The novel Pseudomonas aeruginosa two-component regulator BfmR controls bacteriophage-mediated lysis and DNA release during biofilm development

through PhdA. Molecular Microbiology. 2011;81(3):767-83. doi: https://doi.org/10.1111/j.1365-2958.2011.07733.x.
62. Heydorn A, Ersbøll B, Kato J, Hentzer M, Parsek MR, Tolker-Nielsen T, Givskov M, Molin S. Statistical analysis of Pseudomonas aeruginosa biofilm development: impact of mutations in genes involved in twitching motility, cell-to-cell signaling, and stationary-phase sigma factor expression. Applied and Environmental Microbiology. 2002;68(4):2008-17.
63. Klausen M, Heydorn A, Ragas P, Lambertsen L, Aaes-Jørgensen A, Molin S, Tolker-Nielsen T. Biofilm formation by Pseudomonas aeruginosa wild type, flagella and type IV pili mutants. Molecular microbiology. 2003;48(6):1511-24.
64. O'Toole GA, Kolter R. Flagellar and twitching motility are necessary for Pseudomonas aeruginosa biofilm development. Molecular microbiology. 1998;30(2):295-304.
65. Papenfort K, Bassler BL. Quorum sensing signal-response systems in Gram-negative bacteria. Nat Rev Microbiol. 2016;14(9):576-88. Epub 2016/08/12. doi: 10.1038/nrmicro.2016.89. PubMed PMID: 27510864; PMCID: PMC5056591.
66. Smith P, Schuster M. Antiactivators prevent self-sensing in Pseudomonas aeruginosa quorum sensing. Proceedings of the National Academy of Sciences. 2022;119(25):e2201242119.
67. Schuster M, Greenberg EP. A network of networks: quorum-sensing gene regulation in Pseudomonas aeruginosa. Int J Med Microbiol. 2006;296(2-3):73-81. Epub 2006/02/16. doi: 10.1016/j.ijmm.2006.01.036. PubMed PMID: 16476569.
68. Lee J, Zhang L. The hierarchy quorum sensing network in Pseudomonas aeruginosa. Protein Cell. 2015;6(1):26-41. Epub 2014/09/25. doi: 10.1007/s13238-014-0100-x. PubMed PMID: 25249263; PMCID: PMC4286720.
69. Pearson JP, Gray KM, Passador L, Tucker KD, Eberhard A, Iglewski BH, Greenberg EP. Structure of the autoinducer required for expression of Pseudomonas aeruginosa virulence genes. Proc Natl Acad Sci U S A. 1994;91(1):197-201. Epub 1994/01/04. doi: 10.1073/pnas.91.1.197. PubMed PMID: 8278364; PMCID: PMC42913.
70. Pearson JP, Passador L, Iglewski BH, Greenberg EP. A second N-acylhomoserine lactone signal produced by Pseudomonas aeruginosa. Proc Natl Acad Sci U S A. 1995;92(5):1490-4. Epub 1995/02/28. doi: 10.1073/pnas.92.5.1490. PubMed PMID: 7878006; PMCID: PMC42545.
71. García-Reyes S, Soberón-Chávez G, Cocotl-Yanez M. The third quorum-sensing system of Pseudomonas aeruginosa: Pseudomonas quinolone signal and the enigmatic PqsE protein. Journal of medical microbiology. 2020;69(1):25-34.
72. Mukherjee S, Moustafa DA, Stergioula V, Smith CD, Goldberg JB, Bassler BL. The PqsE and RhlR proteins are an autoinducer synthase-receptor pair that control virulence and biofilm development in Pseudomonas aeruginosa. Proc Natl Acad Sci U S A. 2018;115(40):E9411-E8. Epub 2018/09/19. doi: 10.1073/pnas.1814023115. PubMed PMID: 30224496; PMCID: PMC6176596.
73. Farrow III JM, Sund ZM, Ellison ML, Wade DS, Coleman JP, Pesci EC. PqsE functions independently of PqsR-Pseudomonas quinolone signal and enhances the rhl quorum-sensing system. Journal of bacteriology. 2008;190(21):7043-51.
74. Lee J, Wu J, Deng Y, Wang J, Wang C, Wang J, Chang C, Dong Y, Williams P, Zhang LH. A cell-cell communication signal integrates quorum sensing and stress response. Nat Chem Biol. 2013;9(5):339-43. Epub 2013/04/02. doi: 10.1038/nchembio.1225. PubMed PMID: 23542643.
75. Eickhoff MJ, Bassler BL. SnapShot: bacterial quorum sensing. Cell. 2018;174(5):1328-. e1.
76. Whiteley M, Lee KM, Greenberg E. Identification of genes controlled by quorum sensing in Pseudomonas aeruginosa. Proceedings of the National Academy of Sciences. 1999;96(24):13904-9.

77. Kariminik A, Baseri-Salehi M, Kheirkhah B. Pseudomonas aeruginosa quorum sensing modulates immune responses: an updated review article. Immunology letters. 2017;190:1-6.
78. Taylor IR, Paczkowski JE, Jeffrey PD, Henke BR, Smith CD, Bassler BL. Inhibitor Mimetic Mutations in the Pseudomonas aeruginosa PqsE Enzyme Reveal a Protein–Protein Interaction with the Quorum-Sensing Receptor RhlR That Is Vital for Virulence Factor Production. ACS chemical biology. 2021;16(4):740-52.
79. Pierson LS, Pierson EA. Metabolism and function of phenazines in bacteria: impacts on the behavior of bacteria in the environment and biotechnological processes. Applied microbiology and biotechnology. 2010;86(6):1659-70.
80. Meirelles LA, Newman DK. Both toxic and beneficial effects of pyocyanin contribute to the lifecycle of Pseudomonas aeruginosa. Mol Microbiol. 2018;110(6):995-1010. Epub 2018/09/20. doi: 10.1111/mmi.14132. PubMed PMID: 30230061; PMCID: PMC6281804.
81. Lau GW, Hassett DJ, Ran H, Kong F. The role of pyocyanin in Pseudomonas aeruginosa infection. Trends in molecular medicine. 2004;10(12):599-606.
82. Choi W, Choe S, Lin J, Borchers MT, Kosmider B, Vassallo R, Limper AH, Lau GW. Exendin-4 restores airway mucus homeostasis through the GLP1R-PKA-PPARγ-FOXA2-phosphatase signaling. Mucosal immunology. 2020;13(4):637-51.
83. Diggle SP, Matthijs S, Wright VJ, Fletcher MP, Chhabra SR, Lamont IL, Kong X, Hider RC, Cornelis P, Cámara M. The Pseudomonas aeruginosa 4-quinolone signal molecules HHQ and PQS play multifunctional roles in quorum sensing and iron entrapment. Chemistry & biology. 2007;14(1):87-96.
84. Xiao G, Déziel E, He J, Lépine F, Lesic B, Castonguay MH, Milot S, Tampakaki AP, Stachel SE, Rahme LG. MvfR, a key Pseudomonas aeruginosa pathogenicity LTTR-class regulatory protein, has dual ligands. Molecular microbiology. 2006;62(6):1689-99.
85. Deziel E, Lepine F, Milot S, He J, Mindrinos MN, Tompkins RG, Rahme LG. Analysis of Pseudomonas aeruginosa 4-hydroxy-2-alkylquinolines (HAQs) reveals a role for 4-hydroxy-2-heptylquinoline in cell-to-cell communication. P Natl Acad Sci USA. 2004;101(5):1339-44. Epub 2004/01/24. doi: 10.1073/pnas.0307694100. PubMed PMID: 14739337; PMCID: 337054.
86. Drees SL, Fetzner S. PqsE of Pseudomonas aeruginosa acts as pathway-specific thioesterase in the biosynthesis of alkylquinolone signaling molecules. Chemistry & biology. 2015;22(5):611-8.
87. Simanek KA, Taylor IR, Richael EK, Lasek-Nesselquist E, Bassler BL, Paczkowski JE. The PqsE-RhlR interaction regulates RhlR DNA binding to control virulence factor production in Pseudomonas aeruginosa. Microbiology spectrum. 2022;10(1):e02108-21.
88. Lin J, Cheng J, Wang Y, Shen X. The Pseudomonas quinolone signal (PQS): not just for quorum sensing anymore. Frontiers in cellular and infection microbiology. 2018;8:230.
89. Gallagher LA, McKnight SL, Kuznetsova MS, Pesci EC, Manoil C. Functions Required for Extracellular Quinolone Signaling by Pseudomonas aeruginosa. Journal of Bacteriology. 2002;184(23):6472-80. doi: doi:10.1128/JB.184.23.6472-6480.2002.
90. Wade DS, Calfee MW, Rocha ER, Ling EA, Engstrom E, Coleman JP, Pesci EC. Regulation of Pseudomonas quinolone signal synthesis in Pseudomonas aeruginosa. Journal of bacteriology. 2005;187(13):4372-80.
91. Xiao G, He J, Rahme LG. Mutation analysis of the Pseudomonas aeruginosa mvfR and pqsABCDE gene promoters demonstrates complex quorum-sensing circuitry. Microbiology. 2006;152(6):1679-86.
92. Brouwer S, Pustelny C, Ritter C, Klinkert B, Narberhaus F, Häussler S. The PqsR and RhlR transcriptional regulators determine the level of Pseudomonas quinolone signal synthesis in

Pseudomonas aeruginosa by producing two different pqsABCDE mRNA isoforms. Journal of bacteriology. 2014;196(23):4163-71.
93. Dötsch A, Eckweiler D, Schniederjans M, Zimmermann A, Jensen V, Scharfe M, Geffers R, Häussler S. The Pseudomonas aeruginosa transcriptome in planktonic cultures and static biofilms using RNA sequencing. PloS one. 2012;7(2):e31092.
94. Gallagher LA, Manoil C. Pseudomonas aeruginosa PAO1 kills Caenorhabditis elegans by cyanide poisoning. J Bacteriol. 2001;183(21):6207-14. doi: 10.1128/JB.183.21.6207-6214.2001. PubMed PMID: 11591663; PMCID: PMC100099.
95. Diggle SP, Winzer K, Chhabra SR, Worrall KE, Cámara M, Williams P. The Pseudomonas aeruginosa quinolone signal molecule overcomes the cell density-dependency of the quorum sensing hierarchy, regulates rhl-dependent genes at the onset of stationary phase and can be produced in the absence of LasR. Molecular microbiology. 2003;50(1):29-43.
96. Cao H, Krishnan G, Goumnerov B, Tsongalis J, Tompkins R, Rahme LG. A quorum sensing-associated virulence gene of Pseudomonas aeruginosa encodes a LysR-like transcription regulator with a unique self-regulatory mechanism. Proceedings of the National Academy of Sciences. 2001;98(25):14613-8.
97. Lau GW, Ran H, Kong F, Hassett DJ, Mavrodi D. Pseudomonas aeruginosa pyocyanin is critical for lung infection in mice. Infection and immunity. 2004;72(7):4275-8.
98. Bredenbruch F, Geffers R, Nimtz M, Buer J, Häussler S. The Pseudomonas aeruginosa quinolone signal (PQS) has an iron-chelating activity. Environmental microbiology. 2006;8(8):1318-29.
99. Mashburn LM, Whiteley M. Membrane vesicles traffic signals and facilitate group activities in a prokaryote. Nature. 2005;437(7057):422-5.
100. Mashburn-Warren L, Howe J, Garidel P, Richter W, Steiniger F, Roessle M, Brandenburg K, Whiteley M. Interaction of quorum signals with outer membrane lipids: insights into prokaryotic membrane vesicle formation. Molecular microbiology. 2008;69(2):491-502.
101. Bru J-L, Rawson B, Trinh C, Whiteson K, Høyland-Kroghsbo NM, Siryaporn A. PQS produced by the Pseudomonas aeruginosa stress response repels swarms away from bacteriophage and antibiotics. Journal of bacteriology. 2019;201(23):e00383-19.
102. Doekes HM, Mulder GA, Hermsen R. Repeated outbreaks drive the evolution of bacteriophage communication. Elife. 2021;10. Epub 2021/01/19. doi: 10.7554/eLife.58410. PubMed PMID: 33459590; PMCID: PMC7935489.
103. Stewart FM, Levin BR. The population biology of bacterial viruses: why be temperate. Theor Popul Biol. 1984;26(1):93-117. Epub 1984/08/01. doi: 10.1016/0040-5809(84)90026-1. PubMed PMID: 6484871.
104. Maslov S, Sneppen K. Well-temperate phage: optimal bet-hedging against local environmental collapses. Sci Rep. 2015;5:10523. Epub 2015/06/04. doi: 10.1038/srep10523. PubMed PMID: 26035282; PMCID: PMC4451807.
105. Taylor VL, Fitzpatrick AD, Islam Z, Maxwell KL. The Diverse Impacts of Phage Morons on Bacterial Fitness and Virulence. Adv Virus Res. 2019;103:1-31. Epub 2019/01/13. doi: 10.1016/bs.aivir.2018.08.001. PubMed PMID: 30635074.
106. Silpe JE, Bassler BL. Phage-Encoded LuxR-Type Receptors Responsive to Host-Produced Bacterial Quorum-Sensing Autoinducers. MBio. 2019;10(2). Epub 2019/04/11. doi: 10.1128/mBio.00638-19. PubMed PMID: 30967469; PMCID: PMC6456758.
107. Hendrix H, Zimmermann-Kogadeeva M, Zimmermann M, Sauer U, De Smet J, Muchez L, Lissens M, Staes I, Voet M, Wagemans J, Ceyssens PJ, Noben JP, Aertsen A, Lavigne R. Metabolic

reprogramming of Pseudomonas aeruginosa by phage-based quorum sensing modulation. Cell Rep. 2022;38(7):110372. doi: 10.1016/j.celrep.2022.110372. PubMed PMID: 35172131.
108. Høyland-Kroghsbo NM, Bassler BL. Phage infection restores PQS signaling and enhances growth of a Pseudomonas aeruginosa lasI quorum-sensing mutant. Journal of bacteriology. 2022;204(5):e00557-21.
109. Høyland-Kroghsbo NM, Paczkowski J, Mukherjee S, Broniewski J, Westra E, Bondy-Denomy J, Bassler BL. Quorum sensing controls the Pseudomonas aeruginosa CRISPR-Cas adaptive immune system. Proceedings of the National Academy of Sciences. 2017;114(1):131-5.
110. Secor PR, Michaels LA, Smigiel KS, Rohani MG, Jennings LK, Hisert KB, Arrigoni A, Braun KR, Birkland TP, Lai Y, Hallstrand TS, Bollyky PL, Singh PK, Parks WC. Filamentous Bacteriophage Produced by Pseudomonas aeruginosa Alters the Inflammatory Response and Promotes Noninvasive Infection In Vivo. Infect Immun. 2017;85(1). Epub 2016/11/01. doi: 10.1128/IAI.00648-16. PubMed PMID: 27795361; PMCID: PMC5203648.
111. McElroy KE, Hui JG, Woo JK, Luk AW, Webb JS, Kjelleberg S, Rice SA, Thomas T. Strain-specific parallel evolution drives short-term diversification during Pseudomonas aeruginosa biofilm formation. P Natl Acad Sci USA. 2014;111(14):E1419-27. Epub 2014/04/08. doi: 10.1073/pnas.1314340111. PubMed PMID: 24706926.
112. Rice SA, Tan CH, Mikkelsen PJ, Kung V, Woo J, Tay M, Hauser A, McDougald D, Webb JS, Kjelleberg S. The biofilm life cycle and virulence of Pseudomonas aeruginosa are dependent on a filamentous prophage. Isme J. 2009;3(3):271-82. Epub 2008/11/14. doi: 10.1038/ismej.2008.109. PubMed PMID: 19005496; PMCID: 2648530.
113. Webb JS, Lau M, Kjelleberg S. Bacteriophage and phenotypic variation in Pseudomonas aeruginosa biofilm development. J Bacteriol. 2004;186(23):8066-73. Epub 2004/11/18. doi: 10.1128/JB.186.23.8066-8073.2004. PubMed PMID: 15547279; PMCID: 529096.
114. Webb JS, Thompson LS, James S, Charlton T, Tolker-Nielsen T, Koch B, Givskov M, Kjelleberg S. Cell death in Pseudomonas aeruginosa biofilm development. J Bacteriol. 2003;185(15):4585-92. Epub 2003/07/18. PubMed PMID: 12867469; PMCID: 165772.
115. Petrova OE, Schurr JR, Schurr MJ, Sauer K. The novel Pseudomonas aeruginosa two-component regulator BfmR controls bacteriophage-mediated lysis and DNA release during biofilm development through PhdA. Mol Microbiol. 2011;81(3):767-83. Epub 2011/06/24. doi: 10.1111/j.1365-2958.2011.07733.x. PubMed PMID: 21696457; PMCID: 3214647.
116. Castang S, Dove SL. Basis for the essentiality of H-NS family members in Pseudomonas aeruginosa. J Bacteriol. 2012;194(18):5101-9. Epub 2012/07/24. doi: 10.1128/JB.00932-12. PubMed PMID: 22821971; PMCID: 3430348.
117. Tsao YF, Taylor VL, Kala S, Bondy-Denomy J, Khan AN, Bona D, Cattoir V, Lory S, Davidson AR, Maxwell KL. Phage Morons Play an Important Role in Pseudomonas aeruginosa Phenotypes. J Bacteriol. 2018;200(22). Epub 2018/08/29. doi: 10.1128/JB.00189-18. PubMed PMID: 30150232; PMCID: PMC6199475.
118. Roux S, Krupovic M, Daly RA, Borges AL, Nayfach S, Schulz F, Sharrar A, Matheus Carnevali PB, Cheng JF, Ivanova NN, Bondy-Denomy J, Wrighton KC, Woyke T, Visel A, Kyrpides NC, Eloe-Fadrosh EA. Cryptic inoviruses revealed as pervasive in bacteria and archaea across Earth's biomes. Nat Microbiol. 2019. Epub 2019/07/25. doi: 10.1038/s41564-019-0510-x. PubMed PMID: 31332386.
119. Bondy-Denomy J, Qian J, Westra ER, Buckling A, Guttman DS, Davidson AR, Maxwell KL. Prophages mediate defense against phage infection through diverse mechanisms. ISME J. 2016;10(12):2854-66. Epub 2016/06/04. doi: 10.1038/ismej.2016.79. PubMed PMID: 27258950; PMCID: PMC5148200.

120. Murray TS, Kazmierczak BI. Pseudomonas aeruginosa exhibits sliding motility in the absence of type IV pili and flagella. J Bacteriol. 2008;190(8):2700-8. Epub 2007/12/11. doi: 10.1128/JB.01620-07. PubMed PMID: 18065549; PMCID: PMC2293233.
121. Burgener EB, Secor PR, Tracy MC, Sweere JM, Bik EM, Milla CE, Bollyky PL. Methods for Extraction and Detection of Pf Bacteriophage DNA from the Sputum of Patients with Cystic Fibrosis. Phage (New Rochelle). 2020;1(2):100-8. Epub 2020/07/07. doi: 10.1089/phage.2020.0003. PubMed PMID: 32626852; PMCID: PMC7327540.
122. Lanzarotti E, Biekofsky RR, Estrin DA, Marti MA, Turjanski AG. Aromatic-aromatic interactions in proteins: beyond the dimer. J Chem Inf Model. 2011;51(7):1623-33. Epub 2011/06/15. doi: 10.1021/ci200062e. PubMed PMID: 21662246.
123. Stahelin RV, Cho W. Differential roles of ionic, aliphatic, and aromatic residues in membrane-protein interactions: a surface plasmon resonance study on phospholipases A2. Biochemistry. 2001;40(15):4672-8. Epub 2001/04/11. doi: 10.1021/bi0020325. PubMed PMID: 11294634.
124. Crooks GE, Hon G, Chandonia JM, Brenner SE. WebLogo: a sequence logo generator. Genome Res. 2004;14(6):1188-90. Epub 2004/06/03. doi: 10.1101/gr.849004. PubMed PMID: 15173120; PMCID: PMC419797.
125. Winsor GL, Griffiths EJ, Lo R, Dhillon BK, Shay JA, Brinkman FS. Enhanced annotations and features for comparing thousands of Pseudomonas genomes in the Pseudomonas genome database. Nucleic Acids Res. 2016;44(D1):D646-53. Epub 2015/11/19. doi: 10.1093/nar/gkv1227. PubMed PMID: 26578582; PMCID: 4702867.
126. Jumper J, Evans R, Pritzel A, Green T, Figurnov M, Ronneberger O, Tunyasuvunakool K, Bates R, Zidek A, Potapenko A, Bridgland A, Meyer C, Kohl SAA, Ballard AJ, Cowie A, Romera-Paredes B, Nikolov S, Jain R, Adler J, Back T, Petersen S, Reiman D, Clancy E, Zielinski M, Steinegger M, Pacholska M, Berghammer T, Bodenstein S, Silver D, Vinyals O, Senior AW, Kavukcuoglu K, Kohli P, Hassabis D. Highly accurate protein structure prediction with AlphaFold. Nature. 2021. Epub 2021/07/16. doi: 10.1038/s41586-021-03819-2. PubMed PMID: 34265844.
127. McCallum M, Tammam S, Little DJ, Robinson H, Koo J, Shah M, Calmettes C, Moraes TF, Burrows LL, Howell PL. PilN Binding Modulates the Structure and Binding Partners of the Pseudomonas aeruginosa Type IVa Pilus Protein PilM. J Biol Chem. 2016;291(21):11003-15. Epub 2016/03/30. doi: 10.1074/jbc.M116.718353. PubMed PMID: 27022027; PMCID: PMC4900251.
128. Takhar HK, Kemp K, Kim M, Howell PL, Burrows LL. The platform protein is essential for type IV pilus biogenesis. J Biol Chem. 2013;288(14):9721-8. Epub 2013/02/16. doi: 10.1074/jbc.M113.453506. PubMed PMID: 23413032; PMCID: PMC3617274.
129. Lee YM, Tscherne DM, Yun SI, Frolov I, Rice CM. Dual mechanisms of pestiviral superinfection exclusion at entry and RNA replication. J Virol. 2005;79(6):3231-42. Epub 2005/02/26. doi: 10.1128/JVI.79.6.3231-3242.2005. PubMed PMID: 15731218; PMCID: PMC1075699.
130. Tarafder AK, von Kugelgen A, Mellul AJ, Schulze U, Aarts D, Bharat TAM. Phage liquid crystalline droplets form occlusive sheaths that encapsulate and protect infectious rod-shaped bacteria. Proc Natl Acad Sci U S A. 2020;117(9):4724-31. Epub 2020/02/20. doi: 10.1073/pnas.1917726117. PubMed PMID: 32071243; PMCID: PMC7060675.
131. Pourtois JD, Kratochvil MJ, Chen Q, Haddock NL, Burgener EB, De Leo GA, Bollyky PL. Filamentous Bacteriophages and the Competitive Interaction between Pseudomonas aeruginosa Strains under Antibiotic Treatment: a Modeling Study. mSystems. 2021;6(3):e0019321. Epub 2021/06/23. doi: 10.1128/mSystems.00193-21. PubMed PMID: 34156288.
132. Comolli JC, Hauser AR, Waite L, Whitchurch CB, Mattick JS, Engel JN. Pseudomonas aeruginosa gene products PilT and PilU are required for cytotoxicity in vitro and virulence in a mouse

model of acute pneumonia. Infection and immunity. 1999;67(7):3625-30. Epub 1999/06/22. PubMed PMID: 10377148; PMCID: 116553.
133. Sauer K, Cullen MC, Rickard AH, Zeef LA, Davies DG, Gilbert P. Characterization of nutrient-induced dispersion in Pseudomonas aeruginosa PAO1 biofilm. J Bacteriol. 2004;186(21):7312-26. Epub 2004/10/19. doi: 10.1128/JB.186.21.7312-7326.2004. PubMed PMID: 15489443; PMCID: 523207.
134. Sauer K, Camper AK, Ehrlich GD, Costerton JW, Davies DG. Pseudomonas aeruginosa displays multiple phenotypes during development as a biofilm. J Bacteriol. 2002;184(4):1140-54. Epub 2002/01/25. PubMed PMID: 11807075; PMCID: 134825.
135. Wright A, Hawkins CH, Anggard EE, Harper DR. A controlled clinical trial of a therapeutic bacteriophage preparation in chronic otitis due to antibiotic-resistant Pseudomonas aeruginosa; a preliminary report of efficacy. Clin Otolaryngol. 2009;34(4):349-57. Epub 2009/08/14. doi: 10.1111/j.1749-4486.2009.01973.x. PubMed PMID: 19673983.
136. Bruttin A, Brussow H. Human volunteers receiving Escherichia coli phage T4 orally: a safety test of phage therapy. Antimicrob Agents Chemother. 2005;49(7):2874-8. Epub 2005/06/28. doi: 10.1128/AAC.49.7.2874-2878.2005. PubMed PMID: 15980363; PMCID: PMC1168693.
137. Rhoads DD, Wolcott RD, Kuskowski MA, Wolcott BM, Ward LS, Sulakvelidze A. Bacteriophage therapy of venous leg ulcers in humans: results of a phase I safety trial. J Wound Care. 2009;18(6):237-8, 40-3. Epub 2009/08/08. doi: 10.12968/jowc.2009.18.6.42801. PubMed PMID: 19661847.
138. Schooley RT, Biswas B, Gill JJ, Hernandez-Morales A, Lancaster J, Lessor L, Barr JJ, Reed SL, Rohwer F, Benler S, Segall AM, Taplitz R, Smith DM, Kerr K, Kumaraswamy M, Nizet V, Lin L, McCauley MD, Strathdee SA, Benson CA, Pope RK, Leroux BM, Picel AC, Mateczun AJ, Cilwa KE, Regeimbal JM, Estrella LA, Wolfe DM, Henry MS, Quinones J, Salka S, Bishop-Lilly KA, Young R, Hamilton T. Development and Use of Personalized Bacteriophage-Based Therapeutic Cocktails To Treat a Patient with a Disseminated Resistant Acinetobacter baumannii Infection. Antimicrob Agents Chemother. 2017;61(10). Epub 2017/08/16. doi: 10.1128/AAC.00954-17. PubMed PMID: 28807909; PMCID: PMC5610518.
139. Dedrick RM, Guerrero-Bustamante CA, Garlena RA, Russell DA, Ford K, Harris K, Gilmour KC, Soothill J, Jacobs-Sera D, Schooley RT, Hatfull GF, Spencer H. Engineered bacteriophages for treatment of a patient with a disseminated drug-resistant Mycobacterium abscessus. Nat Med. 2019;25(5):730-3. Epub 2019/05/10. doi: 10.1038/s41591-019-0437-z. PubMed PMID: 31068712; PMCID: PMC6557439.
140. Aslam S, Courtwright AM, Koval C, Lehman SM, Morales S, Furr CL, Rosas F, Brownstein MJ, Fackler JR, Sisson BM, Biswas B, Henry M, Luu T, Bivens BN, Hamilton T, Duplessis C, Logan C, Law N, Yung G, Turowski J, Anesi J, Strathdee SA, Schooley RT. Early clinical experience of bacteriophage therapy in 3 lung transplant recipients. Am J Transplant. 2019;19(9):2631-9. Epub 2019/06/18. doi: 10.1111/ajt.15503. PubMed PMID: 31207123; PMCID: PMC6711787.
141. Oechslin F. Resistance Development to Bacteriophages Occurring during Bacteriophage Therapy. Viruses. 2018;10(7). Epub 2018/07/04. doi: 10.3390/v10070351. PubMed PMID: 29966329; PMCID: PMC6070868.
142. Loc Carrillo C, Atterbury RJ, el-Shibiny A, Connerton PL, Dillon E, Scott A, Connerton IF. Bacteriophage therapy to reduce Campylobacter jejuni colonization of broiler chickens. Appl Environ Microbiol. 2005;71(11):6554-63. Epub 2005/11/05. doi: 10.1128/AEM.71.11.6554-6563.2005. PubMed PMID: 16269681; PMCID: PMC1287621.
143. Scott AE, Timms AR, Connerton PL, Loc Carrillo C, Adzfa Radzum K, Connerton IF. Genome dynamics of Campylobacter jejuni in response to bacteriophage predation. PLoS Pathog.

2007;3(8):e119. Epub 2007/08/29. doi: 10.1371/journal.ppat.0030119. PubMed PMID: 17722979; PMCID: PMC1950947.
144. Carvalho CM, Gannon BW, Halfhide DE, Santos SB, Hayes CM, Roe JM, Azeredo J. The in vivo efficacy of two administration routes of a phage cocktail to reduce numbers of Campylobacter coli and Campylobacter jejuni in chickens. BMC Microbiol. 2010;10:232. Epub 2010/09/03. doi: 10.1186/1471-2180-10-232. PubMed PMID: 20809975; PMCID: PMC2940857.
145. Chung IY, Kim BO, Han JH, Park J, Kang HK, Park Y, Cho YH. A phage protein-derived antipathogenic peptide that targets type IV pilus assembly. Virulence. 2021;12(1):1377-87. Epub 2021/05/20. doi: 10.1080/21505594.2021.1926411. PubMed PMID: 34008466; PMCID: PMC8143254.
146. Hmelo LR, Borlee BR, Almblad H, Love ME, Randall TE, Tseng BS, Lin C, Irie Y, Storek KM, Yang JJ, Siehnel RJ, Howell PL, Singh PK, Tolker-Nielsen T, Parsek MR, Schweizer HP, Harrison JJ. Precision-engineering the Pseudomonas aeruginosa genome with two-step allelic exchange. Nat Protoc. 2015;10(11):1820-41. Epub 2015/10/23. doi: 10.1038/nprot.2015.115. PubMed PMID: 26492139.
147. Li Y, Liu X, Tang K, Wang W, Guo Y, Wang X. Prophage encoding toxin/antitoxin system PfiT/PfiA inhibits Pf4 production in Pseudomonas aeruginosa. Microb Biotechnol. 2020;13(4):1132-44. Epub 2020/04/05. doi: 10.1111/1751-7915.13570. PubMed PMID: 32246813; PMCID: PMC7264888.
148. Qiu D, Damron FH, Mima T, Schweizer HP, Yu HD. PBAD-based shuttle vectors for functional analysis of toxic and highly regulated genes in Pseudomonas and Burkholderia spp. and other bacteria. Appl Environ Microbiol. 2008;74(23):7422-6. Epub 2008/10/14. doi: 10.1128/AEM.01369-08. PubMed PMID: 18849445; PMCID: PMC2592904.
149. Semmler AB, Whitchurch CB, Mattick JS. A re-examination of twitching motility in Pseudomonas aeruginosa. Microbiology. 1999;145 (Pt 10):2863-73. Epub 1999/10/28. doi: 10.1099/00221287-145-10-2863. PubMed PMID: 10537208.
150. Choi KH, Schweizer HP. mini-Tn7 insertion in bacteria with single attTn7 sites: example Pseudomonas aeruginosa. Nat Protoc. 2006;1(1):153-61. Epub 2007/04/05. doi: 10.1038/nprot.2006.24. PubMed PMID: 17406227.
151. Pettersen EF, Goddard TD, Huang CC, Meng EC, Couch GS, Croll TI, Morris JH, Ferrin TE. UCSF ChimeraX: Structure visualization for researchers, educators, and developers. Protein Sci. 2021;30(1):70-82. Epub 2020/09/04. doi: 10.1002/pro.3943. PubMed PMID: 32881101; PMCID: PMC7737788.
152. Holloway BW, Krishnapillai V, Morgan AF. Chromosomal genetics of Pseudomonas. Microbiol Rev. 1979;43(1):73-102. Epub 1979/03/01. PubMed PMID: 111024; PMCID: 281463.
153. Zhao K, Tseng BS, Beckerman B, Jin F, Gibiansky ML, Harrison JJ, Luijten E, Parsek MR, Wong GC. Psl trails guide exploration and microcolony formation in Pseudomonas aeruginosa biofilms. Nature. 2013;497(7449):388-91. Epub 2013/05/10. doi: 10.1038/nature12155. PubMed PMID: 23657259; PMCID: 4109411.
154. Jennings LK, Storek KM, Ledvina HE, Coulon C, Marmont LS, Sadovskaya I, Secor PR, Tseng BS, Scian M, Filloux A, Wozniak DJ, Howell PL, Parsek MR. Pel is a cationic exopolysaccharide that cross-links extracellular DNA in the Pseudomonas aeruginosa biofilm matrix. Proc Natl Acad Sci U S A. 2015;112(36):11353-8. Epub 2015/08/28. doi: 10.1073/pnas.1503058112. PubMed PMID: 26311845; PMCID: PMC4568648.
155. Cruz RL, Asfahl KL, Van den Bossche S, Coenye T, Crabbe A, Dandekar AA. RhlR-Regulated Acyl-Homoserine Lactone Quorum Sensing in a Cystic Fibrosis Isolate of Pseudomonas aeruginosa. MBio. 2020;11(2). Epub 2020/04/09. doi: 10.1128/mBio.00532-20. PubMed PMID: 32265330; PMCID: PMC7157775.

156. Budzik JM, Rosche WA, Rietsch A, O'Toole GA. Isolation and characterization of a generalized transducing phage for Pseudomonas aeruginosa strains PAO1 and PA14. J Bacteriol. 2004;186(10):3270-3. Epub 2004/05/06. doi: 10.1128/JB.186.10.3270-3273.2004. PubMed PMID: 15126493; PMCID: PMC400619.
157. Chan BK, Sistrom M, Wertz JE, Kortright KE, Narayan D, Turner PE. Phage selection restores antibiotic sensitivity in MDR Pseudomonas aeruginosa. Sci Rep. 2016;6:26717. Epub 2016/05/27. doi: 10.1038/srep26717. PubMed PMID: 27225966; PMCID: PMC4880932.
158. Hay ID, Lithgow T. Filamentous phages: masters of a microbial sharing economy. Embo Rep. 2019;20(6). Epub 2019/04/07. doi: 10.15252/embr.201847427. PubMed PMID: 30952693; PMCID: PMC6549030.
159. Schmidt AK, Fitzpatrick AD, Schwartzkopf CM, Faith DR, Jennings LK, Coluccio A, Hunt DJ, Michaels LA, Hargil A, Chen Q, Bollyky PL, Dorward DW, Wachter J, Rosa PA, Maxwell KL, Secor PR. A Filamentous Bacteriophage Protein Inhibits Type IV Pili To Prevent Superinfection of Pseudomonas aeruginosa. mBio. 2022:e0244121. Epub 20220118. doi: 10.1128/mbio.02441-21. PubMed PMID: 35038902.
160. Waldor MK, Mekalanos JJ. Lysogenic conversion by a filamentous phage encoding cholera toxin. Science. 1996;272(5270):1910-4. Epub 1996/06/28. doi: 10.1126/science.272.5270.1910. PubMed PMID: 8658163.
161. Addy HS, Askora A, Kawasaki T, Fujie M, Yamada T. The filamentous phage varphiRSS1 enhances virulence of phytopathogenic Ralstonia solanacearum on tomato. Phytopathology. 2012;102(3):244-51. doi: 10.1094/PHYTO-10-11-0277. PubMed PMID: 22085298.
162. JG H, A M-p, S K, D M, SA R. Environmental cues and genes involved in establishment of the superinfective Pf4 phage of Pseudomonas aeruginosa. Front Microbiol. 2014;5(654). doi: 10.3389/fmicb.2014.00654.
163. Bach MS, de Vries CR, Khosravi A, Sweere JM, Popescu MC, Chen Q, Demirdjian S, Hargil A, Van Belleghem JD, Kaber G, Hajfathalian M, Burgener EB, Liu D, Tran QL, Dharmaraj T, Birukova M, Sunkari V, Balaji S, Ghosh N, Mathew-Steiner SS, El Masry MS, Keswani SG, Banaei N, Nedelec L, Sen CK, Chandra V, Secor PR, Suh GA, Bollyky PL. Filamentous bacteriophage delays healing of Pseudomonas-infected wounds. Cell Rep Med. 2022;3(6):100656. doi: 10.1016/j.xcrm.2022.100656. PubMed PMID: 35732145.
164. Schuster M, Greenberg EP. A network of networks: quorum-sensing gene regulation in Pseudomonas aeruginosa. Int J Med Microbiol. 2006;296(2-3):73-81. Epub 2006/02/16. doi: 10.1016/j.ijmm.2006.01.036. PubMed PMID: 16476569.
165. Tan MW, Mahajan-Miklos S, Ausubel FM. Killing of Caenorhabditis elegans by Pseudomonas aeruginosa used to model mammalian bacterial pathogenesis. Proc Natl Acad Sci U S A. 1999;96(2):715-20. doi: 10.1073/pnas.96.2.715. PubMed PMID: 9892699; PMCID: PMC15202.
166. Saunders SH, Tse ECM, Yates MD, Otero FJ, Trammell SA, Stemp EDA, Barton JK, Tender LM, Newman DK. Extracellular DNA Promotes Efficient Extracellular Electron Transfer by Pyocyanin in Pseudomonas aeruginosa Biofilms. Cell. 2020;182(4):919-32 e19. Epub 2020/08/09. doi: 10.1016/j.cell.2020.07.006. PubMed PMID: 32763156; PMCID: PMC7457544.
167. Glasser NR, Kern SE, Newman DK. Phenazine redox cycling enhances anaerobic survival in Pseudomonas aeruginosa by facilitating generation of ATP and a proton-motive force. Mol Microbiol. 2014;92(2):399-412. Epub 2014/03/13. doi: 10.1111/mmi.12566. PubMed PMID: 24612454; PMCID: PMC4046897.

168. Lau GW, Hassett DJ, Ran H, Kong F. The role of pyocyanin in Pseudomonas aeruginosa infection. Trends Mol Med. 2004;10(12):599-606. Epub 2004/11/30. doi: 10.1016/j.molmed.2004.10.002. PubMed PMID: 15567330.
169. Pesci EC, Milbank JBJ, Pearson JP, McKnight S, Kende AS, Greenberg EP, Iglewski BH. Quinolone signaling in the cell-to-cell communication system of Pseudomonas aeruginosa. Proceedings of the National Academy of Sciences. 1999;96(20):11229-34. doi: doi:10.1073/pnas.96.20.11229.
170. Letizia M, Mellini M, Fortuna A, Visca P, Imperi F, Leoni L, Rampioni G. PqsE Expands and Differentially Modulates the RhlR Quorum Sensing Regulon in Pseudomonas aeruginosa. Microbiology Spectrum. 2022;10(3):e00961-22. doi: doi:10.1128/spectrum.00961-22.
171. McKnight SL, Iglewski BH, Pesci EC. The Pseudomonas Quinolone Signal Regulates rhl Quorum Sensing in Pseudomonas aeruginosa. Journal of Bacteriology. 2000;182(10):2702-8. doi: doi:10.1128/JB.182.10.2702-2708.2000.
172. Soto-Aceves MP, Cocotl-Yanez M, Servin-Gonzalez L, Soberon-Chavez G. The Rhl Quorum-Sensing System Is at the Top of the Regulatory Hierarchy under Phosphate-Limiting Conditions in Pseudomonas aeruginosa PAO1. J Bacteriol. 2021;203(5). Epub 20210208. doi: 10.1128/JB.00475-20. PubMed PMID: 33288622; PMCID: PMC7890550.
173. Dietrich LE, Price-Whelan A, Petersen A, Whiteley M, Newman DK. The phenazine pyocyanin is a terminal signalling factor in the quorum sensing network of Pseudomonas aeruginosa. Mol Microbiol. 2006;61(5):1308-21. Epub 2006/08/02. doi: 10.1111/j.1365-2958.2006.05306.x. PubMed PMID: 16879411.
174. Asfahl KL, Smalley NE, Chang AP, Dandekar AA. Genetic and Transcriptomic Characteristics of RhlR-Dependent Quorum Sensing in Cystic Fibrosis Isolates of Pseudomonas aeruginosa. mSystems. 2022;7(2):e0011322. Epub 20220411. doi: 10.1128/msystems.00113-22. PubMed PMID: 35471121; PMCID: PMC9040856.
175. Smalley NE, Schaefer AL, Asfahl KL, Perez C, Greenberg EP, Dandekar AA. Evolution of the Quorum Sensing Regulon in Cooperating Populations of Pseudomonas aeruginosa. MBio. 2022;13(1):e0016122. Epub 20220222. doi: 10.1128/mbio.00161-22. PubMed PMID: 35294222; PMCID: PMC8863103.
176. Feltner JB, Wolter DJ, Pope CE, Groleau MC, Smalley NE, Greenberg EP, Mayer-Hamblett N, Burns J, Deziel E, Hoffman LR, Dandekar AA. LasR Variant Cystic Fibrosis Isolates Reveal an Adaptable Quorum-Sensing Hierarchy in Pseudomonas aeruginosa. MBio. 2016;7(5). Epub 2016/10/06. doi: 10.1128/mBio.01513-16. PubMed PMID: 27703072; PMCID: PMC5050340.
177. Garigan D, Hsu AL, Fraser AG, Kamath RS, Ahringer J, Kenyon C. Genetic analysis of tissue aging in Caenorhabditis elegans: a role for heat-shock factor and bacterial proliferation. Genetics. 2002;161(3):1101-12. doi: 10.1093/genetics/161.3.1101. PubMed PMID: 12136014; PMCID: PMC1462187.
178. Manago A, Becker KA, Carpinteiro A, Wilker B, Soddemann M, Seitz AP, Edwards MJ, Grassme H, Szabo I, Gulbins E. Pseudomonas aeruginosa pyocyanin induces neutrophil death via mitochondrial reactive oxygen species and mitochondrial acid sphingomyelinase. Antioxid Redox Signal. 2015;22(13):1097-110. Epub 20150318. doi: 10.1089/ars.2014.5979. PubMed PMID: 25686490; PMCID: PMC4403017.
179. O'Malley YQ, Abdalla MY, McCormick ML, Reszka KJ, Denning GM, Britigan BE. Subcellular localization of Pseudomonas pyocyanin cytotoxicity in human lung epithelial cells. Am J Physiol Lung Cell Mol Physiol. 2003;284(2):L420-30. Epub 20021101. doi: 10.1152/ajplung.00316.2002. PubMed PMID: 12414438.

180. Johnstone IL. Cuticle collagen genes. Expression in Caenorhabditis elegans. Trends Genet. 2000;16(1):21-7. doi: 10.1016/s0168-9525(99)01857-0. PubMed PMID: 10637627.
181. Moura-Alves P, Fae K, Houthuys E, Dorhoi A, Kreuchwig A, Furkert J, Barison N, Diehl A, Munder A, Constant P, Skrahina T, Guhlich-Bornhof U, Klemm M, Koehler AB, Bandermann S, Goosmann C, Mollenkopf HJ, Hurwitz R, Brinkmann V, Fillatreau S, Daffe M, Tummler B, Kolbe M, Oschkinat H, Krause G, Kaufmann SH. AhR sensing of bacterial pigments regulates antibacterial defence. Nature. 2014;512(7515):387-92. Epub 2014/08/15. doi: 10.1038/nature13684. PubMed PMID: 25119038.
182. Moura-Alves P, Puyskens A, Stinn A, Klemm M, Guhlich-Bornhof U, Dorhoi A, Furkert J, Kreuchwig A, Protze J, Lozza L, Pei G, Saikali P, Perdomo C, Mollenkopf HJ, Hurwitz R, Kirschhoefer F, Brenner-Weiss G, Weiner J, 3rd, Oschkinat H, Kolbe M, Krause G, Kaufmann SHE. Host monitoring of quorum sensing during Pseudomonas aeruginosa infection. Science. 2019;366(6472). Epub 2019/12/21. doi: 10.1126/science.aaw1629. PubMed PMID: 31857448.
183. Liu Y-C, Chan K-G, Chang C-Y. Modulation of host biology by Pseudomonas aeruginosa quorum sensing signal molecules: messengers or traitors. Frontiers in microbiology. 2015;6:1226.
184. Fujii-Kuriyama Y, Mimura J. Molecular mechanisms of AhR functions in the regulation of cytochrome P450 genes. Biochem Biophys Res Commun. 2005;338(1):311-7. Epub 20050830. doi: 10.1016/j.bbrc.2005.08.162. PubMed PMID: 16153594.
185. Larigot L, Bui LC, de Bouvier M, Pierre O, Pinon G, Fiocca J, Ozeir M, Tourette C, Ottolenghi C, Imbeaud S, Pontoizeau C, Blaise BJ, Chevallier A, Tomkiewicz C, Legrand B, Elena-Herrmann B, Neri C, Brinkmann V, Nioche P, Barouki R, Ventura N, Dairou J, Coumoul X. Identification of Modulators of the C. elegans Aryl Hydrocarbon Receptor and Characterization of Transcriptomic and Metabolic AhR-1 Profiles. Antioxidants (Basel). 2022;11(5). Epub 20220523. doi: 10.3390/antiox11051030. PubMed PMID: 35624894; PMCID: PMC9137885.
186. Diggle SP, Matthijs S, Wright VJ, Fletcher MP, Chhabra SR, Lamont IL, Kong X, Hider RC, Cornelis P, Camara M, Williams P. The Pseudomonas aeruginosa 4-quinolone signal molecules HHQ and PQS play multifunctional roles in quorum sensing and iron entrapment. Chem Biol. 2007;14(1):87-96. Epub 2007/01/27. doi: 10.1016/j.chembiol.2006.11.014. PubMed PMID: 17254955.
187. Evans EA, Kawli T, Tan MW. Pseudomonas aeruginosa suppresses host immunity by activating the DAF-2 insulin-like signaling pathway in Caenorhabditis elegans. PLoS Pathog. 2008;4(10):e1000175. Epub 2008/10/18. doi: 10.1371/journal.ppat.1000175. PubMed PMID: 18927620; PMCID: PMC2568960.
188. Mestre MR, González-Delgado A, Gutiérrez-Rus LI, Martínez-Abarca F, Toro N. Systematic prediction of genes functionally associated with bacterial retrons and classification of the encoded tripartite systems. Nucleic acids research. 2020;48(22):12632-47.
189. Secor PR, Jennings LK, Michaels LA, Sweere JM, Singh PK, Parks WC, Bollyky PL. Biofilm assembly becomes crystal clear - filamentous bacteriophage organize the Pseudomonas aeruginosa biofilm matrix into a liquid crystal. Microb Cell. 2015;3(1):49-52. Epub 2015/12/31. doi: 10.15698/mic2016.01.475. PubMed PMID: 28357315; PMCID: PMC5354590.
190. Alatraktchi FAa, Svendsen WE, Molin S. Electrochemical Detection of Pyocyanin as a Biomarker for Pseudomonas aeruginosa: A Focused Review. Sensors. 2020;20(18):5218. PubMed PMID: doi:10.3390/s20185218.
191. Feltner JB, Wolter DJ, Pope CE, Groleau M-C, Smalley NE, Greenberg EP, Mayer-Hamblett N, Burns J, Déziel E, Hoffman LR, Dandekar AA, Winans SC, Diggle S, Goldberg J. LasR Variant Cystic Fibrosis Isolates Reveal an Adaptable Quorum-Sensing Hierarchy in Pseudomonas aeruginosa. mBio. 2016;7(5):e01513-16. doi: doi:10.1128/mBio.01513-16.

192. Martey CA, Baglole CJ, Gasiewicz TA, Sime PJ, Phipps RP. The aryl hydrocarbon receptor is a regulator of cigarette smoke induction of the cyclooxygenase and prostaglandin pathways in human lung fibroblasts. Am J Physiol Lung Cell Mol Physiol. 2005;289(3):L391-9. Epub 20050429. doi: 10.1152/ajplung.00062.2005. PubMed PMID: 15863442.
193. Scott SA, Fu J, Chang PV. Microbial tryptophan metabolites regulate gut barrier function via the aryl hydrocarbon receptor. Proc Natl Acad Sci U S A. 2020;117(32):19376-87. Epub 20200727. doi: 10.1073/pnas.2000047117. PubMed PMID: 32719140; PMCID: PMC7431026.
194. Ghosh DD, Lee D, Jin X, Horvitz HR, Nitabach MN. C. elegans discriminates colors to guide foraging. Science. 2021;371(6533):1059-63. doi: 10.1126/science.abd3010. PubMed PMID: 33674494; PMCID: PMC8554940.
195. Leong W, Poh WH, Williams J, Lutz C, Hoque MM, Poh YH, Yee BYK, Chua C, Givskov M, Sanderson-Smith M, Rice SA, McDougald D. Adaptation to an Amoeba Host Leads to Pseudomonas aeruginosa Isolates with Attenuated Virulence. Appl Environ Microbiol. 2022;88(5):e0232221. Epub 20220112. doi: 10.1128/aem.02322-21. PubMed PMID: 35020451; PMCID: PMC8904051.
196. Hilbi H, Weber SS, Ragaz C, Nyfeler Y, Urwyler S. Environmental predators as models for bacterial pathogenesis. Environ Microbiol. 2007;9(3):563-75. doi: 10.1111/j.1462-2920.2007.01238.x. PubMed PMID: 17298357.
197. Schulenburg H, Felix MA. The Natural Biotic Environment of Caenorhabditis elegans. Genetics. 2017;206(1):55-86. doi: 10.1534/genetics.116.195511. PubMed PMID: 28476862; PMCID: PMC5419493.
198. Fiedoruk K, Zakrzewska M, Daniluk T, Piktel E, Chmielewska S, Bucki R. Two Lineages of Pseudomonas aeruginosa Filamentous Phages: Structural Uniformity over Integration Preferences. Genome Biol Evol. 2020;12(10):1765-81. doi: 10.1093/gbe/evaa146. PubMed PMID: 32658245; PMCID: PMC7549136.
199. Kurachi M. Studies on the Biosynthesis of Pyocyanine.(I): On the Cultural Condition for Pyocyanine Formation. Bulletin of the Institute for Chemical Research, Kyoto University. 1958;36(6):163-73.
200. Essar DW, Eberly L, Hadero A, Crawford IP. Identification and characterization of genes for a second anthranilate synthase in Pseudomonas aeruginosa: interchangeability of the two anthranilate synthases and evolutionary implications. Journal of Bacteriology. 1990;172(2):884-900. doi: doi:10.1128/jb.172.2.884-900.1990.
201. Choi K-H, Kumar A, Schweizer HP. A 10-min method for preparation of highly electrocompetent Pseudomonas aeruginosa cells: application for DNA fragment transfer between chromosomes and plasmid transformation. Journal of microbiological methods. 2006;64(3):391-7.
202. Qin H, Powell-Coffman JA. The Caenorhabditis elegans aryl hydrocarbon receptor, AHR-1, regulates neuronal development. Dev Biol. 2004;270(1):64-75. doi: 10.1016/j.ydbio.2004.02.004. PubMed PMID: 15136141.
203. Burgener EB, Secor PR, Tracy MC, Sweere JM, Bik EM, Milla CE, Bollyky PL. Methods for Extraction and Detection of Pf Bacteriophage DNA from the Sputum of Patients with Cystic Fibrosis. Phage. 2020;1(2):100-8. Epub 2020/07/07. doi: 10.1089/phage.2020.0003. PubMed PMID: 32626852; PMCID: PMC7327540.
204. King CD, Singh D, Holden K, Govan AB, Keith SA, Ghazi A, Robinson RAS. Proteomic identification of virulence-related factors in young and aging C. elegans infected with Pseudomonas aeruginosa. J Proteomics. 2018;181:92-103. Epub 20180412. doi: 10.1016/j.jprot.2018.04.006. PubMed PMID: 29656019.

205. Thomas PD, Ebert D, Muruganujan A, Mushayahama T, Albou LP, Mi H. PANTHER: Making genome-scale phylogenetics accessible to all. Protein Sci. 2022;31(1):8-22. Epub 20211125. doi: 10.1002/pro.4218. PubMed PMID: 34717010; PMCID: PMC8740835.
206. Moribe H, Yochem J, Yamada H, Tabuse Y, Fujimoto T, Mekada E. Tetraspanin protein (TSP-15) is required for epidermal integrity in Caenorhabditis elegans. J Cell Sci. 2004;117(Pt 22):5209-20. Epub 20040928. doi: 10.1242/jcs.01403. PubMed PMID: 15454573.
207. Miller MB, Bassler BL. Quorum sensing in bacteria. Annu Rev Microbiol. 2001;55:165-99. Epub 2001/09/07. doi: 10.1146/annurev.micro.55.1.165. PubMed PMID: 11544353.
208. Whiteley M, Lee KM, Greenberg EP. Identification of genes controlled by quorum sensing in Pseudomonas aeruginosa. P Natl Acad Sci USA. 1999;96(24):13904-9. Epub 1999/11/26. PubMed PMID: 10570171; PMCID: 24163.
209. Hoque MM, Naser IB, Bari SM, Zhu J, Mekalanos JJ, Faruque SM. Quorum Regulated Resistance of Vibrio cholerae against Environmental Bacteriophages. Sci Rep. 2016;6:37956. Epub 20161128. doi: 10.1038/srep37956. PubMed PMID: 27892495; PMCID: PMC5124996.
210. Hoyland-Kroghsbo NM, Maerkedahl RB, Svenningsen SL. A quorum-sensing-induced bacteriophage defense mechanism. MBio. 2013;4(1):e00362-12. Epub 2013/02/21. doi: 10.1128/mBio.00362-12. PubMed PMID: 23422409; PMCID: PMC3624510.
211. Patterson AG, Jackson SA, Taylor C, Evans GB, Salmond GPC, Przybilski R, Staals RHJ, Fineran PC. Quorum Sensing Controls Adaptive Immunity through the Regulation of Multiple CRISPR-Cas Systems. Mol Cell. 2016;64(6):1102-8. Epub 20161117. doi: 10.1016/j.molcel.2016.11.012. PubMed PMID: 27867010; PMCID: PMC5179492.
212. Hoyland-Kroghsbo NM, Paczkowski J, Mukherjee S, Broniewski J, Westra E, Bondy-Denomy J, Bassler BL. Quorum sensing controls the Pseudomonas aeruginosa CRISPR-Cas adaptive immune system. Proc Natl Acad Sci U S A. 2017;114(1):131-5. Epub 20161114. doi: 10.1073/pnas.1617415113. PubMed PMID: 27849583; PMCID: PMC5224376.
213. Blasdel BG, Ceyssens P-J, Chevallereau A, Debarbieux L, Lavigne R. Comparative transcriptomics reveals a conserved Bacterial Adaptive Phage Response (BAPR) to viral predation. bioRxiv. 2018:248849. doi: 10.1101/248849.
214. De Smet J, Zimmermann M, Kogadeeva M, Ceyssens PJ, Vermaelen W, Blasdel B, Bin Jang H, Sauer U, Lavigne R. High coverage metabolomics analysis reveals phage-specific alterations to Pseudomonas aeruginosa physiology during infection. Isme J. 2016;10(8):1823-35. Epub 20160216. doi: 10.1038/ismej.2016.3. PubMed PMID: 26882266; PMCID: PMC5029163.
215. Moreau P, Diggle SP, Friman VP. Bacterial cell-to-cell signaling promotes the evolution of resistance to parasitic bacteriophages. Ecol Evol. 2017;7(6):1936-41. Epub 20170221. doi: 10.1002/ece3.2818. PubMed PMID: 28331600; PMCID: PMC5355186.
216. Bru JL, Rawson B, Trinh C, Whiteson K, Hoyland-Kroghsbo NM, Siryaporn A. PQS Produced by the Pseudomonas aeruginosa Stress Response Repels Swarms Away from Bacteriophage and Antibiotics. J Bacteriol. 2019;201(23). Epub 2019/08/28. doi: 10.1128/JB.00383-19. PubMed PMID: 31451543; PMCID: PMC6832071.
217. Hoyland-Kroghsbo NM, Bassler BL. Phage Infection Restores PQS Signaling and Enhances Growth of a Pseudomonas aeruginosa lasI Quorum-Sensing Mutant. J Bacteriol. 2022;204(5):e0055721. Epub 20220407. doi: 10.1128/jb.00557-21. PubMed PMID: 35389255; PMCID: PMC9112912.
218. Schwartzkopf CM, Robinson AJ, Ellenbecker M, Faith DR, Schmidt AK, Brooks DM, Lewerke L, Voronina E, Dandekar AA, Secor PR. Tripartite interactions between filamentous Pf4 bacteriophage, Pseudomonas aeruginosa, and bacterivorous nematodes. PLoS Pathog. 2023;19(2):e1010925. Epub 20230217. doi: 10.1371/journal.ppat.1010925. PubMed PMID: 36800381.

219. Tortuel D, Tahrioui A, David A, Cambronel M, Nilly F, Clamens T, Maillot O, Barreau M, Feuilloley MGJ, Lesouhaitier O, Filloux A, Bouffartigues E, Cornelis P, Chevalier S. Pf4 Phage Variant Infection Reduces Virulence-Associated Traits in Pseudomonas aeruginosa. Microbiology Spectrum. 2022;0(0):e01548-22. doi: doi:10.1128/spectrum.01548-22.
220. Tortuel D, Tahrioui A, David A, Cambronel M, Nilly F, Clamens T, Maillot O, Barreau M, Feuilloley MGJ, Lesouhaitier O, Filloux A, Bouffartigues E, Cornelis P, Chevalier S. Pf4 Phage Variant Infection Reduces Virulence-Associated Traits in Pseudomonas aeruginosa. Microbiol Spectr. 2022:e0154822. Epub 20220829. doi: 10.1128/spectrum.01548-22. PubMed PMID: 36036571.
221. Chang YW, Rettberg LA, Treuner-Lange A, Iwasa J, Sogaard-Andersen L, Jensen GJ. Architecture of the type IVa pilus machine. Science. 2016;351(6278):aad2001. Epub 20160310. doi: 10.1126/science.aad2001. PubMed PMID: 26965631; PMCID: PMC5929464.
222. Kim S, Jeon TJ, Oberai A, Yang D, Schmidt JJ, Bowie JU. Transmembrane glycine zippers: physiological and pathological roles in membrane proteins. Proc Natl Acad Sci U S A. 2005;102(40):14278-83. Epub 20050922. doi: 10.1073/pnas.0501234102. PubMed PMID: 16179394; PMCID: PMC1242278.
223. Giltner CL, Nguyen Y, Burrows LL. Type IV pilin proteins: versatile molecular modules. Microbiol Mol Biol Rev. 2012;76(4):740-72. doi: 10.1128/MMBR.00035-12. PubMed PMID: 23204365; PMCID: PMC3510520.
224. Coleman JP, Hudson LL, McKnight SL, Farrow JM, 3rd, Calfee MW, Lindsey CA, Pesci EC. Pseudomonas aeruginosa PqsA is an anthranilate-coenzyme A ligase. J Bacteriol. 2008;190(4):1247-55. Epub 2007/12/18. doi: 10.1128/JB.01140-07. PubMed PMID: 18083812; PMCID: PMC2238192.
225. Witzgall F, Ewert W, Blankenfeldt W. Structures of the N-Terminal Domain of PqsA in Complex with Anthraniloyl- and 6-Fluoroanthraniloyl-AMP: Substrate Activation in Pseudomonas Quinolone Signal (PQS) Biosynthesis. Chembiochem. 2017;18(20):2045-55. Epub 20170918. doi: 10.1002/cbic.201700374. PubMed PMID: 28834007.
226. DiMaio D. Viral miniproteins. Annu Rev Microbiol. 2014;68:21-43. Epub 20140410. doi: 10.1146/annurev-micro-091313-103727. PubMed PMID: 24742054; PMCID: PMC4430842.
227. Fremin BJ, Bhatt AS, Kyrpides NC, Global Phage Small Open Reading Frame C. Thousands of small, novel genes predicted in global phage genomes. Cell Rep. 2022;39(12):110984. doi: 10.1016/j.celrep.2022.110984. PubMed PMID: 35732113; PMCID: PMC9254267.
228. Eriksson JM, Haggard-Ljungquist E. The multifunctional bacteriophage P2 cox protein requires oligomerization for biological activity. J Bacteriol. 2000;182(23):6714-23. doi: 10.1128/JB.182.23.6714-6723.2000. PubMed PMID: 11073917; PMCID: PMC111415.
229. Ziegelin G, Scherzinger E, Lurz R, Lanka E. Phage P4 alpha protein is multifunctional with origin recognition, helicase and primase activities. Embo J. 1993;12(9):3703-8. doi: 10.1002/j.1460-2075.1993.tb06045.x. PubMed PMID: 8253092; PMCID: PMC413647.
230. Hernandez AJ, Richardson CC. Gp2.5, the multifunctional bacteriophage T7 single-stranded DNA binding protein. Semin Cell Dev Biol. 2019;86:92-101. Epub 20180328. doi: 10.1016/j.semcdb.2018.03.018. PubMed PMID: 29588157; PMCID: PMC6162179.
231. Calfee MW, Coleman JP, Pesci EC. Interference with Pseudomonas quinolone signal synthesis inhibits virulence factor expression by Pseudomonas aeruginosa. Proceedings of the National Academy of Sciences. 2001;98(20):11633-7. doi: doi:10.1073/pnas.201328498.
232. Tortuel D, Tahrioui A, David A, Cambronel M, Nilly F, Clamens T, Maillot O, Barreau M, Feuilloley MGJ, Lesouhaitier O, Filloux A, Bouffartigues E, Cornelis P, Chevalier S. Pf4 Phage Variant Infection Reduces Virulence-Associated Traits in Pseudomonas aeruginosa. Microbiology Spectrum. 2022;10(5):e01548-22. doi: doi:10.1128/spectrum.01548-22.

233. Liao Y, Smyth GK, Shi W. The R package Rsubread is easier, faster, cheaper and better for alignment and quantification of RNA sequencing reads. Nucleic Acids Research. 2019;47(8):e47-e. doi: 10.1093/nar/gkz114.
234. Robinson MD, McCarthy DJ, Smyth GK. edgeR: a Bioconductor package for differential expression analysis of digital gene expression data. Bioinformatics. 2009;26(1):139-40. doi: 10.1093/bioinformatics/btp616.
235. Team RC. R: A language and environment for statistical computing. MSOR connections. 2014;1.
236. Villanueva RAM, Chen ZJ. ggplot2: Elegant Graphics for Data Analysis (2nd ed.). Measurement: Interdisciplinary Research and Perspectives. 2019;17(3):160-7. doi: 10.1080/15366367.2019.1565254.